

Removal of sulfur and nitrogen compounds from gas oil by adsorption

A thesis submitted to the College of Graduate and Postdoctoral Studies

In partial fulfillment of the Requirements for the

Degree of Master in Science

In the Department of Chemical and Biological Engineering

University of Saskatchewan

Saskatoon, SK

Canada

By

Anakaren Botana de la Cruz

PERMISSION TO USE

In presenting this thesis in partial fulfillment of the requirements for a Postgraduate degree from the University of Saskatchewan, I agree that the libraries of this University may make it freely available for inspection. I further agree that permission for copying of this thesis in any manner, in whole or in part, for scholarly purposes may be granted by Dr. Ajay Dalai and Dr. John Adjaye, who supervised my thesis work, or in their absence, by the Head of the Department or the Dean of the College of Engineering. It is understood that any copying or publication or use of this thesis or parts thereof for financial gain is prohibited and shall not be allowed without my written permission. It is also understood that due recognition shall be given to me and to the University of Saskatchewan in any scholarly use which may be made of any material in my thesis. Requests for permission to copy or to make other uses of materials in this thesis/dissertation in whole or part should be addressed to:

Head of the Department
Chemical and Biological Engineering
University of Saskatchewan
57 Campus Drive
Saskatoon, Saskatchewan
S7N 5A9 Canada

OR

Dean
College of Graduate and Postdoctoral Studies
University of Saskatchewan
116 Thorvaldson Building, 110 Science Place
Saskatoon, Saskatchewan S7N 5C9 Canada

ABSTRACT

Catalytic hydrotreatment is known worldwide as the process where concentrations of species like nitrogen, sulfur, oxygen and various metals are reduced to acceptable levels in the refining process. This process involves high temperatures and pressures, which results in major economic expense to refineries. These process conditions are dependent on the nature of the petroleum feedstock to be processed. Bitumen-derived gas oils from Athabasca oil sands can have high concentrations of organo-sulfur (~ 4 wt.%) and nitrogen (~ 0.4 wt.%) species; thus, posing a major challenge to downstream processing in refineries. Due to the challenge represented by these heteroatoms (S, N) during conventional catalytic hydrotreatment, other methods that involve non-catalytic processes using π -acceptor-immobilized adsorbents have garnered immense interest of researchers in this field due to its low temperature and pressure requirements. Though, mixed metal oxides such as mesoporous alumina with desirable textural properties (surface area, pore diameter and pore volume) have the tendency to be used as adsorbent support for the immobilization of π -acceptor moieties via a linker, their potential has been less explored. In this study, an attempt was made to investigate the mesoporous alumina support-linker- π acceptor, charge-transfer complex (CTC) structure for the adsorption of these heteroatoms present in the oil. This novel alumina-based adsorbent, combined with the non-catalytic adsorption method, was effective to selectively remove the refractory sulfur and nitrogen compounds from model feedstocks under milder conditions (room temperature and atmospheric pressure) as compared to catalytic hydrotreatment.

The research work was divided in 3 phases. Phase 1 was focused on the synthesis and characterization of the alumina-based adsorbents and their characterization. Three adsorbents were synthesized using a charge-transfer complex (CTC) moiety consisting of a support, linker and π -acceptor. Alumina was selected to be the supporting materials for its textural properties; three different alumina-based supports were used: mesoporous alumina, titania-substituted alumina and commercial alumina for comparison purposes. These three supports went under reaction to get a linker, ethylenediamine (EDA) attached to them and then a π -acceptor, 2,7-Dinitro-9-fluorenone (DNF). The adsorbents and supports were characterized using BET, FTIR, TGA techniques to ascertain their physicochemical properties. The extent of π -acceptor functionalization on supports was characterized using XRD, TGA and XPS techniques. In phase 2, the adsorbents were

examined for the desulfurization of a model oil feed with 500 ppm of sulfur. The commercial γ - Al_2O_3 -EDA-DNF adsorbent successfully removed 90.4 wt% of sulfur. The substitution of Ti in the framework of mesoporous Al_2O_3 did not promote its desulfurization efficiency. The higher desulfurization activity of the commercial γ - Al_2O_3 based adsorbent than that of others is attributed to its textural properties.

Among the three adsorbents screened a commercial γ - Al_2O_3 CTC adsorbent (Adsorbent C) showed the highest desulfurization in a short time period. Therefore, in Phase 3, the sulfur adsorption isotherms and kinetic were examined. The kinetics of sulfur adsorption followed a pseudo-second-order model with the CTC adsorbents. The regeneration of used adsorbent was studied with three different polar solvents such as chloroform, dichloromethane and carbon tetrachloride. Dichloromethane was found to be the most suitable solvent for extracting a major part of sulfur compounds contained in the pores of the spent adsorbent. Thermodynamic parameters such as E_a , ΔG , ΔH and ΔS provided a better insight into the adsorption.

ACKNOWLEDGEMENT

I want to take the opportunity to thank everyone that supported me through my MSc. Program. Firstly, I would like to express my gratitude to my supervisors, Dr. Dalai and Dr. John Adjaye for giving me a once in a lifetime opportunity to pursue my master's degree under their guidance and for all the shared knowledge. I am extremely thankful for having the opportunity to achieve another level of education under their supervision and constant support.

I thank my advisory Committee members, Drs. Amira Abdelrasoul and Lifeng Zhang for their input during my research and their availability when it was needed. I will also like to thank Drs. Misra Prachee, Philip Boahene and Sundaramurthy Vedachalam for their continuous support in the laboratory and through my program. I will to extend my gratitude to Heli Eunike, Richard Blondin, Dushmanthi Jayasinge and Rosa Do for their assistance for analytical instruments' use.

I would also like to thank fellow students in Catalysis and Chemical Reaction Engineering Laboratories (CCREL) for making a support community among our research group. I thank my friend and fellow student Dylan, with whom I have shared so many memories and personal experiences.

Lastly, on a personal note, I would like to thank my parents, Araceli de la Cruz Cruz and Jorge Alberto Botana Ponce and my brother Jorge Alberto Botana de la Cruz, for their constant support, love and encouragement through the distance. You are my everyday motivation. I also want to thank all my family back in Mexico who have always showed me their love and support. I thank Jacob, for giving me the words of encouragement when I needed them and your constant love and support to make hard days easier.

DEDICATION

This thesis is dedicated to my parents

Araceli de la Cruz Cruz and Jorge Alberto Botana Ponce

My accomplishments will always be dedicated to you

Table of Contents

PERMISSION TO USE	i
ABSTRACT	ii
ACKNOWLEDGEMENT	iv
DEDICATION	v
TABLE OF CONTENTS	vi
LIST OF TABLES	viii
LIST OF FIGURES	ix
NOMENCLATURE	xi
ABBREVIATIONS	xii
Chapter 1 : Introduction and Thesis Outline	1
1.1 Introduction	1
1.2 Knowledge gaps	6
1.3 Hypothesis	6
1.4 Research Objectives	6
1.5 Organization of the thesis	7
Chapter 2 : Literature review	8
2.1 Global energy consumption and oil reserves	8
2.2 Alternative non-catalytic methods	9
2.3 Materials used for nitrogen and sulfur impurities adsorption	10
2.4 Synthesis of mesoporous materials	16
2.4.1 Al ₂ O ₃ -based materials syntheses and adsorption performance with linker and π -acceptor	22
2.5 Adsorption kinetics and thermodynamics	23
2.6 Regeneration and reusability	24
Chapter 3 : Synthesis, characterization and batch adsorption experiments	25
3.1 Abstract	25
3.2 Introduction	26
3.3 Experimental	28
3.3.1 Materials	28
3.3.2 Synthesis of adsorbents	28

3.3.3	Characterization of supports and adsorbents	30
3.3.4	Procedure for adsorption experiments	31
3.4	Results and discussion	32
3.4.1	N ₂ -adsorption measurement	32
3.4.2	Fourier transform infrared analysis	35
3.4.3	Thermogravimetric analysis	37
3.4.4	X-ray diffraction	38
3.4.5	X-ray photoelectron spectroscopy	39
3.4.6	CHNS elemental analysis	40
3.4.7	Adsorption experiments using ultra-low sulfur diesel (ULSD) feedstock	42
3.4.8	Effects of adsorption time	44
3.4.9	Effects of feed concentration on adsorption capacity	45
3.5	Conclusions	46
Chapter 4	: Optimization, regeneration and kinetic studies	48
4.1	Experimental methods	48
4.1.1	Materials/ Chemicals	48
4.1.2	Preparation of adsorbents	48
4.2	Process parameter Optimization	49
4.2.1	Adsorption parameters optimization studies	50
4.3	Adsorption kinetics	52
4.3.1	Kinetic studies	53
4.4.1	Adsorption thermodynamic studies	57
4.5.1	Regeneration and reusability studies	60
Chapter 5	: Conclusions and recommendations	62
5.1	Conclusions	62
5.2	Recommendations	63
References		64
Appendix A:	Permission to reuse submitted paper Tables and Figures	73
Appendix B:	Additional table of results from process parameter optimization studies and activation energy (E_a) plots for adsorbents A, B and C	74

LIST OF TABLES

Table 1.1 Adsorbents used and applications	3
Table 2.1 Feed characteristics of Bitumen derived gas oil, adapted from Yang et al., 2020.	8
Table 2.2 Different methods use for desulfurization and denitrogenation of petroleum feedstock	10
Table 2.3 Various materials used as adsorbents for the removal of nitrogen and sulfur of petroleum feed.	11
Table 2.4 Textural properties of the materials. Adapted from Baia et al., 2017.	12
Table 2.5 Adsorption capacities of alumina and clays towards nitrogen and sulfur compounds based on Model 1: First Order	13
Table 2.6 Textural properties of the adsorbents. Adapted from Silveira et al.,2015.	17
Table 2.7 Characteristics of the mesoporous alumina samples. Adapted from Alphonse et al., 2013.	18
Table 2.8 Textural properties from various Al ₂ O ₃ supported materials. Adapted from Badoga et al. 2014.	20
Table 3.1 Textural properties of the synthesized support, support-linker, and support-linker- π -acceptor.	35
Table 3.2 CHNS elemental composition of supports, support + linker and final adsorbent	41
Table 4.1 Optimization parameters and their corresponding range used for the Central Composite Design.	49
Table 4.2 Design of experiments for adsorption of sulfur and nitrogen species	50
Table 4.3 Linear equations for adsorbents A, B and C from Composite Design Expert based on the proposed set of experiments.	52
Table 4.4 Kinetic parameters for pseudo-first and pseudo-second-order model	55
Table 4.5 Activation energy calculated values for adsorbents A, B and C.	57
Table 4.6 Free activation energy values for adsorbents A, B and C.	58
Table 4.7 Enthalpy and entropy values for adsorbents A, B and C.	58

LIST OF FIGURES

Figure 3.1 Schematic of synthesized adsorbent for desulfurization	28
Figure 3.2 N ₂ -adsorption/desorption isotherms for Al ₂ O ₃ ,Ti-substituted meso-alumina and commercial gamma-alumina their corresponding DNF-immobilized supports (Al ₂ O ₃ -EDA-DNF and Ti-substituted meso-alumina -EDA-DNF).	33
Figure 3.3 Pore size distribution of the DNF immobilized support Al ₂ O ₃ -EDA-DNF, Ti-substituted Al ₂ O ₃ -EDA-DNF and commercial alumina-EDA-DNF.	34
Figure 3.4 FT-IR spectra of the alumina-based supports	36
Figure 3.5 FT-IR spectra of adsorbents, ethylenediamine and dinitrofluorenone.	36
Figure 3.6 Thermal degradation profiles of adsorbents and dinitrofluorenone	37
Figure 3.7 X-ray diffraction for alumina supports. (A) Mesoporous alumina support, (B) Ti-substituted meso-Al ₂ O ₃ and (C) commercial γ -alumina supports.	38
Figure 3.8 X-ray diffraction for alumina based adsorbents and π -acceptor compound.	39
Figure 3.9 X-ray photoelectron spectroscopy of Adsorbent B.	40
Figure 3.10 Comparison of sulfur removal efficiency of Adsorbents A, B and C. Adsorption parameters: Feed = 500 ppm of sulfur in ULSD, T = 22 °C, stirring = 400 rpm, atmospheric pressure, adsorbent to feed ratio = 1:5, time = 24 h).	42
Figure 3.11 Sulfur and nitrogen removal efficiency of adsorbents A, B and C with ULSD non-spiked feed. Adsorption parameters: T = 22 °C, stirring = 400 rpm, atmospheric pressure, adsorbent to feed ratio = 1:5, time = 24 h.	43
Figure 3.12 Effects of adsorption time on sulfur removal (Adsorption parameters: T = 22 °C, stirring = 400 rpm, atmospheric pressure, adsorbent to feed ratio = 1:5, time = 0 to 96 h).	44
Figure 3.13 Effects of initial concentration of sulfur model feed on adsorption capacity of adsorbents A, B and C (Adsorption parameters: T = 22 °C, stirring = 400 rpm, atmospheric pressure, adsorbent to feed ratio = 1:5, time = 24 h).	46
Figure 4.1 The three-dimensional response surfaces: effects of temperature and adsorbent loading on desulfurization activity of adsorbents A, B and C.	51

Figure 4.2 Pseudo first-order adsorption kinetics of adsorbents A, B and C. Temperature =22°C, feed to adsorbent ratio=5. The solid line is the results for the kinetic model; the dash line is pseudo first-order-model simulation	54
Figure 4.3. Pseudo first-order adsorption kinetics of adsorbents A, B and C. Temperature =22°C, feed to adsorbent ratio=5. The solid line is the results for the kinetic model; the dash line is pseudo first-order-model simulation.	55
Figure 4.4 Schematic of Soxhlet extraction set-up used for regeneration.	59
Figure 4.5 Sulfur removal from Adsorbent A after 8 h of regeneration with chloroform, carbon tetrachloride and dichloromethane	60
Figure 4.6 Reusability results for adsorbent A using dichloromethane as solvent	61
Figure A.1 Permission to use published article, tables and figures for Chapter 3	73
Figure B.1 Optimization result table for adsorbent A	74
Figure B.2 Optimization result table for adsorbent B	75
Figure B.3 Optimization result table for adsorbent C	76
Figure B.4 Activation energy (E_a) plot $\ln K_D$ vs $1/T$ (K^{-1}) for adsorbent A	76
Figure B.5 Activation energy (E_a) plot $\ln K_D$ vs $1/T$ (K^{-1}) for adsorbent B	77
Figure B.6 Activation energy (E_a) plot $\ln K_D$ vs $1/T$ (K^{-1}) for adsorbent C	77
Figure B.7 Free activation energy, enthalpy and entropy plots for adsorbents A, B and C	78

NOMENCLATURE

<i>F-127</i>	tri-block copolymer
<i>FT-IR</i>	Fourier-transform infrared spectroscopy
<i>HPLC</i>	high performance liquid chromatography
<i>keV</i>	kiloelectronvolt
<i>Kv</i>	kilovolt
<i>nm</i>	nanometers
<i>P-123</i>	tri-block copolymer
<i>SBA-15</i>	Mesoporous alumina
<i>SDAs</i>	structure directing agents
<i>ZSM-5</i>	aluminosilicate zeolite
ΔG^0	free activation energy
ΔS^0	entropy
ΔH^0	enthalpy

ABBREVIATIONS

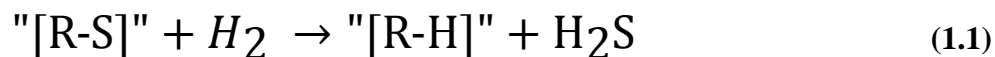
<i>BET</i>	Brunauer-Emmett-Teller
<i>BJH</i>	Barrett-Joyner-Halenda
<i>BN</i>	basic nitrogen
<i>CTC</i>	charge transfer complex
<i>DCM</i>	dichloromethane
<i>DNF</i>	2,7 – dinitro – fluorenone
<i>EDA</i>	ethylenediamine
<i>HDN</i>	hydrodenitrogenation
<i>HDS</i>	hydrodesulfurization
<i>HGO</i>	heavy gas oil
<i>LGO</i>	light gas oil
<i>MDF</i>	model diesel fuel
<i>NBN</i>	non-basic nitrogen
<i>PGMA</i>	Poly (glycidyl methacrylate)
<i>PPD</i>	Process parameter design
<i>ppm</i>	parts per million
<i>ppmw</i>	parts per million
<i>PTFE</i>	Polytetrafluoroethylene
<i>rpm</i>	revolutions per minute
<i>TGA</i>	Thermogravimetric analysis
<i>ULSD</i>	ultra low sulfur diesel
<i>XPS</i>	X-ray photoelectron spectroscopy
<i>XRD</i>	X-ray diffraction

Chapter 1 : Introduction and Thesis Outline

1.1 Introduction

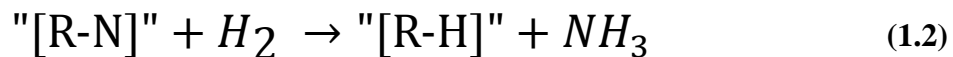
As the population of the world increases and the impact of industry, transportation, greenhouse emissions and other pollutants grow, emissions from combustion of fuels are being regulated (Yoosuk et al., 2020). Due to this situation, more effort is being put towards delivering and meeting the energy demand while meeting environmental regulations. Current oil reserves in the world place Canada as number 7 with most of their oil reserves contained in the Athabasca, Alberta region (Speight, 2020). Naturally, this oil deposits are in the form of oil sands, a combination of sand, clay, water and bitumen. That bitumen is then refined and transformed into a variety of fuels; many different processes are involved in order to achieve the quality of fuels required (McCabe, 2020). Among the processes that are involved in the refining process, hydrotreatment is an important one since it is where impurities like sulfur, nitrogen, oxygen and aromatics are removed. The removal of these impurities happens in the presence of excess hydrogen, high temperature and pressure (260-427°C and up to 13 MPa) using a catalyst typically CoMo/Al₂O₃ or NiMo/Al₂O₃. Sulfur removal (Hydrodesulfurization (HDS)), Nitrogen removal (Hydrodenitrogenation (HDN)), saturation of aromatics (Hydrodearomatization (HAD HDA)) and metals removal (Hydrodemetallation (HDM)) are some of the reactions that take place during a typical hydrotreating process (Satterfield 1996).

HDS is the catalytic process where sulfur is removed from petroleum products; organic sulfur species are converted to sulfur dioxide (H₂S) after reacting with the excess hydrogen (H₂) present in the system (Bu et al., 2011). The reaction for HDS is shown below, where R represents the hydrocarbon units contained on the hydrotreatment feed.



The concentration and nature of the sulfur organic compounds changes over the boiling range. Thiols, sulfides and disulfides, thiophenes, benzothiophenes, dibenzothiophenes are the major sulfur compounds present in gas oil (Song, 2003). On the other hand, nitrogen in the gas oil

feedstock is present predominantly as heterocyclic aromatic compounds. Non-basic (five membered ring) and basic (six-membered ring) are the two types of aromatic nitrogen compounds present predominantly in the Athabasca bitumen (Fu et al., 2006). The reaction for HDN is shown below:



Where R represents the hydrocarbon chains contained on the hydrotreatment feed. Some of the nitrogen compounds present in the bitumen-derived gas oil are indole, carbazoles, indoline, acriline and aniline (Fu et al., 2006). As it was mentioned before, the government has set the maximum content of sulfur in fuels of 10 parts per million (ppm); concentration that will be achieved after hydrotreating the feed (Yitzhaki et al., 1995). In order to explain the importance of nitrogen removal an insight to the catalyst used on the hydrotreatment process is needed. A catalyst is a substance that in a small amount causes a large change as it increases the rate of reaction toward equilibrium without being appreciably consumed in the process. The rate of reaction depends on pressure, temperature, concentration of reactants and products, and other variables (Satterfield, 1996).

However, the catalyst may undergo through some major changes in its structure and composition as a result of its participation in the reaction. Catalysts are usually synthesized using a support with textural properties such as high surface area, pore size and pore volume (Bu et al., 2011). They can also use different metals to act as promoter and enhance the activity during the reaction; however, it may lose its activity by a variety of different reasons. Poisoning is the presence of elements such as phosphorous (P), arsenic (As), silica (Si), sodium (Na), vanadium (V), tungsten (W) and/or iron (Fe). Another phenomenon that can occur is fouling, reduction of the active area by sintering or migration and the loss of active species (Satterfield, 1996).

There are some challenges on processing high N and S compound concentration on gas oil, where crude oils with more than 0.5%wt sulfur need to be treated extensively during petroleum refining. The distillation process segregates sulfur species in higher concentrations into the higher-boiling fractions and distillation residues. Removing sulfur from petroleum products is one of the most

important processes in a refinery to produce fuels compliant with environmental regulations. Basic nitrogen compounds are particularly undesirable in crude oil fractions as they deactivate the acidic sites on catalyst. Some nitrogen compounds are also corrosive. An alternative to prevent catalyst deactivation are non-catalytic methods to remove the sulfur and nitrogen present in gas oil (Song et al., 2003). Some of the materials that have been used as adsorbent and its application are shown in Table 1.1.

Table 1.1 Adsorbents used and applications

Adsorbent	Applications
Silica Gel	Drying of gases, refrigerants, organic solvents, transformer oils Desiccant in packings and double glazing (Ziolo et al., 1995; Ullah et al., 2013)
Activated Alumina	Removal of HCl from hydrogen (Fleming et al.,1988; Ullah et al., 2013) Removal of fluorine in alkylation process (Heilig 1994; Weber et al., 1991)
Carbons	Removal of SOX and NOX (Mochida et al., 2000; Sumathi et al., 2009, 2010) Purification of helium (Chang and Wu, 2009; Favvas et al., 2015) Clean-up of nuclear off-gases (Munakata et al., 1999)
Zeolites	Oxygen from air (Li et al., 1998) Drying of gasses (Auerbach et al., 2003; Li et al., 2008)
Functionalized Polymers and resins	Water purification (Akelah and Sherrington, 1981; Puoci, et al., 2008) Recovery and purification of steroids, amino acids (Hentze and Antonietti, 2002) Separation of fatty acids from water and toluene (Kale et al., 2015)
Clay	Treatment of edible oils (Bokade and Yadav, 2009; Richardson, 1978) Removal of organic pigments (Espantaleón et al., 2003; Zhou et al., 2014) Refining of mineral oils (Vural, 2020; Wu et al., 2017)

The focus of this study will be adsorption, defined as the adhesion of molecules (adsorbates) in an extreme thin layer to the surfaces of solid bodies (adsorbents) with which they are in contact (Baia et al., 2017). It has also been widely used due to less operational cost, specific target and high efficiency removing undesired compounds. The adsorption process is generally classified as physisorption (characteristic of weak van der Waals forces and hydrogen bonding) or chemisorption (characteristic of covalent bonding). Physical adsorption resembles

the condensation of gases to liquids and depends on the physical, or van der Waals, force of attraction between the solid adsorbent and the adsorbate molecules. Chemical adsorption is adsorption in which the forces involved are valence forces of the same kind as those operating in the formation of chemical compounds (Nathan and Scobell, 2012).

The technique here proposed is charge-transfer complex (CTC) which occurs between a π -acceptor compound functionalized with a support and π -donor compounds that can be found on the gas oil (Macaud et al., 2004). The functionalized particles consist of support, linker and π -acceptor. The support would bring the mesoporous surface to the linker to be attached to, using a linker could have an effect on the selective adsorption of NBN compounds and lastly, the π -acceptor would be the electron poor donor compounds contributing to the selective adsorption of π -donor compounds present in the oil (Rizwan et al., 2013).

The support is an inner substance that helps spreading out an expensive catalyst onto its surface such as Pt, it can also help stabilize the activity towards the adsorption process. It may be used in pellet or powder form (Maity et al., 2003). Also, in a similar process are the catalysts, which are promoted with active metals. The presence of an active metal onto the support, might improve the textural properties of the support, leading to an increase of activity towards the adsorption process (Wachs, 2005).

Activated alumina is a mesoporous material that has high surface area: 100 to 600 m²/g, its pore size distribution is mesoporous in nature, it is a low cost material when compared to titania (Ti) and it has shown thermal stability (Badoga et al., 2017). On the other hand, Ti helps in NO_x reduction emissions in hydrotreating, is more acidic than alumina, which enhances the hydrogen sulfide (H₂S) formations (affinity towards sulfur compounds). Metal oxide supports contain alkali, alkaline and noble metals, also have been widely employed as solid catalysts; either as active phases or supports (Wachs, 2005). Both are used for their acid-base and redox properties and constitute the largest family of catalysts in heterogeneous catalysis.

The function of the linker is to immobilize the π -acceptor onto the mesoporous supports (Misra, 2017). Amines, hydrazines and hydroxylamine have been used as linkers and have been reported in the literature. The linker allows the immobilization to take place on the support without substituting an electron-withdrawing group (on the support) with an electron-donor compound, compounds present in gas oil (Sévignon et al. 2005).

Previous reported studies have calculated theoretically (Milenkovic et al. 2004) and demonstrated (Meille et al. 1998; Milenkovic et al. 1999; Sévignon et al. 2005) that symmetrical π -acceptor compounds based on polynitrosubstituted 9-fluorenones have showed selectivity towards sulfur compounds such as dibenzothiophenes, benzothiophenes and aromatic compounds. As mentioned before, the sulfur compounds present in the oil contain electron rich aromatic systems; this characteristic might enhance the affinity of the adsorbate towards the adsorbent and create an attraction to facilitate the adsorption of the sulfur compounds. Based on the available literature, there are many adsorbents that have been tested based on the CTC complex formation, but to the best of our knowledge, the meso- porous alumina-based supports with the CTC complex formation has not been reported for desulfurization. Mesoporous alumina seems to be good support as it has a high surface area, pore diameter and pore volume for anchoring the π -acceptor. In this study, 2,7-dinitro-9- fluorenone (DNF) functionalized pristine mesoporous Al_2O_3 , Ti-substituted mesoporous Al_2O_3 and commercial $\gamma\text{-Al}_2\text{O}_3$ were prepared, characterized and evaluated in the aim to treat a model feed for desulfurization. Afterwards, kinetic studies and thermodynamic parameters were calculated to bring an insight into the adsorption taking place. Lastly, regeneration and reusability of adsorbent A was tested using solvent removal method.

1.2 Knowledge gaps

1. The performance of π -acceptor functionalized particles for the adsorption of nitrogen and sulfur compounds is limited in the literature. The synthesis of functionalized mesoporous Al_2O_3 and Ti-incorporated Al_2O_3 supported adsorbents via π -acceptor and their application for sulfur and nitrogen removal is limited in the literature.
2. Regenerability, optimization and kinetic studies of mesoporous Al_2O_3 based adsorbents are scarce in the literature.

1.3 Hypothesis

1. Post-treatment of processed oil using non-catalytic methods may successfully remove nitrogen and sulfur compounds, using mesoporous Al_2O_3 support and π -acceptor may increase selectivity. Incorporating TiO_2 onto mesoporous Al_2O_3 support would increase the adsorption capacity.
2. Optimization, kinetics and regeneration studies will determine the suitability of these adsorbents for liquid feedstocks containing sulfur and nitrogen impurities

1.4 Research Objectives

To study the performance of π -acceptor immobilized alumina-based materials as adsorbent for the removal of sulfur and nitrogen impurities from liquid fuels. The goal is to improve the efficiency of hydrotreating in terms of less catalyst loading, lower reaction temperature, and severity of hydrotreating conditions (T, P, space velocity, hydrogen/oil ratio...)

Sub-objectives:

- To investigate the effects of the proposed synthesis method and its impact on the adsorbent properties for sulfur and nitrogen compounds present in liquid fuels.
- To study process optimizations, kinetics and long-term stability of potential adsorbent identified in above sub-objective.

1.5 Organization of the thesis

This thesis contains 5 chapters covering detailed synthesis, characterization, experimental testing and conclusions from all the phases of the research. Chapter 2 focuses on the literature review starting with the Global energy consumption and oil reserves, followed by the alternative non-catalytic methods, materials used for nitrogen and sulfur impurities adsorption. Synthesis of mesoporous materials and Al₂O₃-based materials and their adsorption performance with linker and π -acceptor. Lastly, adsorption kinetics, thermodynamics and regeneration were further studied.

Chapter 3 presents the synthesis of alumina-based adsorbents followed by the characterization and batch adsorption experiments performed using a diesel model feed. Chapter 4 describes the process optimization studies, regeneration experiments, kinetic study of the adsorption process and the thermodynamics of the process.

Chapter 5 summarizes the key findings from this work and provides recommendations for possible future work in this area.

Chapter 2 : Literature review

This chapter discusses the review of the literature related to this research. Non-catalytic methods have been discussed as an alternative due to its simplicity as compared to hydrotreatment. Among many different methods, adsorption seems to be the most widely studied. However, its success depends on finding an ideal adsorbent that can effectively remove nitrogen and sulfur species from liquid fuels.

2.1 Global energy consumption and oil reserves

The world depends on different energy resources to function. The demand for oil started to increase after World War II and correlated to the rapid growth of the world's economy.

The main energy sources used worldwide are oil (32 %), coal (26%), gas (23%), biomass (10%), electricity from hydro and nuclear (9%) and heat (<1%). The United States dominated the world production until other countries started their own production. Currently, 60 % of the world's oil production are from mostly six countries (Yang et al., 2020).

Canada's oil reserve is in 7th place with 4 % of the global oil reserve (Ha et al., 2018). These reserves are mostly contained in the oil sands in Cold Lake and Peace River regions of Northern Alberta. Alberta's oil sands contain around 166 billion barrels of oil (Yang et al., 2020), which by nature contain more minerals, metals and other polluting compounds. These oil reserves are known as oil sands due to their high concentration in sand, clay and water as compared to those present in crude oil. It contains up to 80-85 % of sand and clay, 4-6 % of water, and 10-12% of bitumen.

Table 2.1 Feed characteristics of Bitumen derived gas oil, adapted from Yang et al., 2020.

Parameter	Light Gas Oil (LGO)	Heavy Gas Oil (HGO)
Sulfur content (ppm)	29000	38000
Nitrogen content (ppm)	1700	4000

Three major stages are used for converting crude oil to fuels. The stages can be referred to as separation, conversion and treating, and involve processes such as distillation, cracking, reforming

and hydrotreating just to mention a few. The Canadian government has set the sulfur content in gasoline to be 10 ppm (Ha et al., 2018), therefore, special consideration has to be taken when designing processes for feed with high sulfur concentration to meet the environmental regulations. Hydrotreating is the process in which contaminants in the hydrocarbons are removed in the presence of excess hydrogen (H_2) using high temperature (350-400°C) and pressure (5-10 MPa). Table 2.1 shows the amount of sulfur and nitrogen compounds typically contained in LGO and HGO feeds; sulfur content varies from 0.3-5 wt.% and nitrogen from 0.1-0.8 wt. In the presence of a catalyst, sulfur and nitrogen compounds react with H_2 to be removed as hydrogen sulfide (H_2S) and ammonia (NH_3), respectively. The vehicular emission from fuel combustion can contribute greatly when the sulfur species in fuels is converted to sulfur oxides after combustion; this can ultimately lead to acid rain. Nitrogen compounds present in oil, on the other hand, also contribute to the nitrogen oxide emissions (NO_x) and causes other problems in refineries such as catalyst deactivation, coke formation, and they can be found to be poison for acid functionality in catalysts (Satterfield, 1996).

2.2 Alternative non-catalytic methods

Extensive research (Bu et al., 2011; Li et al., 2015; Liu et al., 2020; Misra et al., 2018; Qi et al., 2020; Zolotareva et al., 2019) has been done over the last years in an effort to find different non-catalytic methods other than hydrotreating. As it was mentioned before, high H_2 consumption, high temperature and pressure used in hydrotreating process can be costly; thus impacting on the cost of fuels (Li et al., 2009). Among different technologies that can be used for reducing sulfur and nitrogen concentrations in refineries feedstock, the non-catalytic methods are gaining significant attention. There are many advantages when using non-catalytic methods, low temperatures and pressures are used as compared to the conventional hydrotreating methods. (Zolotareva et al., 2019) has recently reported Ionic liquids (IL) as an effective method due to its low temperature and pressure; they can also be more selective than some solvents such as acetone, pyrimidinone, polyalkylene glycol, imidazolidinone, dimethyl sulfoxide and polyethylene glycol that are found to have high volatility, flammability and toxicity (Toor et al., 2013). Bedda et al., 2019, reported the DS of light cycle oil using extraction solvents such as acetonitrile, N-methylpyrrolidone, and N,N-dimethylformamide. The performance of the solvent was evaluated and it was concluded that a solvent/feed ratio from 1.0 to 2.5 has a higher sulfur removal as the

ratio increased. Acetronitile removed 53.3 ppmw%, N-methylpyrrolidone 74.8 ppmw% and N,N-dimethylformamide removed 73.3% from the total sulfur content of initially 2157 ppmw. Table 2.2 shows different methods used with advantages and disadvantages for comparison purposes.

Table 2.2 Different methods use for desulfurization and denitrogenation of petroleum feedstock

Method	Advantages	Disadvantages
Adsorption (Mckav and Ireland, 1985; Misra et al., 2015a; Sampanthar et al., 2006)	<ul style="list-style-type: none"> ✓ Require less material. ✓ Process can be carried at room temperatura. ✓ Control of the properties and surfaces. ✓ Solid applications. ✓ Non-catalytic method 	<ul style="list-style-type: none"> ✓ Large amount of adsorbents needed for industrial applications. ✓ Regenerability needs to be studied.
Absorption (Li et al., 2009; Wachs, 2005)	<ul style="list-style-type: none"> ✓ Liquid and gas applications. ✓ Not necessarily require elevated pressure. ✓ Conversion of a hazardous chemical to a safe compound. 	<ul style="list-style-type: none"> ✓ Extensive areas of liquid surfaces in contact with gas phases. ✓ Not enough information for further comparison.
Ultrasound assisted oxidative desulfurization (Liu et al., 2020; Zolotareva et al., 2019)	<ul style="list-style-type: none"> ✓ Efficient desulfurization method ✓ Complements the HDS process. 	<ul style="list-style-type: none"> ✓ Only focus on sulfur compounds. ✓ Widely study in the industry

Based on the literature review, adsorption was found to be a more suitable method for the removal of sulfur and nitrogen compounds from liquid fuels. Several adsorbents have been reported in the literature, most of them are described in the following.

2.3 Materials used for nitrogen and sulfur impurities adsorption

The aim of this section is to provide an extensive literature review on what has been done on the adsorption of nitrogen and sulfur compounds from liquid fuels. Many different materials have been used as adsorbents, such as zeolites, activated carbon, silica, alumina, ion exchange resins, titania nanotubes just to mentioned a few. Based on the characteristics of the materials, alumina was

found as the more suitable adsorbent support, having a relatively high surface area from 100 to 600 m²/g, being mesoporous in nature, thermally stable and having a relatively low cost compared to titania, which has shown to have high efficiency for nitrogen and sulfur removal (Badoga et al., 2017; Maity et al., 2003).

Some of the different materials used as adsorbents are mentioned in Table 2.3. Many different adsorbents and feed materials have been tested, however, there is limited information on the adsorption of sulfur and nitrogen compounds from model and real oil fractions using alumina-based adsorbents.

Table 2.3 Various materials used as adsorbents for the removal of nitrogen and sulfur of petroleum feed.

Method	Feedstock	Adsorption capacity (mg S,N /g adsorbent)	Temperature (°C)	Highlights	Reference
Activated carbon	Real diesel- 398 ppmw (S) Model diesel – 400 ppmw (S)	77mg/g, 88 mg/g	25, 30, 75	Polycyclic aromatics and sulfur removal	(Bu et al., 2011)
Ion exchange resins	Model feed (benzene and thiophene)	Not stated. Reduction of 97% of sulfur	120	Effective for basic nitrogen species removal	(Yang et al., 2004)
Copper zeolites	Gasoline- 335 ppmw (S) Diesel- 430 ppmw (S)	8.89 and 13.12 mg S/g adsorbent	23	Effective adsorption for sulfur compounds	(Hernández-Maldonado and Yang, 2003)
Titania based nanotubes	Model diesel blends	14.6 mg S/ g adsorbent	20	Adsorption of nitrogen and sulfur compounds	(Rendon-Rivera et al., 2016)

Baia et al. 2017, studied the adsorption of sulfur and nitrogen compounds contained in a straight run diesel feedstock using three different types of clay, designated as A, B and C. Their study

included kinetic and isotherm experiments. A commercial alumina was used for comparison purposes due to its properties of adsorbing many different substances. The textural properties of the alumina and clays are shown in Table 2.4. Straight run diesel was used as a feed with a composition of 3906 mg kg⁻¹ of sulfur and 522 mg kg⁻¹ of nitrogen. Kinetic tests were performed in a Dubnoff reciprocal shaking bath, using a shaking frequency of 150 rpm at 40°C. Seven flasks containing 10 mL of diesel and 2 g of adsorbent were used and samples at 10, 30, 60, 120, 180, 240 and 300 minutes were analyzed.

Table 2.4 Textural properties of the materials. Adapted from Baia et al., 2017.

Sample	Pore volume (cm ³ g ⁻¹)			
	Specific area (m ² g ⁻¹)	Mesoporous	Microporous	Pore diameter (nm)
Alumina	357	0.34	0.02	5
Clay A	95	0.45	0.01	22
Clay B	198	0.21	0.01	6
Clay C	273	0.30	0.02	9

During the adsorption experiments, it was observed that the rate of adsorption was high during the first 10 minutes, thereafter, it decreased. This was attributed to the large number of pores that are available at the beginning of the process as compared to those available after a determined period of time. By measuring the solution concentration at the equilibrium point, the authors noted that the adsorption process in the liquid phase involved a competition between the solvent and the solute.

As we can see from Table 2.5, Clay B showed better performance than the other materials in both, nitrogen and sulfur adsorption capacities. This can be attributed to the presence of Brønsted acids and higher specific surface area than the other materials. In addition, Clay B and Clay C showed different adsorption steps for both sulfur and nitrogen compounds, this particular characteristic can be noticed on their respective adsorption-desorption isotherms. In another study carried by Sano et al. (Sano et al., 2004), where the surface area of various activated carbons was the selection criteria for its expected performance, straight run gas oil (SRGO) was fed into a tube containing activated carbons and activated fibers. Among the materials that were used for these experiments,

MAXSORB-II showed the largest adsorption capacity for nitrogen species in gas oil. Even though MAXSORB-II and MAXSORB-III both showed equally large surface areas ($> 2000 \text{ m}^2/\text{g}$) which is considered a key characteristic for adsorption capacity, MAXSORB-II had a better performance (Sano et al., 2004).

Table 2.5 Adsorption capacities of alumina and clays towards nitrogen and sulfur compounds based on Model 1: First Order

Adsorbent	qe, cal (mol·kg-1) nitrogen	qe, cal (mol·kg-1) sulfur
Alumina	0.058	0.059
Clay A	0.074	0.018
Clay B	0.125	0.174
Clay C	0.116	0.126

Other materials, such as zeolites have been used as adsorbents as well with a π -complexation structure (Yang et al., 2001). Yang and co-workers reported the adsorption process took place in a fixed-bed reactor operated at ambient temperature and pressure. This chemical complexation has been barely utilized. Even though there are some studies in the literature that mention this model, few of them have achieved remarkable removal of nitrogen and sulfur compounds. Added to the π -complexation characteristic of this material, during the adsorption process, a thin layer of AC was used and showed that it can significantly increase the sulfur adsorption capacities of the π -complexation sorbent. This copper-based zeolite is highly hydrophilic but no other properties of this particular zeolite are mentioned. However, the fixed-bed adsorption results showed that the sulfur contents of those commercial fuels used (gasoline and diesel) were drastically decreased.

In a different study by Santos et al. (Santos et al., 2012), diesel was used as feed for an adsorption pre-treatment with the aim to remove nitrogen and sulfur compounds. Commercial silica-alumina samples were calcined and then impregnated with various mixed metal oxides such as cerium, nickel and molybdenum. The commercial name of the silica-alumina material is SIRAL 40 and is composed by 60:40 $\text{Al}_2\text{O}_3/\text{SiO}_2$ mass ratio. First, this material was calcined under atmospheric pressure for 4 h at 823 K. Then, aqueous solutions containing the metal oxides were prepared for wet impregnation of the parent material with $\text{Ni}(\text{NO}_3)_3 \cdot 6\text{H}_2\text{O}$, $(\text{NH}_4)_6\text{Mo}_7\text{O}_{24} \cdot 4\text{H}_2\text{O}$ or $\text{Ce}(\text{NO}_3)_3 \cdot 6\text{H}_2\text{O}$. The concentration was aimed to be 0.17 mol of metal per 100 g of adsorbent, this

wet impregnation was carried out in a rotary evaporator at 353 K for 5 h. Finally, the material was dried and calcined once more. For the adsorption experiments, 10 mL of the commercial diesel containing 229 mg of total sulfur and 196 mg of total nitrogen per kg of diesel were mixed with the adsorbent in different weights. Using 0.50 g, 0.75 g, 1.00 g, 1.50 g, 2.00 g and 2.50 g at 313 K under stirring, the temperature was raised after 45 minutes to 343 K and kept constant for 45 minutes and then it was cool down. After this pre-treatment, the adsorption experiments were carried out for 7 h.

The increase on the adsorption capacity per area of the materials can be attributed to the incorporation of metal oxides. Molybdenum species showed the best performance, however a reduction in the specific surface area was observed. An increase on the adsorption capacity was not observed on a mass basis; therefore, it can be assume that incorporating molybdenum is promising as long as there is a control on the loss of the surface area of the material.

Another type of material that has been studied for pre-treating oil feed are titania nanotubes. Rendon-Rivera et al., 2016, used TiO₂ nanoparticles and TiO₂ nanotubes as adsorbents to study their selective adsorption properties on liquid phase with sulfur and nitrogen organic compounds. Using dibenzothiophenes (DBT), 4, 6-dimethyl DBT (4, 6-DMDBT), pyrrole and quinoline which are compounds that represent some of those ones contained in diesel fuels. Model diesel blends and these compounds were mixed to emulate a real diesel blend. Adsorption isotherms for the compounds were determined at ambient temperature and pressure and fitted into Langmuir or Tempkin models. To establish the influence of TiO₂ nanoparticles transformation into nanotubes, the commercial version of this material was used as the reference adsorbent. For the batch adsorption experiments, four different model diesel fuels (MDF) were prepared. The adsorption was carried out in a batch system at room temperature (20°C) at atmospheric pressure. TiO₂ was added in different quantities but keeping the model diesel fuels volume constant, then, the mixtures were shaken using a magnetic stirrer to reach the equilibrium phase (typically, 0.5 h). After that, some liquid was extracted, it was passed through PTFE syringe filters and it was stored in vials. The fixed bed adsorption experiments were carried out at ambient conditions as well, using titanate nanotubes or anatase as particles and only two of the MDF. A gas column was packed with 2 g of adsorbent of between 80-100 mesh and placed in a special furnace. The materials were heated to 300°C prior to adsorption experiments for 3 h in the presence of nitrogen as a pretreatment. After

this, the adsorbent was allowed to cool down to room temperature and then hexane was used to remove any entrapped gas.

In addition, another study from the same group were another type of zeolites, Cu-Y and Ag-Y, as selective sorbents for the desulfurization of liquid fuels (Li et al., 2009). Compared to Na-Y, which is one of the sorbents presented in the previous study Takahashi et al., 2002, Cu⁺-Y was prepared by ion exchange zeolites with Na-Y, followed by reduction, the same process described in their previous paper (Munakata et al., 1999). Molecular orbital computational technique was used to determine the details on the materials. The bonding energies of the materials were calculated based on the following equation:

$$E_{ads} = E_{adsorbate} + E_{adsorbent} - E_{adsorbent-adsorbate} \quad (2.1)$$

Where $E_{adsorbate}$ is the total energy of thiophene; $E_{adsorbent}$ is the total energy of the bare adsorbent and $E_{adsorbent-adsorbate}$ is the total energy of the adsorbate/adsorbent system. E is measured in kcal/mol. Isotherms of benzenes and thiophene on Ag-Y and Cu-Y were fitted by the Langmuir-Freundlich isotherms and then compared. These sorbents showed more adsorption capacity towards thiophene and benzene than Na-Y at lower pressures than 10^{-3} atm and nearly the same amounts at high partial pressures. Even though, the paper states that this is due to the π -complexation with Ag and Cu, further research was done to confirm these theoretical findings. In order to understand the strengths of this complexation between Ag and Cu. The neutron activation analyses of the sorbent samples showed that the Ag exchange was 100% but the Cu exchange was 23%. On a per-cation basis, the π -complexation with Cu was stronger than the one with Ag. Results showed that 0.92 thiophene molecule per Cu was obtained at 2×10^{-5} atm at 120°C, whereas only 0.42 thiophene molecule/Ag was obtained.

Hernández-Maldonado et al., 2003, studied the desulfurization of commercial liquid fuels by π -complexation with Cu(I)-Y Zeolite. The experimental section was developed in a fixed bed adsorber operated at ambient temperature and pressure, and the results yield to a concentration of below the limit of detection of the instrument used, Flame photometric detection (FPD). As mentioned in the previous papers by Takahashi et al., 2002, and Yang et al., 2001, molecular orbital

calculations have shown that the π -complexation bonds between Ag or Cu and thiophene are stronger than those ones with benzene, this sorbents are suitable for a selective desulfurization of transport fuels. The procedure was the same as previous sorbents, initially the adsorbents were loaded inside the adsorber and heated in presence of helium, and then a sulfur freed hydrocarbon feed was passes through the sorbent at a rate of 0.5 cm³/min. From this paper there is only so little that can be discussed. Most of the key findings have already been mentioned in the two previous papers; however, they also conducted a study with a guard bed reactor. When used, Cu(I)-Y showed higher adsorption capacities at both, breakthrough and saturation points.

Velu et al. 2002, conducted a study using zeolites on the selective adsorption for removing sulfur (SARS). The aim of this study was to explore some selective-zeolite based materials for removing organic sulfur compounds from transportation fuels. In this research, commercial zeolites were ion-exchanged with transition metal ions using three to five time the excess amount of a concentration of 0.1 M metal nitrates at 80°C for 24 h. After this, the suspension was filtered, washed with deionized water and dried at 80°C overnight and then calcined at 450°C for 6 h in air atmosphere. After the preparation of these materials, adsorption took place in a batch reactor using JP-8 jet fuel as the feed. In a 100 mL round bottom flask, 1 g of ion-exchange zeolite and 6 g of feed were stirred at 80°C for 4-5 h. The treated jet fuel was then separated from the adsorbent and analyzed by a GC equipped with a pulsed flame photometric detector (PFPD) using dibenzothiophenes as a standard. The study showed that those zeolites ion-exchanged with Cerium and Palladium, CeY-Zeolite and PdY-Zeolite respectively, removed the highest amount of sulfur, 60 and 58 wt.%, respectively. The species that were found in the untreated jet fuel were 2, 3-DMBT and 2, 3, 7-TMBT. The sulfur concentration of the feed was around 736 ppm and higher selectivity for the adsorption of 2, 3-DMBT.

2.4 Synthesis of mesoporous materials

In a different study by Silveira et al. 2015, the influence of nickel, cerium, molybdenum and cobalt oxides impregnated on silica-alumina was evaluated for removing nitrogen and sulphur compounds from a hydrotreated fuel stream. Silica-alumina with 40 wt. % of SiO₂ was used as a support for the materials used in this study. This support was calcined at 550°C for 4 h before it was used to confirm the presence of metal oxides. The material was sieved to a particle size range of +100 to 325 mesh. The addition of nickel, cerium, molybdenum and cobalt was carried out by

wet impregnation method resulting on a 2.5 wt. % present in the silica-alumina support. Adsorption experiments were carried out in a 1:20 adsorbent to fuel ratio kept at 40°C for 45 minutes under stirring at 150 rpm. Then the temperature was raised up to 70°C and kept for 45 minutes, and then the temperature was reduced to room temperature and maintained for 15 hours. Specific surface area and pore volume are fundamental characteristics that help in the explanation of the adsorption performance. This study concluded that the addition of metal oxides can decrease the surface area up to 25%.

As shown in Table 2.6, an approximate of 25% of the support area was lost after the wet impregnation of metal oxides; however, there was not a significant reduction in the mesoporous volume. The adsorption performance of these materials was measured by mmol of sulfur or nitrogen removed per adsorbent area, where molybdenum was better than the other metal oxides. In this particular case, a higher percentage of nitrogen was removed than that of sulfur. Several alumina synthesis methods are available in the literature (Alphonse and Faure, 2013a, 2013b; Badoga et al., 2015; Khodabandeh and Davis, 2014; Niesz et al., 2005; Yuan et al., 2008). The general synthesis is based on a sol-gel process associated with a non-ionic block copolymer as templates using ethanol as a solvent (Yuan et al., 2008). These mesoporous aluminas have large surface areas (around 400 m²/g), pore volumes (around 0.70 cm³/g) and narrow pore size distributions. Compared to silica, alumina is more used in the petroleum sector as catalysts supports.

Table 2.6 Textural properties of the adsorbents. Adapted from Silveira et al.,2015.

Adsorbent	Specific surface area (m²/g)	Mesoporous volume (cm³/g)
Silica-alumina	451	0.84
Silica-alumina Mo	329	0.79
Silica-alumina Ce	328	0.80
Silica-alumina Ni	352	0.80
Silica-alumina Co	341	0.80

Non-siliceous materials used surfactants as structure-directing agents (SDAs) or by using the nano-casting method. According in previous reports (Alphonse and Faure, 2013a; Niesz et al., 2005), the hydrolysis behavior of alumina is very complicated and it is significantly affected by acid, water, temperature, humidity and other factors giving arise to different conditions for ordered

mesoporous aluminas. Among the different Al precursors, the most commonly used is the aluminum isopropoxide. Different acids such as HNO₃ and HCl are also added as the pH adjustors for the hydrolysis of the precursors. The use of a polymer as a surfactant combined with an acid has shown that large surface area alumina supports can be developed. Surfactants such as P-123 and F-127 were tested using different acid molar ratios. Narrow pore size distributions are obtained whereas after calcination they tend to decrease to some extent. These supports have shown high thermal stability up to 1000 °C. These three characteristics combined, result in enhancing the potential of these mesoporous alumina and their applications. Also, Niesz et al., 2005, reported a different synthesis method, that applies the same concept as Yuan et al. 2008. This material has a similar arrangement of that of SBA-15, known as one of the groups of ordered mesoporous silica materials. During this synthesis, two solutions were prepared, one containing the surfactant (P-123) in a solvent (ethanol), and the second one containing the alumina precursor (aluminum tri-tert-butoxide) and the acid (HCl). This mixture was left for aging at 75°C for 4.5 days, followed by vacuum drying at 70°C for 12 h prior to calcination at 600°C for 5 h. Hydrolysis steps is the key to achieving mesoporous morphology of the material. Also, using small amounts of water and acid showed that this hydrolysis process slows down, so the right amount of water and acid is crucial for this process to happen in a control rate and hence the formation of the mesoporous structure of the material. The BET surface areas resulting from this process are shown in Table 2.7.

Table 2.7 Characteristics of the mesoporous alumina samples. Adapted from Alphonse et al., 2013.

Sample names	BET surface area (m ² /g)	Pore volume (cm ³ /g)	Pore diameter (Å)
MP-Al ₂ O ₃ _2 ^a	206	0.44	39-150
MP-Al ₂ O ₃ _6 ^a	410	0.80	67
MP-Al ₂ O ₃ _12 ^a	349	0.62	39-90

^a the numbers in the samples stand for the [H₂O]:[Al₂O₃] ratios.

Considering that surface characteristics of the supporting material are key for the adsorption performance, many different researchers have tried to develop a synthesis method that results in having large surface area, large pore volume and tunable pore size distribution. For instance,

Alphonse et al., 2013, synthesized alumina-based materials with the above mentioned characteristics by adding triblock copolymers. In the procedure, 185 mL of hot water (85°C) was added fast to 25.3 g of aluminum-tri-sec-butoxide, under vigorous stirring. After the aluminum was dissolved into the water, 0.474 mL of nitric acid (HNO₃, 68%) was added and kept for stirring at 85°C for 24 h. As a last synthesis step, an additive was incorporated to the mixture and kept for stirring at room temperature during 24 h and the material was calcined at 500°C for 24 h. Since this particular study incorporated different additives and nitrates, there was a wide range of surface areas and pore volumes varying from 354-501 m²/g and 1.53-2.63 cm³/g. Also, Gonz and Sastre 2001 obtained samples of mesoporous aluminas with a similar synthesis procedure. In their study, non-ionic surfactants were used in different ratios and the alumina source was aluminum sec-butoxide. First, the surfactant was dissolved in sec-butanol and aluminum sec-butoxide. Then, a solution containing water, dipropylamine and half of the required sec-butanol were added. The resulting mixture was stirred for 3 h, and then cooled to room temperature. After this, the sol-gel solution was filtered, washed with ethanol and dried at 40°C for two days. The dried gel was heated at 95°C for 6 h. The surfactant was removed by Soxhlet extraction with ethanol for 15 h prior to drying of the solid at 40°C for 2 days followed by calcination. The obtained materials had large surface area varying from 229 to 534 m²/g, due to different calcination temperatures. It was observed that the lower the calcination temperature (550°C), the higher the surface area. This was not the case for the pore volume, which showed little relationship with calcination temperatures. The methodology for this research will aim to obtain a novel material to use for the adsorption of nitrogen and sulfur species from bitumen derived gas oil.

As alumina has been a widely studied (Biswas et al., 2011; Tursiloadi et al., 2004) support material for catalysts, so has other metal oxides incorporated in alumina (Badoga et al., 2017; Maity et al., 2006; Vosoughi et al., 2017). Studies (Badoga et al., 2014; Guevara et al., 2008; Herbert et al., 2005; Silva et al., 2015) have shown that addition of other metals such as TiO₂ have increased the activity around 3-5 times in hydrodesulfurization (HDS) process. So, in the aim to experiment with different approaches than the ones available in the literature, a mixed metal oxide will be used as support for the adsorbents in this study. There are certain characteristics that the support and the metal oxide need to have, such as, active metal dispersion, metal-support interaction and the textural properties shown by the support material (Badoga et al., 2014). Based on a study by Badoga et al., 2014, 10 wt. % TiO₂, Zr and Sn were supported on Al₂O₃ for a catalytic reaction.

Even though this study is not adsorption based, the synthesis of the materials was the focus of attention due to the material properties. In Table 2.8, the textural properties of some of the materials synthesized on this research are shown.

Table 2.8 Textural properties from various Al₂O₃ supported materials. Adapted from Badoga et al. 2014.

Material	BET surface area, m ² /g	Pore volume, cm ³ /g	Pore diameter, nm
γ-Al ₂ O ₃	275	0.80	7.6
Mesoporous Al ₂ O ₃	320	0.57	5.8
TiO ₂ - Al ₂ O ₃	480	0.86	5.2

Taking into consideration that surface characteristics of the supporting material are key for the adsorption performance, many different researchers have tried to develop a synthesizing method that results in having large surface area, large pore volume and tunable pore size distribution. One of many synthesis methods available in the literature is from Alphonse and Faure, 2013. In their work alumina based materials with the above mentioned characteristics were synthesized by adding triblock copolymers. In the procedure, 185 mL of hot water (85°C) were added fast to 25.3 g of aluminum-tri-sec-butoxide, under vigorous stirring. After the aluminum source was dissolved into the water, 0.474 mL of nitric acid (HNO₃, 68%) were added and kept for stirring at 85°C for 24 h. As a last synthesis step, an additive was incorporated to the mixture and the resulting mixture was stirred at room temperature for 24 h; the material was then calcined at 500°C for 24 h. Since this particular study incorporated different additives and nitrates, there was a wide range of surface areas and pore volumes, ranging from 354-501 m²/g and 1.53-2.63 cm³/g, respectively.

Also, Gonz and Sastre 2001, obtained samples of mesoporous aluminas with a similar synthesis procedure. In this study, non-ionic surfactants were used in different ratios and the alumina source was aluminum sec-butoxide. First, the surfactant was dissolved in sec-butanol and aluminum sec-butoxide. Then, a solution containing water, dipropylamine and half of the required sec-butanol were added. The resulting mixture was stirred for 3 h and then cooled down for 24 h at room temperature. After this, the sol-gel solution was filtered, wash with ethanol and dried at 40°C for two days. After this, the dried gel was heated at 95°C for 6 h in an open propylene bottle; the

surfactant was removed by Soxhlet extraction with ethanol for 15 h. then, this solid was dried for 48 h at 40°C prior to calcination for 4 h at 550°C. Part of this material was calcined a second time in an air oven at 600 and 700°C for 3 h. The resulting materials had large surface areas ranging from 229 to 534 m²/g; this is considering the different temperatures the samples were calcined. It was observed that the lower the calcination temperature (550°C), the higher the surface area. This was not the case for the pore volume, which showed little relation to the different calcination temperatures. Another alumina synthesis procedure performed by Khodabandeh and Davis, 2014, even though the application was for an alumina catalyst, the material preparation is not that different from the previous ones already discussed. Aluminum sec-butoxide (1 g) was hydrolyzed in water (15.10 g), followed by stirring for 1 h. A solution of sodium dodecylbenzenesulfonate (0.49 g) in formamide (5.05 g) was added to the mixture. It was aged for 5 min and then heated at 110°C for 48 h. The solid was recovered by filtration, washed with deionized water and then dried at room temperature. Several alumina precursors are used and based on their molecular composition the correspondent materials for the procedure are calculated. Only the support preparation and characterization will be discussed. The support properties are not thoroughly discussed in this paper, however, the preparation method is not that much different from the ones available in the literature (Alphonse and Faure, 2013a; Khodabandeh and Davis, 2014). According to the authors, performing the synthesis with different ethanol/formamide/water solvents and ethanol/water showed that it plays an important role for the material to have good surface properties. However, other factors like synthesis time and temperature may also affect the final properties of this one.

Niesz et al., 2005, reported a synthesis method for ordered mesoporous alumina using different templates as structure directing agents. Even though several papers have been published regarding the use of templates, until 2005, none of them was about the synthesis of ordered mesoporous alumina. The paper here discussed presents a reproducible method for synthesizing mesoporous alumina with an SBA-15-like arrangement of ordered channels, high surface area and narrow pore size distribution. As a surfactant, Pluronic P123 was used, 1 g was dissolved in 12 ml of ethanol and stirred for 15 minutes at 40°C, and this was named solution A. At the same time, solution B was prepared with different amounts of hydrochloric acid (37 wt. %) and 6 mL of ethanol. Then, 2.46 g of aluminum tri-sec-butoxide was added to solution B slowly under vigorous stirring, the

two solutions were mixed together and continued to be stirred at 40°C. This homogeneous solution was then left for aging in a Teflon container for three days at 40°C under N₂ flow.

2.4.1 Al₂O₃-based materials syntheses and adsorption performance with linker and π -acceptor

The technique here suggested, the support + linker + π -acceptor, is the formation of a charge transfer complex (CTC), which occurs between a π -acceptor compound (immobilized on a support) and π -donor compounds (that can be found in the gas oil). These could be basic nitrogen (BN) and non-basic nitrogen (NBN) compounds. The support would provide the porous surface for the attachment of the linker. The contribution of the linker (linear diamines) to the adsorbent system will be dependent on the length of the amine, which could potentially influence the selective adsorption of the NBN compounds. In this regard, the CTC formation could be affected by how far the π -acceptor is extended from the support. The length on this linker may be the factor that allows more interaction between the adsorbent and adsorbate (Chitanda et al., 2015). In this study three different linkers were tested. Using a polymeric support, polyglycidyl methacrylate (PGMA), followed by linker and then the π -acceptor compounds, four different materials were synthesized. The results showed that the length of the linker had little to no effect on the loading during the adsorption experiments. The adsorbent that showed a better performance compared to the others was that one with diaminopropane as linker, followed by diaminobutane. There was no significant difference between the other two adsorbents reported in the paper (Abedi et al., 2015).

The π -acceptor characteristic is present among several nitrogen compounds, these compounds are electron poor due to the withdrawing of an electron caused by the nitro groups; therefore, these compounds can act as π -acceptors. This is relevant due to the affinity or selectivity they can have towards non basic nitrogen compounds, that are known to have a lone pair of electrons in their nitrogen atoms localized in the aromatic system (Abedi et al., 2015). In contrast, the basic nitrogen compounds have the lone pair of electron located on the nitrogen atom. Hence, these π -acceptor compounds are major contributors to enhancing the adsorbents selectivity towards nitrogen compound (both basic and non-basic). Compounds with characteristics to act as π -acceptors include 2, 4, 7-trinitro-9-fluorenone (TriNF) and 2, 4, 5, 7-tetranitro-9-fluorenone (TENF); hence there in different adsorbent materials for desulfurization and denitrogenation reactions. Attention has been brought to metal oxides, particularly alumina, which is going to be used in this research

as the support material for the adsorbents to be developed. Many different synthesis methods of alumina supports have been developed. Abedi et al., 2016, modified alumina support with P-toluene sulfonic acid powder, linker and π -acceptor compounds dissolved in dioxane. The resulting alumina-polyglycidyl methacrylate-co-ethylene glycol dimethacrylate polymer (Al-PGMA-DAP-TENF) and its alumina-free derivative (PGMA-DAP-TENF) were synthesized, characterized and evaluated for the sulfur and nitrogen removal performances. FT-IR spectra show that the characteristics peaks of C-O and C=O groups are both represented, as well as the attachment of the π - acceptor by the appearance of stretching frequencies at 1361 cm^{-1} . Alumina particles were stable between 30°C to 800°C as confirmed by TGA technique. Al-PGMA-DAP-TENF particles were decomposed at lower temperature and the amount of residue after 800 °C was lower than that in case of Al-PGMA, which indicates a successful grafting and the formation of a new compound. The performance of Al-PGMA- DAP-TENF was found to be superior to that of PGMA-DAP-TENF as it removed about twice as much nitrogen compounds as other polymers did in LGO, and HGO feeds. Both polymers removed more sulfur compounds in HGO feed than in LGO feed. This is due to the high sulfur content of HGO as compared to that of LGO feed (Misra et al., 2015a).

Based on these properties, mesoporous Al_2O_3 and TiO_2 - Al_2O_3 synthesis were explored. As a reference is commercial γ - Al_2O_3 which properties can compete to the ones of the materials synthesized.

2.5 Adsorption kinetics and thermodynamics

To test and prove the capacity of an adsorbent, adsorption capacity is calculated. In the adsorption process, the liquid (adsorbate) is exposed to the solid phase (adsorbent) and the distribution of adsorbate-adsorbent depends on the affinity of the adsorbent towards the adsorbate. Adsorption capacity is the amount of adsorbate that the adsorbent takes per unit mass of the adsorbent; usually mg/g (El Qada et al., 2006). This adsorption equilibrium capacity is achieved when the rate the molecules attached onto the adsorbent are equal to the rate at which they desorb from it (McKay et al., 1985). Along with the adsorption capacity, adsorption isotherms are often determined in order to study the adsorption performance of an adsorbent (Lin et al., 2007). Establishing equilibrium is key to compare the adsorbent behavior for different adsorption systems

quantitatively; this parameter helps to design the adsorption system and calculate other adsorption parameters.

Kinetic models provide insight to adsorption using equations to fit experimental behavior (Lin and Wang, 2009). Fitting the kinetic data and discuss the possible mechanisms of adsorption based on the model parameters are the best way to provide insight into the adsorption process (Pan and Xing, 2010).

Furthermore, thermodynamic parameters may also provide an insight into the type of adsorption taking place. Activation energy (E_a) can be calculated to determine if the adsorption process is a diffused-controlled process (physical adsorption) or a chemical adsorption (Sismanoglu and Pura, 2001). To calculate E_a , the rate constant parameter k_2 for pseudo-second order model widely used to describe adsorptive behavior in different materials can be applied to the Arrhenius equation (Chiou and Li, 2002; Foo and Hameed, 2010; Sismanoglu and Pura, 2001; Tang et al., 2012). In addition, more thermodynamic parameters can be calculated based on the adsorption experiments such as Gibbs energy, enthalpy and entropy, also reported to be calculated for adsorption systems (Foo and Hameed, 2010; Schirmer, 1999; Tang et al., 2012; Zhang et al., 2017).

2.6 Regeneration and reusability

Among materials used as adsorbents, regeneration studies have been studied using mostly two common methods: thermal treatment and solvent extraction (Almarri et al., 2009; Fei et al., 2017; Shan et al., 2008; Yoosuk et al., 2020). Reusability of the material is important as it can provide information for the industrial application of the process. Considering that in this work, we are studying a charge-transfer complex (CTC) adsorbent, the π -acceptor characteristic becomes a factor when selecting the solvents to use for regeneration. Ideally, an electron donor type of solvent should be used since its polarity can successfully clean the pores of the adsorbent (Misra et al., 2018); the remaining solvent in the adsorbent can be removed afterwards.

Chapter 3 : Synthesis, characterization and batch adsorption experiments

A similar version of this chapter has been published as a research article:

Botana de la Cruz, Anakaren, Philip Boahene, Sundaramurthy Vedachalam, Ajay K. Dalai, and John Adjaye. 2020. “Adsorptive Desulfurization through Charge-Transfer Complex Using Mesoporous Adsorbents.” *Fuel* 269, 117379.

Contribution of the MSc candidate:

Adsorbent synthesis, characterization, testing of the materials and data analysis was done by Anakaren Botana de la Cruz. Anakaren Botana de la Cruz and Dr. Misra Prachee designed synthesis method; adsorption experiments and set-up were designed by Anakaren Botana de la Cruz. Anakaren Botana de la Cruz with suggestions and reviews from Drs. Ajay Dalai, Philip Boahene and Sundaramurthy Vendachalam did all the manuscript writing and revision work.

Contribution of this chapter in the overall MSc. Work:

This part of the research work was focused on the synthesis of the functionalized adsorbents, characterization and adsorption of sulfur model feed of the materials here developed.

3.1 Abstract

Mesoporous supports with a π -acceptor were developed for adsorptive desulfurization of petroleum distillates. Pristine mesoporous Al_2O_3 and Ti-substituted mesoporous Al_2O_3 were synthesized and used as supports along with commercial γ - Al_2O_3 for immobilizing ethylenediamine (EDA) linker followed by the π -acceptor, 2, 7- Dinitro-9-fluorenone (DNF). The adsorbents and supports were characterized using BET, FTIR, TGA techniques to ascertain their physicochemical properties. The extent of π -acceptor functionalization on supports was characterized using XRD, TGA and XPS techniques. Adsorbents were examined for the desulfurization of a model oil feed with 500 ppm of sulfur. The commercial γ - Al_2O_3 -EDA-DNF adsorbent successfully removed 90.4 wt% of sulfur. The substitution of Ti in the framework of mesoporous Al_2O_3 did not promote its desulfurization efficiency. The higher desulfurization

activity of the commercial γ - Al_2O_3 based adsorbent than that of others is attributed to its textural properties.

3.2 Introduction

Refineries perform hydrodesulfurization (HDS) and hydrodenitrogenation (HDN) of petroleum feedstock using NiMo/γ - Al_2O_3 and CoMo/γ - Al_2O_3 catalysts at the temperatures and pressures ranges of 360-420°C and 8 to 9 MPa with excess supply of hydrogen for the removal of sulfur and nitrogen species. The conventional HDS process is ineffective for the removal of refractory sulfur compounds such as dibenzothiophenes and alkyl substituted dibenzothiophenes. Typically, 96-98% of HDS activity is obtained by using the conventional hydrotreating technology; however, the remaining 2-4% sulfur removal is difficult to achieve due to the presence of refractory sulfur species (Lemaire et al., 2002). In addition, the refractory sulfur compounds are responsible for catalyst deactivation and poisoning (Jayaraman et al., 2006). Tremendous efforts have been made to improve the HDS process for desulfurization of refractory compounds by altering the process parameters including temperature, pressure, and liquid hourly space velocity. Feed quality, which is one of the three major factors in hydrotreating process efficiency, depends on the origin and nature of crude oil. Heavy gas oil derived from Canadian oil sands contains about 4 wt.% sulfur as compared to ~ 2.5 wt.% sulfur present in the oil shell formations. Canadian government limited the sulfur content of gasoline and diesel to 14 and 15 ppm, respectively for the on-road vehicles (www.canada.ca). The refractory sulfur compounds present in heavy gas oil should be desulfurized to get ultra-low sulfur fuels that are required to comply with the regulations. The production of ultra-low sulfur fuels by HDS requires a higher reactor temperature, pressure, as well as an increased hydrogen rate. As the severe HDS increases fuel production costs, refineries are developing and testing new HDS catalyst formulations by changing the active metals, promoters and catalyst supports to reduce the cost of deep-desulfurization.

Highly efficient desulfurization technologies are required for the selective removal of refractory sulfur compounds. Extensive research was performed in the area of alternate technologies including oxidative desulfurization and adsorption (Almarri et al., 2009; Hernández-Maldonado et al., 2003; Kim et al., 2006; Shan et al., 2008). Among the different techniques, adsorption has shown many advantages such as relatively lower temperatures and pressures when compared to the conventional HDS process. However, for this method to be effective, the development of the

adsorbents is key. In the literature, several materials were used as adsorbents for the removal of sulfur and nitrogen species from gas oil. Velu et al., 2002, used Y-zeolite-based adsorbents for selective desulfurization of jet-fuel. Activated carbon applications as adsorbent have also been reported by Sano et al. 2004. Using a distilled fraction feed from an atmospheric distillatory, the carbon-based supports were packed into a stainless-steel tube and were put in contact by pumping the distilled fraction feed. This study suggested that adsorbent surface properties, as large surface area and pore size might be important factors for better adsorption efficiency. Another highly used material for desulfurization is silica-alumina. Silveira et al., 2015, reported silica-alumina impregnated with different metal oxides. The loading of mixed metal oxides on silica-alumina promoted the sulfur adsorption. In another study, Sarda et al. 2012, used Ni and Cu loaded alumina and ZSM-5 supports for removing sulfur from a commercial diesel containing 325 ppm total sulfur. This study concluded that the sulfur removal strongly depended on the nature of the metal, its amount and the supporting material.

Recently, charge-transfer complex (CTC) adsorption has been reported for desulfurization (Abedi et al., 2016; Hernández-Maldonado et al., 2003; Macaud et al., 2004; Misra et al., 2016; Song, 2003; Yang et al., 2001). This involves the formation of electron-donor acceptor complexes through the interaction of aromatic π -donor compounds and π -acceptor molecules on support. The refractory sulfur compounds of petroleum fuels contain electron-rich aromatic π -systems. They can be adsorbed with electron-deficient systems through the CTC adsorption. The technique here studied involves adsorptive desulfurization through a charge-transfer complex. Mesoporous supports were functionalized with 2,7-Dinitro-9-fluorenone (π -acceptor) to create a sorbent that binds sulfur compounds (π -donor compounds) via charge-transfer complexation. The π -acceptor is electron-deficient and is known to attract heterocyclic sulfur compounds due to their electron-rich nature. In this study, the π -acceptor is bound to mesoporous supports with the help of ethylenediamine, a linker. The CTC complex formation is shown in Figure 3.1. Based on the available literature, there are many adsorbents that have been tested based on the CTC complex formation, but to the best of our knowledge, the mesoporous alumina-based supports with the CTC complex formation has not been reported for desulfurization. Mesoporous alumina seems to be good support as it has a high surface area, pore diameter and pore volume for anchoring the π -acceptor. In this study, 2,7-dinitro-9-fluorenone (DNF) functionalized pristine mesoporous Al_2O_3 ,

Ti-substituted mesoporous Al_2O_3 and commercial γ - Al_2O_3 were prepared, characterized and evaluated for desulfurization of a model feed.

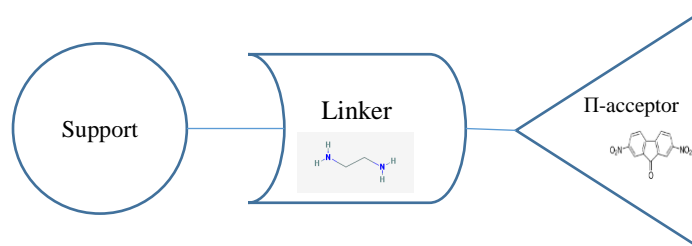


Figure 3.1 Schematic of synthesized adsorbent for desulfurization

3.3 Experimental

3.3.1 Materials

Poly (ethylene oxide)- block poly (propylene oxide) - block poly (ethylene oxide) (P123) was purchased from Sigma Aldrich, Canada. Nitric acid ($\geq 70.0\%$), methanol ($>99.0\%$), toluene ($>99.0\%$) and acetic acid ($>99.0\%$) were purchased from Fisher Chemical, Canada. Aluminum isopropoxide (98.0%) and ethylenediamine (99.0%) were purchased from Alfa Aesar, Canada. Titanium isopropoxide (98.0%) and hydrochloric acid (37.0%) were purchased from Acros Organics, Canada. 2, 7- Dinitro-9-fluorenone was purchased from Tokyo chemical industry and anhydrous ethanol (100%) was purchased from Commercial alcohols, Canada.

3.3.2 Synthesis of adsorbents

Adsorbent A, adsorbent B, and adsorbent C were prepared with the mesoporous Al_2O_3 , Ti-substituted mesoporous Al_2O_3 and commercial γ -alumina supports, respectively. There were three steps involved in the syntheses of adsorbents. First, the supports, mesoporous Al_2O_3 , Ti-substituted mesoporous Al_2O_3 were synthesized, afterward, ethylenediamine (linker) was added onto the three supports and as the third and final step, the immobilization of the π -acceptor onto the three materials was performed.

The synthesis of mesoporous alumina and Ti-substituted mesoporous alumina followed the method reported by Badoga et al. 2014 and Duprez and Wilson 2009 with a few modifications. The synthesis procedures of adsorbents are described below.

Synthesis of Al₂O₃ and Ti-substituted mesoporous Al₂O₃ supports

For the synthesis of pristine alumina support, 39.5 g of aluminum isopropoxide was dissolved in 130 mL of ethanol contained in a 250 mL beaker placed in a hot plate with a mechanical stirrer for 1 h at 40°C (Solution A). Simultaneously, 260 mL of ethanol was placed in a 500 mL beaker at 40°C incorporated with a mechanical stirrer, and then 19.4 g of P-123 was added. The mixture was stirred for 2 h at 40°C in order to dissolve P-123 (Solution B). Then, 29 mL of HNO₃ was added with an HNO₃/H₂O ratio of 0.2 (14 mL of HNO₃ and 70 mL of H₂O). The next step was the addition of the content of solution A to solution B dropwise and stirred for 2 h at 40°C. The resulting material was aged for 4.5 days at 65°C in a Teflon bottle prior to calcination at 600°C in a muffle furnace for 5 h with a ramp rate of 0.5°C/min.

For the synthesis of Ti-substituted mesoporous Al₂O₃ support, 43 g of aluminum isopropoxide and 3.5 g of titanium isopropoxide were dissolved in 117 mL of ethanol in a 500 mL beaker under mechanical agitation for 30 min. Simultaneously, 17.9 g of P123 was dissolved in 240 mL of ethanol at 40 °C for 30 min in another 500 mL beaker. Subsequently, 27 mL of HNO₃ (70 wt.%) was added to the beaker containing P123 solution and allowed to stir for another 15 min. Afterward, the first mixture was added dropwise to the content of the second beaker under vigorous stirring for 2 h. The mixture was then transferred into a Teflon bottle for aging at 65°C for 4.5 days. Finally, the solid material was recovered under vacuum filtration, dried at 80°C and calcined at 600 °C for 5 h at a ramp rate of 0.5°C/min.

Amine functionalization on supports

The functionalization of the synthesized supports with ethylenediamine (EDA) provides anchoring sites for the π -acceptor. The procedure for the immobilization of the amine linker on supports is described below. Firstly, 12.1 g of EDA was added to a beaker containing 144 ml of methanol under vigorous stirring until complete dissolution of the solid particles. Secondly, 10 g of the support was added under continuous stirring for 3h. The resulting mixture was filtered, washed

with methanol and dried in a vacuum oven at 70 °C for 12 h. For comparison purposes, commercial γ -alumina was also functionalized using the same linker.

Immobilization of π -acceptor on supports

87 mL of toluene and 6 mL of acetic acid were added to a 500 mL two-necked flask equipped with a mechanical stirrer immersed in an oil bath at 100°C. Then, 1.06 g of DNF π -acceptor was added under continuous stirring until completely dissolved. Subsequently, the functionalized support (i.e. support + linker matrix) was added and stirred at 400 rpm under reflux at 100°C for 3 days. Once the reaction was completed, the materials were recovered via vacuum filtration and washed with toluene. Then it was dried under vacuum at 85 °C for 48 h.

3.3.3 Characterization of supports and adsorbents

To determine the textural properties of the synthesized supports, supports + linker as well as the formulated support-linker- π acceptor adsorbents, the N₂ adsorption-desorption BET technique was used. The nitrogen physisorption was performed using a Micrometrics ASAP 2020 analyzer with liquid nitrogen at a temperature of 77 K to determine the specific surface area, pore volume and average pore diameter. The Brunauer-Emmett-Teller (BET) method was used in the pressure range (P/P₀) of 0.05-0.30. The adsorption-desorption sections of isotherms were used to calculate the pore diameter and pore size of the synthesized materials using the Barrett-Joyner-Halenda (BJH) method. Using the N₂ amount adsorbed by the materials at a P/P₀ = 0.4, the volume of the mesopore was calculated. Using the amount of N₂ adsorbent at a P/P₀=0.95, the total pore volume was calculated with the assumption that the external surface was negligible as compared to the one in the pores. In all cases, a correlation coefficient of 0.99 was obtained.

The Fourier transformed infrared spectrometer (FT-IR) was used to qualitatively determine the π -acceptor presence on the materials. The spectra were recorded in the range of 400-4000 cm⁻¹ wavenumbers, which used 128 scans with a nominal resolution of 4 cm⁻¹ with a VERTEX 70 FT-IR instrument equipped with a diamond ATR.

The thermal stability of the samples was determined using a TA instruments Q500 series thermogravimetric analyzer (TGA). Nitrogen was used to purge the samples and then the analysis was performed. Using 10-20 mg of sample weighed into a high-temperature platinum pan, the

sample was heated to 800°C at a ramp rate of 10°C/min. As the sample was being heated, the weight loss of the samples was measured as a function of the increasing temperature.

The X-ray diffraction (XRD) patterns of the supports and synthesized adsorbents were obtained using a Bruker D8 Advance X-ray diffractometer (Bruker AXS, Karlsruhe, Germany). The XRD analysis was acquired with the application of monochromatic CuK α radiation ($\lambda = 0.15418$ nm) generated at 40 kV voltage and 130 mA. The diffraction patterns were measured between the wide-angle (2θ) of 10° and 90° at a scanning speed of 0.2°/min.

Around 4-6 mg of each sample were combusted using an El Vario III CHSN elemental analyzer (Elemental Americas Inc., Mt. Laurel, NJ, USA) was used to determine the percent content (wt/wt) of carbon (C), hydrogen (H), and nitrogen (N) atoms. It was also used to determine the nitrogen concentration in between synthesis stages.

All X-ray Photoelectron Spectroscopy (XPS) measurements were collected using a Kratos (Manchester, UK) AXIS Supra system at the Saskatchewan Structural Sciences Centre (SSSC), the University of Saskatchewan. This system is equipped with a 500 mm Rowland circle monochromatic Al K- α (1486.6 eV) source and combined hemi-spherical analyzer (HSA) and spherical mirror analyzer (SMA). A spot size of hybrid slot (300x700 microns) was used. All survey scan spectra were collected in the 5-1200 binding energy range in 1 eV steps with a pass energy of 160 eV. High-resolution scans of multiple regions were also conducted using 0.05 eV steps with a pass energy of 20 eV. An accelerating voltage of 15 keV and an emission current of 15 mA were used for the analysis.

3.3.4 Procedure for adsorption experiments

A model feed was prepared in order to test the adsorption efficiency towards sulfur compounds of the synthesized materials in a batch reactor system. For the model feed, thiophene was dissolved in ultra-low sulfur diesel (ULSD). The ULSD contains 27 and 12 ppm for nitrogen and sulfur, respectively. For the desired concentration of 500 ppm, 0.0656 g of thiophene was diluted in 50 ml of ULSD, based on the formula shown below.

$$ppm (S) = wt. thiophene (g) \times \frac{32.065}{84.14} \times \frac{1}{50} \times 10^6 \quad (3.1)$$

Then, the adsorption studies were carried out by adding adsorbent to model feed (1:5 ratio, by weight). The feed was contacted with the adsorbent by placing 0.5 g of the adsorbent and 2.5 g of the model feed in a glass vial with a cap. Using a magnetic stirrer at 400 rpm, the adsorbent and the model feed were mixed at 22°C, for 12 hours. After mixing, the liquid product was separated from the adsorbent by vacuum filtration and analyzed using an Antek N/S analyzer. The sulfur removal efficiency of adsorbent was calculated based on the formula:

$$\text{S removal efficiency (\%)} = \frac{\text{S content in untreated feed (ppm)} - \text{S content in treated feed (ppm)}}{\text{S content in untreated feed (ppm)}} \times 100 \quad (3.2)$$

3.4 Results and discussion

3.4.1 N₂-adsorption measurement

The isotherms, as well as pore size distributions for pristine supports and their corresponding adsorbents, were determined by N₂-adsorption/desorption measurement. Figure 3.2 shows the isotherms of the three supports (mesoporous Al₂O₃, Ti-substituted mesoporous Al₂O₃ and commercial γ - alumina) and DNF-immobilized supports (Al₂O₃-EDA-DNF and Ti-substituted Al₂O₃-EDA-DNF and commercial γ - alumina-EDA-DNF). The type IV isotherm confirms the presence of textural mesoporosity in the pristine supports and their respective adsorbents (Satterfield 1996). Since adsorption predominantly proceeds on the surface, the porosity of the adsorbent material plays a crucial role. This is because the porosity controls the mass transfer processes via charge transfer complexation between the π -acceptor of the adsorbent material and sulfur compounds (π donors) of the feed; thus, facilitating the adsorption of sulfur compounds and their subsequent desulfurization.

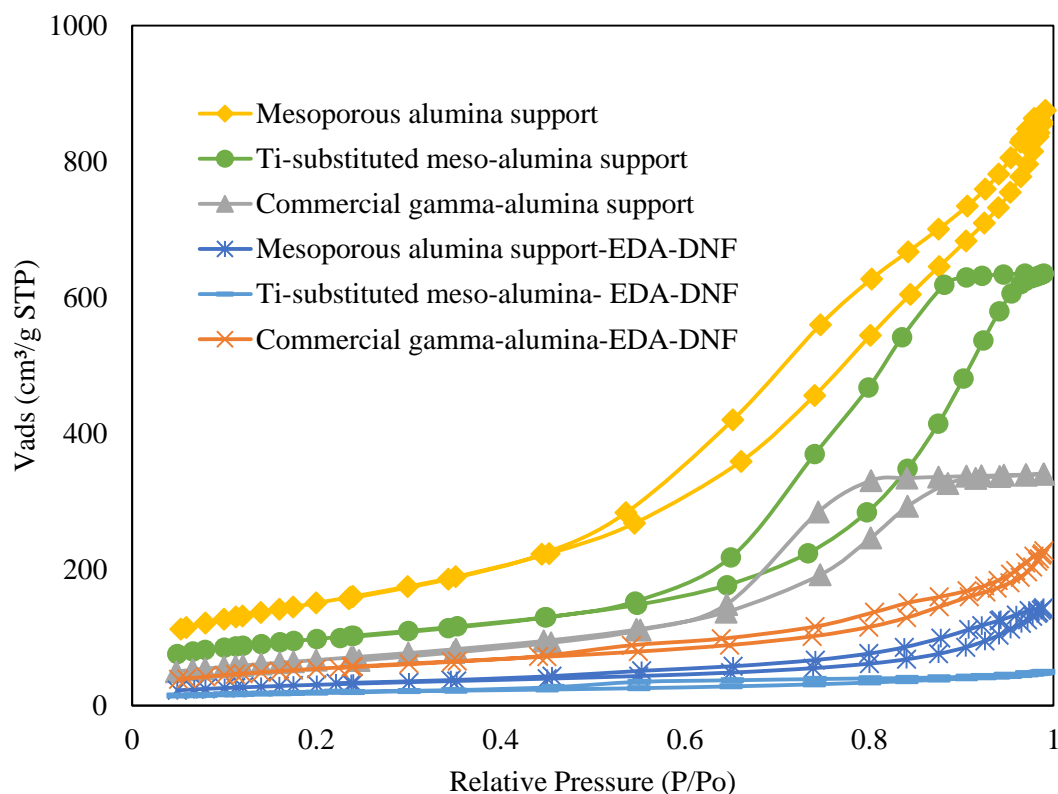


Figure 3.2 N₂-adsorption/desorption isotherms for Al₂O₃, Ti-substituted meso-alumina and commercial gamma-alumina their corresponding DNF-immobilized supports (Al₂O₃-EDA-DNF and Ti-substituted meso-alumina -EDA-DNF).

The pore size distribution profiles of the prepared adsorbents are given in Figure 3.3. It can be observed from the figure that the cumulative volume of N₂ desorbed by the adsorbent A is more than that of the adsorbent B. As given in Table 3.1, the incorporation of Ti in the framework of Al₂O₃ significantly changed the textural properties of mesoporous alumina. It can be noticed that the surface area and pore volume significantly decreased after the immobilization of the linker and π -acceptor on all three supports.

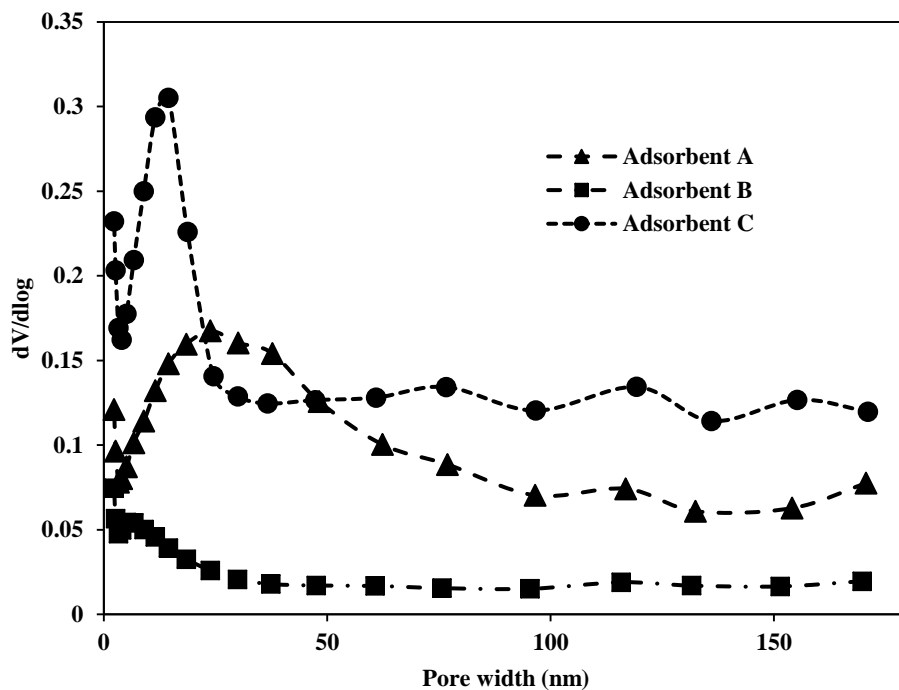


Figure 3.3 Pore size distribution of the DNF immobilized support Al₂O₃-EDA-DNF, Ti-substituted Al₂O₃-EDA-DNF and commercial alumina-EDA-DNF.

The Al₂O₃-EDA and Ti-substituted Al₂O₃-EDA materials suffered a 23.9 and 26.7 % reduction in surface areas, respectively; while a reduction of 28.5 and 27.3 %, respectively, was recorded in their pore volumes. That notwithstanding, significant losses of both surface areas and porosities were observed in the final adsorbents after the DNF π -acceptor was immobilized, whereas the reduction in specific surface area for the final material was in the range of 80-85% and that of pore volume was in the range of 84-95% for the Al₂O₃ and Ti-substituted meso- Al₂O₃ based adsorbents. The observed drastic changes in textural properties, typically, the pore volume, could be attributed to the bulky nature of the DNF π -acceptor. The adsorbent C, which is based on γ - alumina did not show significant changes in the textural properties like the adsorbents A and B.

Table 3.1 Textural properties of the synthesized support, support-linker, and support-linker- π -acceptor.

Sample name	BET surface area (m ² /g)	Pore volume (cm ³ /g)	Pore diameter (nm)
<u>Supports</u>			
Alumina	548	1.37	6.7
Titania-alumina*	341	0.99	7.6
Commercial alumina	241	0.53	6.0
<u>Supports + EDA</u>			
Alumina-ethylenediamine	417	0.98	6.3
Titania-alumina-ethylenediamine	250	0.72	7.0
Commercial alumina-ethylenediamine	264	0.63	6.2
<u>Supports + EDA + DNF</u>			
Alumina-ethylenediamine-dinitrofluorenone (A)	108	0.22	8.7
Titania-alumina-ethylenediamine-dinitrofluorenone (B)	66	0.07	5.0
Commercial alumina-ethylenediamine-dinitrofluorenone (C)	195	0.35	7.7

3.4.2 Fourier transform infrared analysis

Figure 3.4 displays the FTIR spectra of the alumina-based supports used, the broad bands from 400 to 1100 cm⁻¹ are observed in all mixed oxides, it can be attributed to the superimposition of the Al-O vibrations bands. The spectra of mixed oxides show a broad band between 2700-3750 cm⁻¹ that corresponds to hydroxyl groups of oxides and surface adsorbed water (Badoga et al., 2014). The strong peak at 1660 cm⁻¹ can be attributed to the stretching of -OH (Ahmed, 2011; Duprez et al., 2011). The bands for Ti-O were obscured by the bands related to Al-O bonds, hence, could not be identified (Silva et al., 2015). The π -acceptor, DNF contains two nitro groups on fluorenone moiety. Figure 3.5 shows the adsorbents, ethylenediamine and dinitrofluorenone spectra. The immobilization of the π -acceptor on all three supports is evidenced by the appearance

of nitro group (O=N–O) bands at 1340 cm^{-1} and 1570 cm^{-1} (Misra et al., 2015). The FTIR study indicates that the desired adsorbents with the π -acceptor were synthesized successfully.

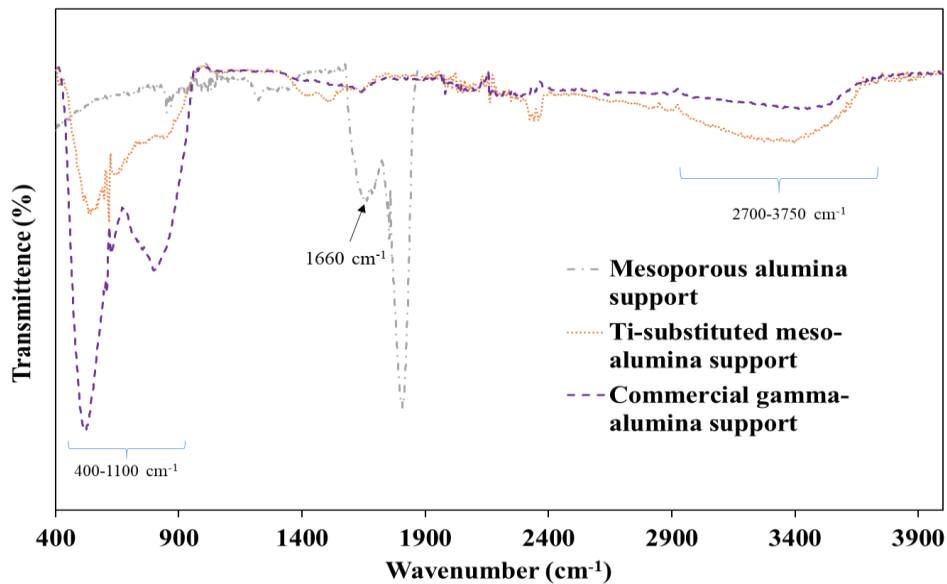


Figure 3.4 FT-IR spectra of the alumina-based supports

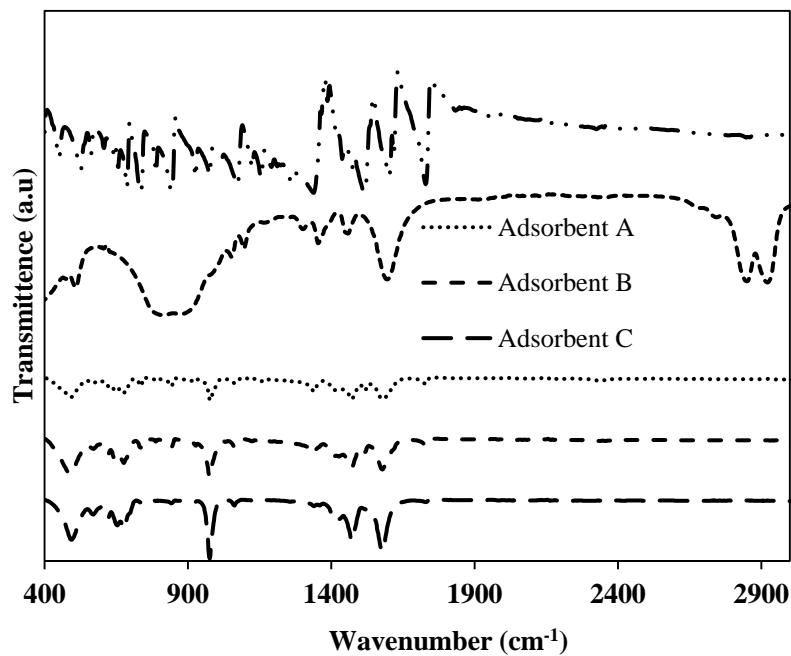


Figure 3.5 FT-IR spectra of adsorbents, ethylenediamine and dinitrofluorenone.

3.4.3 Thermogravimetric analysis

Thermal degradation profiles of the three adsorbents are shown in Figure 3.6. The prepared adsorbents are stable up to 200 °C, a temperature that is within the working range of adsorption reactions. The adsorbents showed significant weight loss after 280°C.

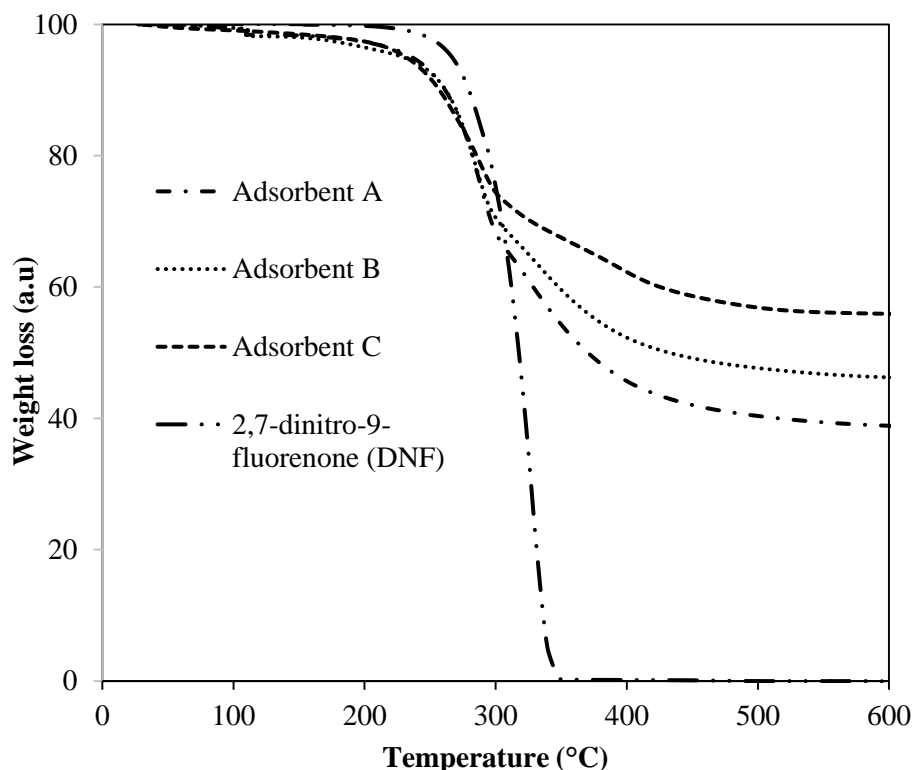


Figure 3.6 Thermal degradation profiles of adsorbents and dinitrofluorenone

As discussed earlier, the FTIR and XRD studies proved the presence of significant amount of DNF in all three adsorbents. Prior to immobilization, supports were calcined at 600°C, and no other compounds or impurities other than DNF is expected in this temperature region. TGA of pure DNF was conducted to validate the above prediction. TGA of pure DNF also shows the weight loss in the same temperature region as adsorbents (Figure 3.6). This result confirms that the weight loss of adsorbents after 280°C is due to thermal degradation of DNF. As discussed previously, the surface area and pore volume values drop as the concentration of DNF increases in adsorbents. The TGA study showed ~20 % more DNF in adsorbent A than adsorbent C.

Adsorbent A showed a significant drop in the surface area and pore volume values due to the presence of the higher amount of DNF in it.

3.4.4 X-ray diffraction

X-ray diffraction of supports and adsorbents are shown in Figures 3.7 and 3.8. The XRD patterns concluded that the mesoporous alumina and Ti-substituted mesoporous alumina supports are mostly amorphous and the commercial alumina support contains the crystalline γ -alumina phase (peaks at 46.3° and 67°). The XRD patterns of the synthesized adsorbents (A, B and C) shown in Figure 3.7 match to the π -acceptor, DNF, which is highly crystalline, therefore its peaks dominant over the support XRD peaks.

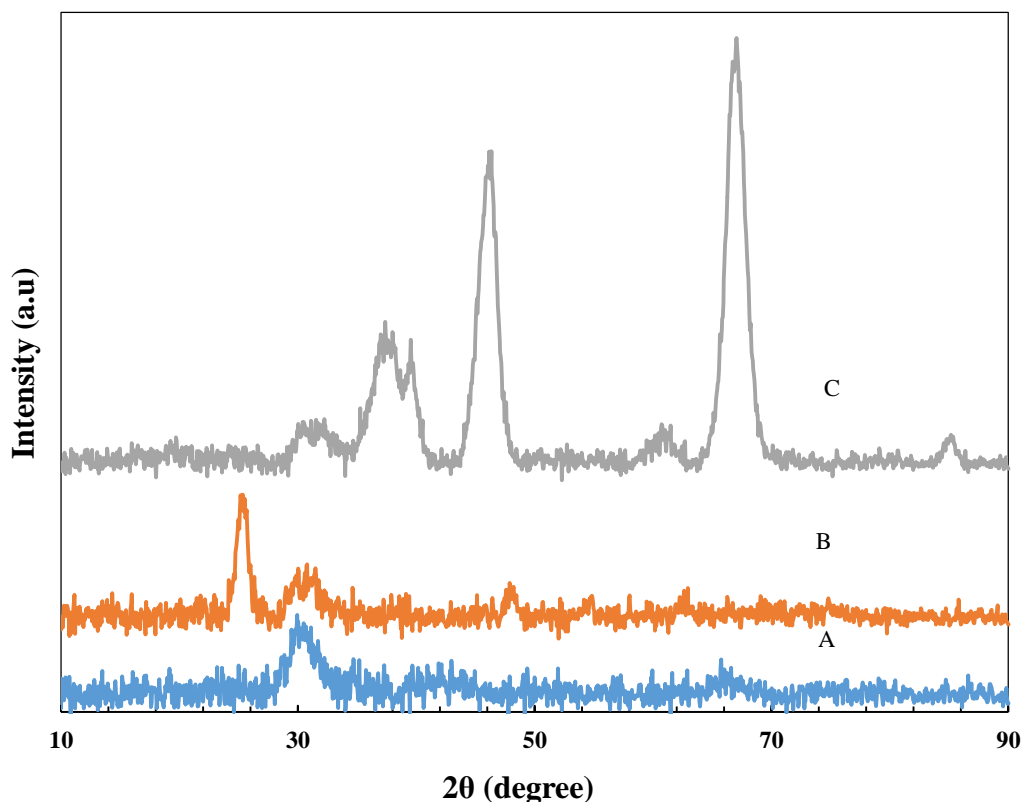


Figure 3.7 X-ray diffraction for alumina supports. (A) Mesoporous alumina support, (B) Ti-substituted meso- Al_2O_3 and (C) commercial γ -alumina supports.

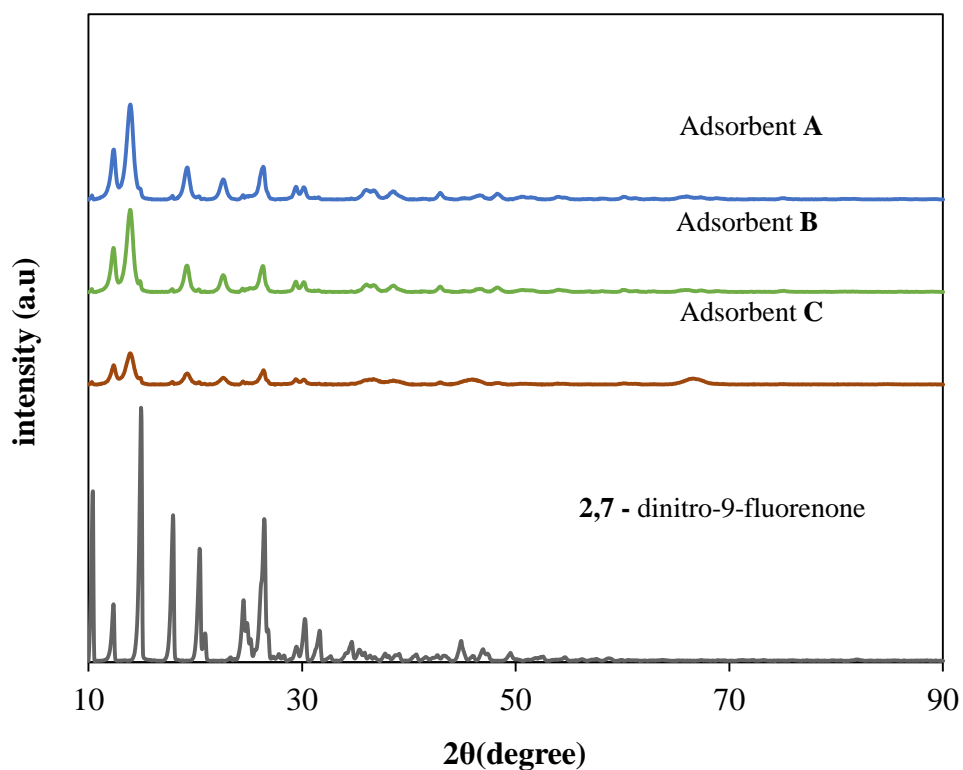


Figure 3.8 X-ray diffraction for alumina based adsorbents and π -acceptor compound.

3.4.5 X-ray photoelectron spectroscopy

Adsorbent B was investigated by XPS to determine its Titanium coordination. In the mesoporous materials, the framework and non-framework Ti species exist in the tetrahedral and octahedral coordination, respectively. The XPS spectrum of adsorbent B shown in Figure 3.9 evidences the presence of only tetrahedrally coordinated titanium by the appearance of characteristic bands at 458 and 462 eV. This values are in accordance with the other reports (Gonzalez-Elipé et al., 1989; Biesinger et al., 2010; Lazzaroni and Hecq, 2003; Pouilleau et al., 1997).

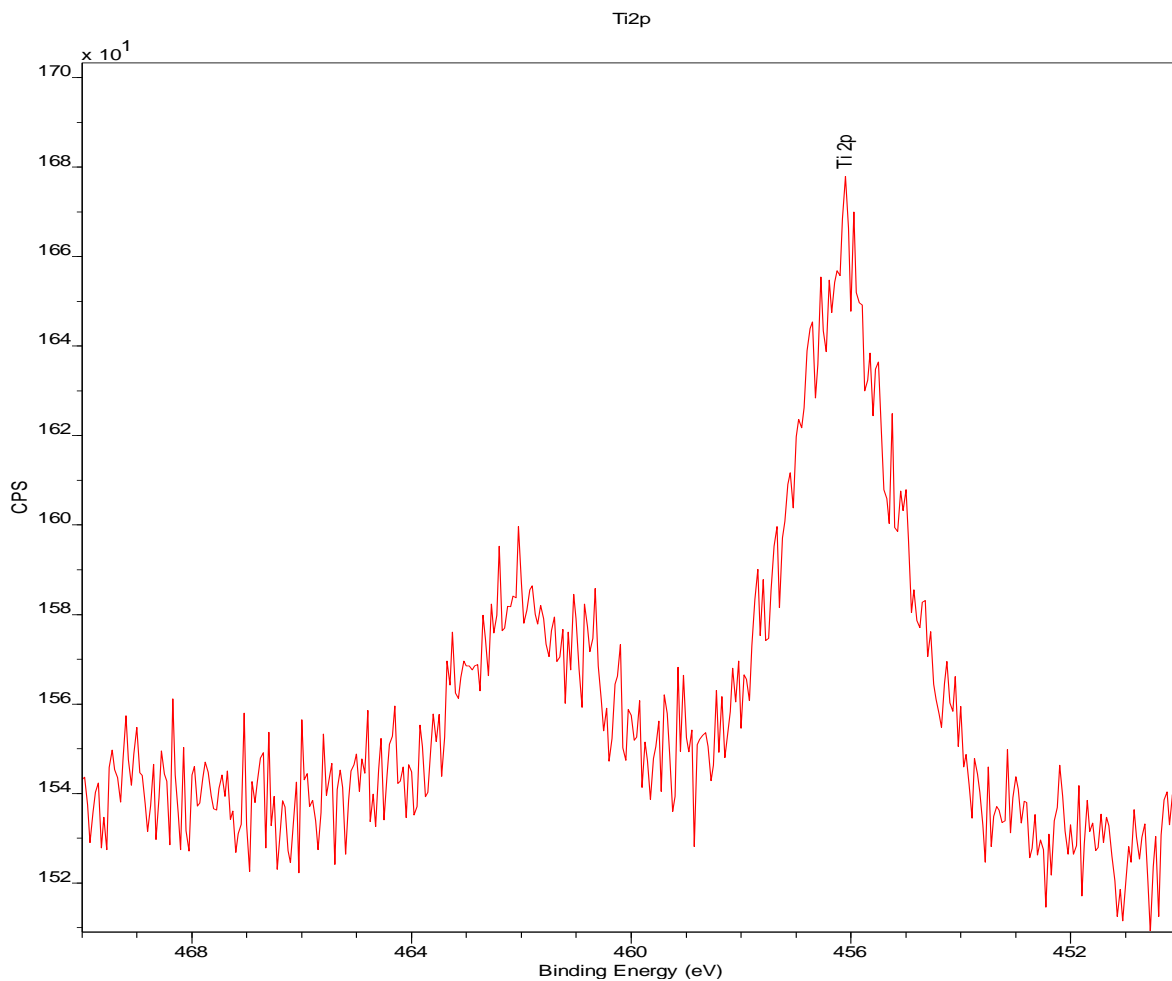


Figure 3.9 X-ray photoelectron spectroscopy of Adsorbent B.

3.4.6 CHNS elemental analysis

The results and their respective standard deviations are shown on Table 3.2. It can be observed that when the linker (EDA) was attached to mesoporous alumina, the nitrogen composition increases to 1.17%, this change in the nitrogen composition was expected as the linker (EDA) is an amine, therefore its structure $C_2H_4(NH_2)_2$ containing nitrogen. Then, when the π -acceptor is added we see that the nitrogen composition did not change significantly, this can be explained with the synthesis procedure. Attaching the linker to the support does not involve a higher temperature

other than 22°C, however, when the π -acceptor was synthesized, a temperature of 100°C was needed for the reaction. With this being said, it might be possible that some of the linker was not washed out after its synthesis onto the support and when the π -acceptor immobilization took place, the linker in excess was washed off but the composition did not decreased, as the π -acceptor (DNF) is high in nitrogen composition. The DNF chemical formula, $C_{13}H_6N_2O_5$, shows that is not only rich in nitrogen, but also in carbon (C). This can explained why after immobilizing the π -acceptor onto the supports and linkers, each sample shows an increase on its carbon composition. This nitrogen composition behavior was not the case for the three supports, Ti-substituted meso-alumina and commercial γ -alumina, where nitrogen compositions increased after adding the linker and π -acceptor. However, the carbon composition behavior was the same in all of the materials.

Table 3.2 CHNS elemental composition of supports, support + linker and final adsorbent

Sample name	Elemental composition % (wt/wt)			
	N (%)	C (%)	H (%)	S (%)
Mesoporous alumina support	0.00 ± 0.00	0.49 ± 0.00	3.44 ± 0.26	0.08 ± 0.11
Mesoporous alumina support-EDA	1.17 ± 0.00	2.30 ± 0.05	3.04 ± 0.01	0.07 ± 0.02
Mesoporous alumina support-EDA-DNF	1.17 ± 0.07	27.38 ± 0.36	3.77 ± 0.08	0.11 ± 0.03
Ti-substituted meso-alumina	0.07 ± 0	0.77 ± 0.06	3.28 ± 0.97	0.02 ± 0.02
Ti-substituted meso-alumina-EDA	0.70 ± 0.00	2.83 ± 0.81	3.40 ± 0.02	0.05 ± 0.01
Ti-substituted meso-alumina-EDA- DNF	0.82 ± 0.02	21.63 ± 1.43	3.40 ± 0.59	0.05 ± 0.00
Commercial γ -alumina	0.00 ± 0.00	0.15 ± 0.17	3.60 ± 0.33	0.04 ± 0.00
Commercial γ -alumina -EDA-DNF	1.82 ± 0.11	15.46 ± 0.75	2.90 ± 0.88	0.03 ± 0.01

3.4.7 Adsorption experiments using ultra-low sulfur diesel (ULSD) feedstock

Adsorption experiments were performed for a 24 h duration to measure the desulfurization abilities of adsorbents using a model feed with 500 ppm sulfur in ULSD. As shown in Figure 3.10, adsorbents A, B and C removed 85.7, 55.3 and 90.4 wt. % sulfur, respectively. Among the adsorbents, adsorbents A and C appear to be suitable materials for desulfurization. These adsorbents are based on alumina supports, whereas the adsorbent B is made of Ti substituted Al_2O_3 support. As compared with alumina supports, Ti substituted Al_2O_3 has inferior surface area and pore volume. In the same way, adsorbent B, which is formulated with Ti substituted Al_2O_3 , has lower surface textural properties. The poor surface area and pore volume of adsorbent B are accountable for its inferior sulfur adsorption tendency.

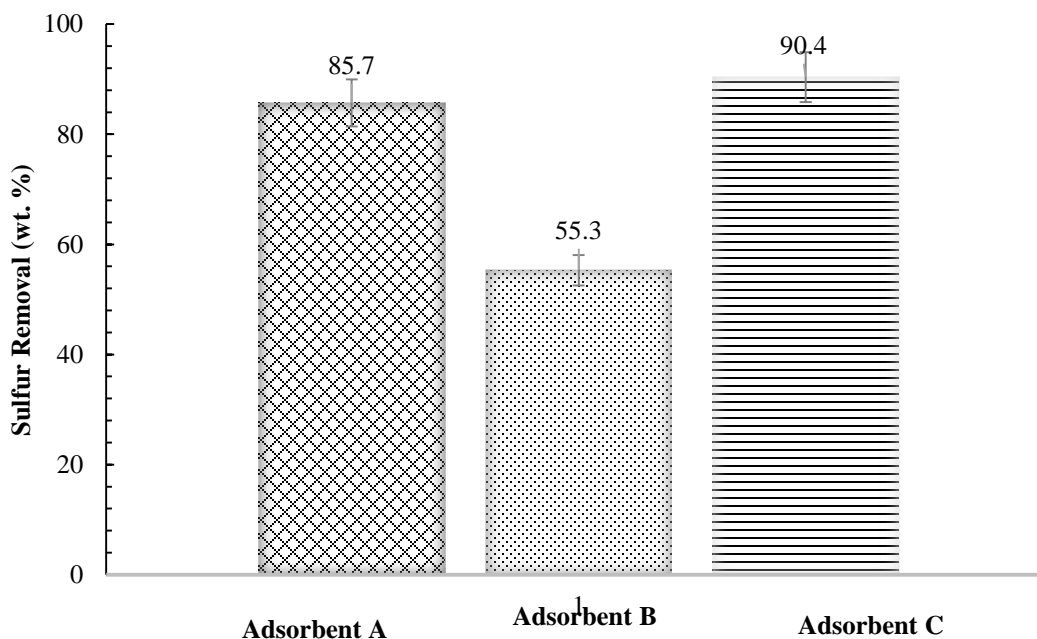


Figure 3.10 Comparison of sulfur removal efficiency of Adsorbents A, B and C. Adsorption parameters: Feed = 500 ppm of sulfur in ULSD, T = 22 °C, stirring = 400 rpm, atmospheric pressure, adsorbent to feed ratio = 1:5, time = 24 h).

All adsorbents contain ethylenediamine and DNF on them. The possibilities of leaching of these compounds were checked by conducting adsorption experiments using ULSD non-spiked feed

with 27 and 12 ppm for nitrogen and sulfur, respectively. As shown in Figure 3.11, all three adsorbents removed completely the total sulfur content, however, this was not the case for nitrogen. The nitrogen contents of liquid products of adsorbents A and C are lower than that of the starting feed. On the contrary, a slight increase in the nitrogen concentration is observed with the adsorbent B. The linker and π -acceptor are nitrogen-based compounds. The leaching of these compounds during adsorption can lead to an increase in the nitrogen concentration of the liquid product. The increase of nitrogen concentration with the adsorbent B in Figure 3.11 evidences the possibility of some leaching of either the linker or the π -acceptor compounds from the adsorbent B.

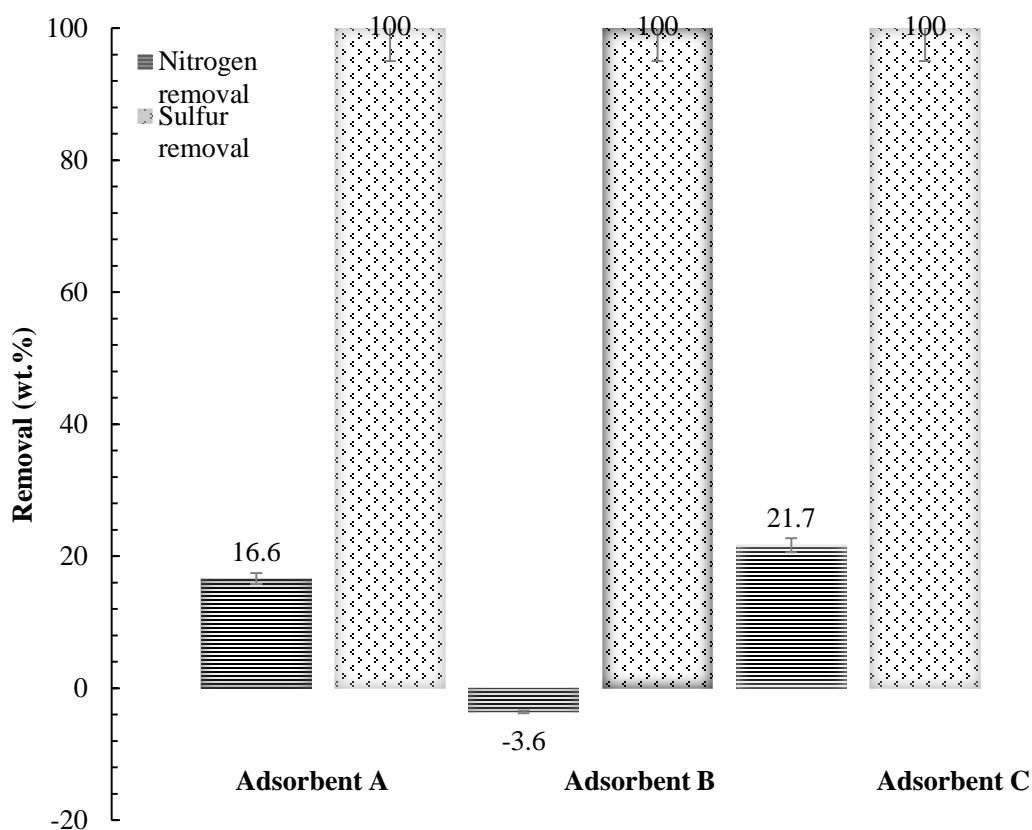


Figure 3.11 Sulfur and nitrogen removal efficiency of adsorbents A, B and C with ULSD non-spiked feed. Adsorption parameters: T = 22 °C, stirring = 400 rpm, atmospheric pressure, adsorbent to feed ratio = 1:5, time = 24 h.

3.4.8 Effects of adsorption time

The time it takes by an adsorbent to remove sulfur and nitrogen impurities is important as it can impact the adsorption capacity. Therefore, the effects of contact time of the adsorption process can be considered as an important factor to determine whether a material is suitable for the adsorption application or not. The effect of time on adsorption of sulfur species was studied by performing the experiments for 1, 6, 12, 24, 48, 72 and 96 h by using the ULSD spiked feed with 500 ppm of sulfur. As shown in Figure 3.12, the adsorption capacity is found to increase with the contact time. During the first hour of the experiment, around 60% of sulfur impurities were removed by adsorbent C and around 20% with adsorbents A and B. Then in the second sample, which was taken after 6 h, there is an increase in the sulfur removal with all three adsorbents.

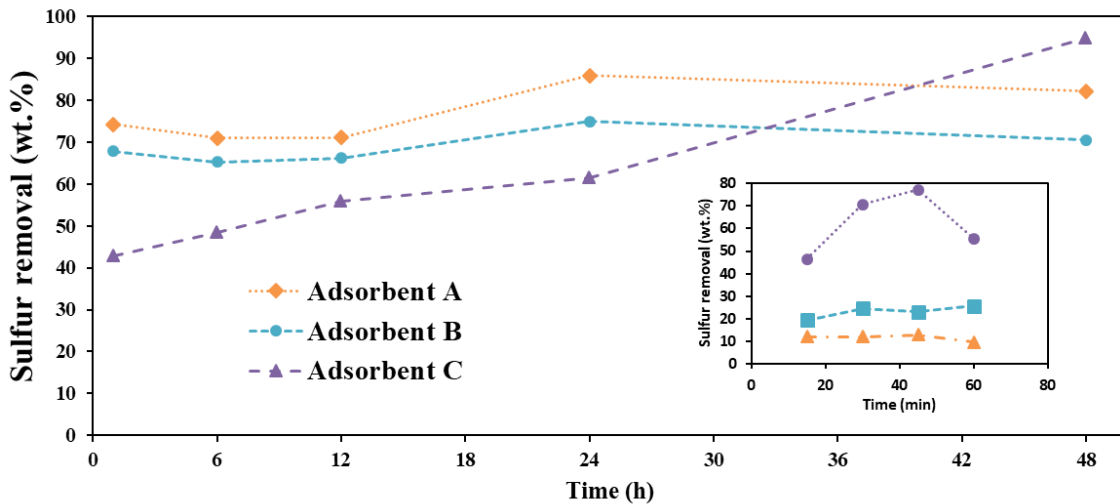


Figure 3.12 Effects of adsorption time on sulfur removal (Adsorption parameters: $T = 22\text{ }^{\circ}\text{C}$, stirring = 400 rpm, atmospheric pressure, adsorbent to feed ratio = 1:5, time = 0 to 96 h).

Adsorbent A removed 60%, adsorbent B removed around 40% and adsorbent C removed over 90%. The consecutive time samples for adsorbents B and C seem to stay within the same range, however, the adsorption activity of the adsorbent A gradually increases and reaches its maximum value at the contact time of 72 h. Though adsorbents A and C showed similar desulfurization activities after 72 h, the adsorbent C is most preferred for the adsorptive desulfurization process,

as it needs the shorter equilibrium time. The most suitable adsorbent for industrial applications is the one that possess a shortest contact time (shortest equilibrium time). As the contact time and flow rate of feedstock are indirectly proportional, high flow rate operation can provide a cost-effective adsorptive desulfurization process.

3.4.9 Effects of feed concentration on adsorption capacity

Adsorption isotherms are the equilibrium relationships that provide insights into the distribution of adsorbate between two phases for a particular adsorbate and adsorbent system (Foo and Hameed, 2010). Studying the equilibrium capacity of an adsorbent is helpful as it can help to determine the maximum adsorption capacity of adsorbent in relation to adsorbate (Mckav and Ireland, 1985). This adsorption equilibrium capacity is achieved when the rate at which the molecules adsorb into the adsorbent is equal to the rate at which they desorb from it; this is considered a dynamic concept. The concentration of the solute should not change in equilibrium either in the solid or in the bulk solution, as the equilibrium is considered a characteristic of the entire system (El Qada et al., 2006).

Here, sulfur model feeds with varying initial concentrations of thiophene in ULSD were used for determining the adsorption capacity data. The sulfur adsorption capacity, q (mg/g) of the adsorbents was calculated according to the following equation:

$$q = \frac{M_f (C_i - C_e)}{M_s} \quad (3.3)$$

Where, M_f is the model feed weight (g), C_i and C_e are the initial and final concentrations of the sulfur in the model feed (ppm), respectively and M_s is the mass of solid adsorbent (g).

There are two types of adsorption; physical and chemical. Chemical adsorption constitutes creating bonds in between adsorbate (sulfur compounds) and adsorbent, whereas physical adsorption is based on weak intermolecular bonds forces like Van der Waals and hydrogen bonding (Nathan and Scobell, 2012). The adsorbate can adsorbed on any sites of the adsorbent and in two different ways: monolayer or multilayer. The monolayer adsorption constitutes one molecule getting attached onto the surface of the adsorbent and multilayer is when several molecules may stack onto the surface of the adsorbent (Hendricks, 2011).

As shown in Figure 3.13, the relation between the various initial feed concentrations compared to their adsorption capacity seems to show the curve, which increases quickly in the beginning, but the adsorption gain decreases and becomes more difficult as the sulfur concentration increases. This adsorption pattern indicates that the adsorption surface of adsorbents A, B and C were heterogeneous, resulting in both monolayer and multilayer adsorptions. Similar results of increase in the adsorption capacity with an increasing amount of the initial adsorbent concentration were reported (Fei et al., 2017; Ha et al., 2018). Increase of adsorbate concentration increases the probability of collision between adsorbate and adsorbent, also the driving force of the concentration gradient and thus causes an increase in adsorption capacity.

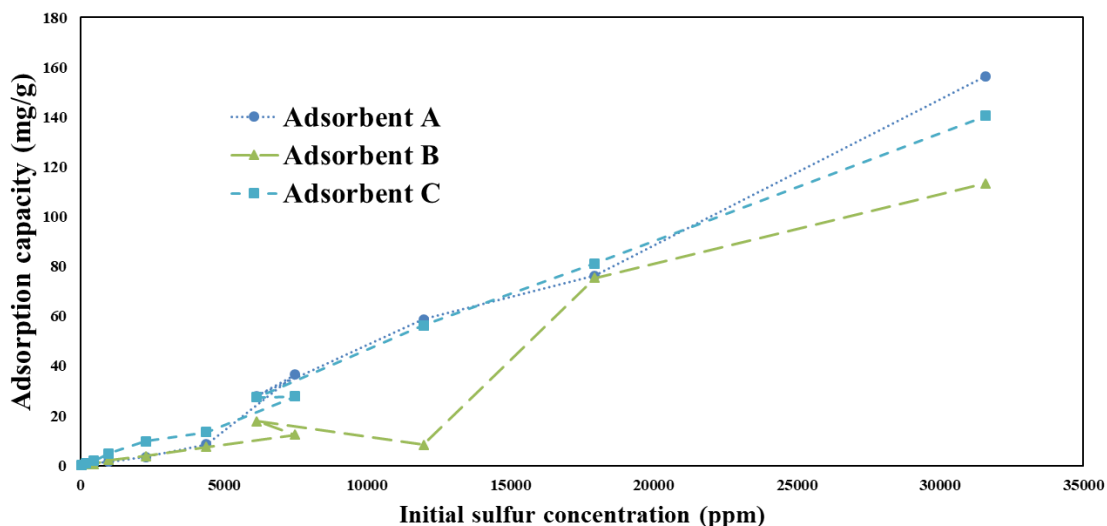


Figure 3.13 Effects of initial concentration of sulfur model feed on adsorption capacity of adsorbents A, B and C (Adsorption parameters: T = 22 °C, stirring = 400 rpm, atmospheric pressure, adsorbent to feed ratio = 1:5, time = 24 h).

3.5 Conclusions

Three different charge-transfer complex (CTC) adsorbents for desulfurization of liquid fuels were prepared and characterized. The BET-N₂ study evidenced the mesoporous nature of all three adsorbents. The FTIR, TGA and XRD studies confirmed the successful incorporation of the π -acceptor on the support. Adsorption experiments were conducted with a model feed of 500 ppm sulfur. The CTC adsorbents prepared based on mesoporous alumina (Adsorbent A) and commercial γ -alumina (Adsorbent C) showed higher sulfur removal than the Ti incorporated material (Adsorbent B). The poor performance of adsorbent B is due to leaching of the linker and

π -acceptor in the adsorption medium (ULSD). No leaching of the linker and π -acceptor was observed with adsorbents A and C. The adsorption capacity profiles of adsorbents A and C are logarithmic with the monolayer and multilayer adsorptions. Among adsorbent A and C, it is concluded that adsorbent C is more suitable for sulfur removal due to the shorter equilibrium time of adsorption.

Chapter 4 : Optimization, regeneration and kinetic studies

This chapter presents the experimental results and discussions of the third phase of this research work. Section 4.1 details the chemical used in this part of the research along with those used for the synthesized adsorbents; it also briefly describes the preparation of the adsorbents previously detailed in Chapter 3. In section 4.2, the optimization design of the experiments is presented and the results are further discussed. Kinetic studies are discussed in section 4.3, two kinetic models were used to fit the data and further explain the adsorptive behavior of the adsorbents. Thermodynamic studies are presented in section 4.4 where free activation energy, enthalpy, entropy and activation energy are calculated and provide an insight of the thermodynamic side of the adsorptive behavior of these alumina-based adsorbents.

4.1. Experimental methods

4.1.1 Materials/ Chemicals

Poly (ethylene oxide)- block poly (propylene oxide) - block poly (ethylene oxide) (P123), carbon tetrachloride (CCl_4) and dichloromethane were purchased from Sigma Aldrich, Ontario, Canada. Nitric acid ($\geq 70.0\%$), methanol ($>99.0\%$), toluene ($>99.0\%$) and acetic acid ($>99.0\%$) were purchased from Fisher Chemical, Saskatoon, Canada. Aluminum isopropoxide (98.0%) and ethylenediamine (99.0%) were purchased from Alfa Aesar, Saskatoon, Canada. Titanium isopropoxide (98.0%) and hydrochloric acid (37.0%) were purchased from Acros Organics, Saskatoon, Canada. 2, 7- Dinitro-9-fluorenone was purchased from Tokyo chemical industry and anhydrous ethanol (100%) was purchased from Commercial alcohols, Saskatoon, Canada.

4.1.2 Preparation of adsorbents

The synthesis method of the charge transfer adsorbents used in this study was described in detail in our previous publication (Botana de la Cruz et al., 2020). In brief, adsorbents A, B, and C were prepared with the mesoporous Al_2O_3 , Ti-substituted mesoporous Al_2O_3 and commercial γ -alumina supports, respectively. The syntheses of adsorbents involved (i) preparation of supports, (ii) anchoring of linker, ethylenediamine on supports, and (iii) immobilization of a π -acceptor, 2,7-dinitro-9-fluorenone on supports.

4.2 Process parameter Optimization

To investigate the influence of process parameters and their combined interactions on the adsorptive desulfurization process, a set of experiments was designed by varying process parameters, namely, temperature, adsorption time and adsorbent loading. The model feed concentration was kept constant. Experiments were designed by the Central Composite Design (CCD) approach using the Design Expert® software (version 6.0.11, State-Ease Inc., Minneapolis, USA). Briefly, the CCD method is used to optimize the conditions of a known multi-variable system as it evaluates the influence of the independent variables in a set of experiments given (Vaez et al., 2012).

Table 4.1 Optimization parameters and their corresponding range used for the Central Composite Design.

Variables	Symbols	Range	
Temperature (°C)	X	22	60
Time (min)	Y	15	60
Adsorbent loading (g)	Z	0.25	0.75

Table 4.1 shows the ranges of variables used to design. As given in Table 4.2, a set of 19 experiments (14 unique) was designed, with the center point experiment replicated 5 times. Experiments were repeated to check reproducibility under the same set of conditions. The model feed used in this study contained 541 ppm of sulfur which was prepared by dissolving thiophene in ultra-low sulfur diesel (ULSD). The typical adsorption experiment was carried out placing 0.5 g of the adsorbent and 2.5 g of the model feed in a glass vial with a cap. Using a magnetic stirrer at 400 rpm, the adsorbent and the model feed were mixed at 22°C for 24 h and the liquid product was separated from the adsorbent by vacuum filtration and analyzed using an Antek N/S analyzer.

Table 4.2 Design of experiments for adsorption of sulfur and nitrogen species

Run number	Adsorbent loading (g)	Temperature (°C)	Time (min)
1	0.75	22	60
2	0.75		27
3	0.25		60
4	0.25		27
5	0.75	60	60
6	0.75		27
7	0.25		60
8	0.25		27
9	0.5	41	43
10	0.5		43
11	0.5		71
12	0.5		43
13	0.5		43
14	0.5		43
15	0.5		15
16	0.5		43
17	0.92		43
18	0.08	43	
19	0.5	73	43

4.2.1 Adsorption parameters optimization studies

The effects of time, temperature and adsorbent loading on sulfur removal were determined by plotting a three-dimensional (3D) response surface and control graphs (see Figure 4.1). Adsorbent A shows its highest adsorption activity with 76.3% of sulfur removal at an adsorbent loading of 20%, 41°C and a reaction time of 43 min. However, at a temperature of 22°C, an adsorbent loading of 30% and a reaction time of 27 min, adsorbent A shows 74.0% sulfur removal. In terms of energy requirements, adsorption at 41°C might not be ideal as compared to 22°C.

Besides, raising the temperature by 20°C increased the sulfur removal only by 2 wt.%. Adsorbent B showed a maximum sulfur removal of 57.2 wt.% at an adsorbent loading of 10% (0.25 g), a temperature of 60°C and an adsorption time of 27 min. Similarly, adsorbent C reached its maximum adsorption capacity at an adsorbent loading of 30% (0.75 g), a temperature of 22°C and

an adsorption time of 27 min, resulting a sulfur removal of 88.7 wt. %.

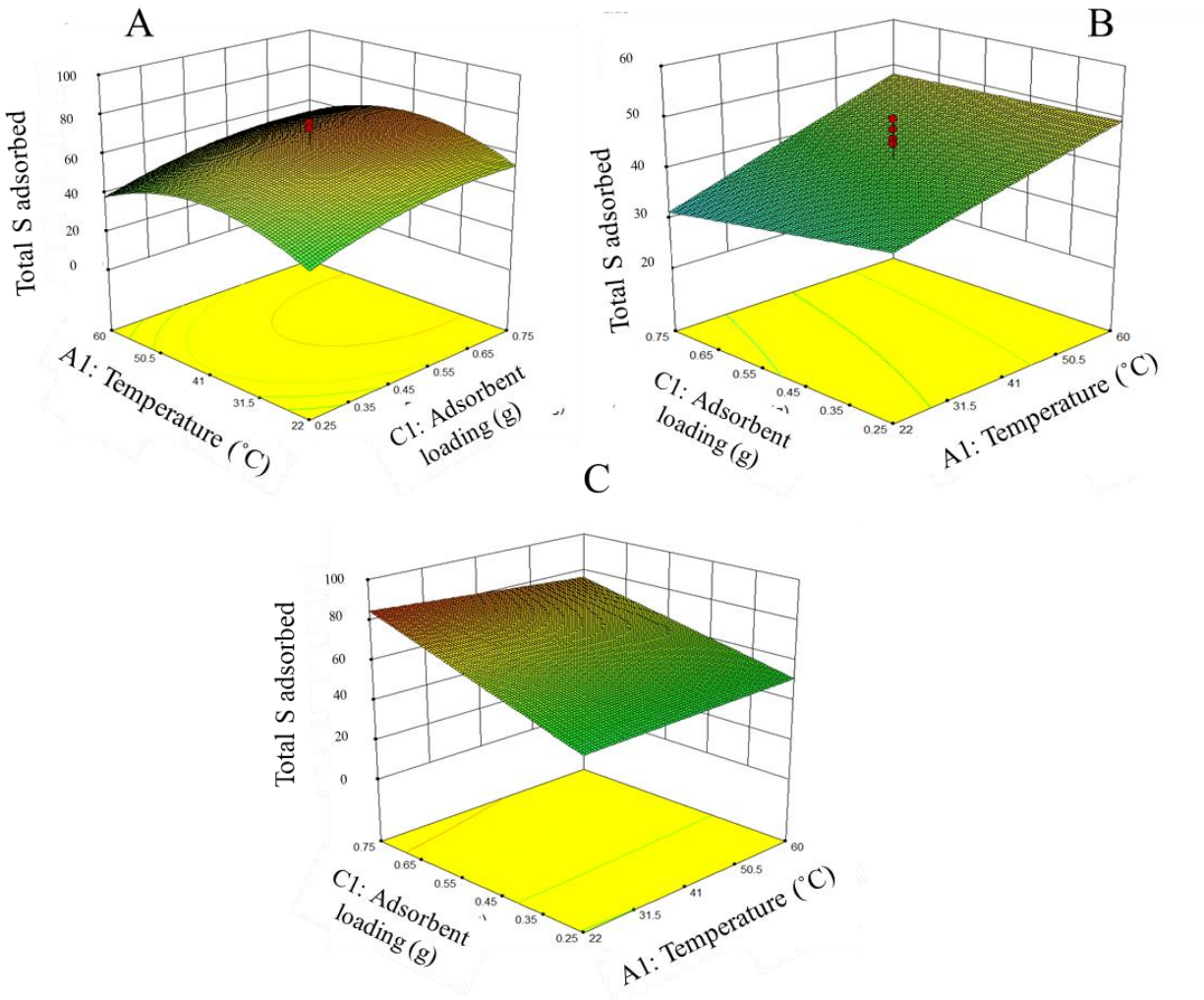


Figure 4.1 The three-dimensional response surfaces: effects of temperature and adsorbent loading on desulfurization activity of adsorbents A, B and C.

To fit the response function on sulfur removal, regression analysis was performed. The model equation for sulfur removal for adsorbents A, B and C are shown in Table 3. The individual effect of each of the process parameters such as temperature (X), time (Y) and adsorbent loading (Z), and combined effects of two of the process parameters on sulfur adsorption can be distinguished by using equations given in Table 3. For example, the effects of X-Y, X-Z, and Y-Z are not as significant as the individual effect of X, Y and Z on the sulfur adsorption capacity of the adsorbent A.

Table 4.3 Linear equations for adsorbents A, B and C from Composite Design Expert based on the proposed set of experiments.

Adsorbent	Linear equation
A	Total S removal= $-5.37+0.17X + 111.04Y +68.99Z - 0.60XY - 0.44XZ - 75.31YZ$
B	Total S removal= $50.73 + 0.34X - 55.31Y - 19.13Z + 0.30XY - 0.17XZ + 48.46 YZ$
C	Total S removal = $103.46 - 0.01X - 1.63Y - 104.90Z - 0.54XY + 0.27XZ + 116.77YZ$

Note: Where X,Y and Z are temp.(°C), time (h) and adsorbent loading (wt.%), respectively.

4.3 Adsorption kinetics

Apart from the results of the experimental studies, mathematical modeling is an efficient method for analysis of any chemical process. Theoretical and empirical models are used to fit experimental data. Using this method provides information to understand and simulate the adsorptive removal of sulfur in from fuels that can potentially reduce the cost of experiments and increase the feasibility of the adsorption process. In this case, empirical models were used, pseudo-first and pseudo-second order kinetic model; these models are known for their simplicity when modelling experimental data.

Kinetic studies were conducted in a stirred batch system consisting of a 15 mL glass vial in which a mixture of the adsorbent and the model feed was stirred at 400 rpm. The adsorbent to feed ratio was maintained at 1:5. To determine the minimum time required for the adsorbent to reach adsorption equilibrium, the experiments were carried at different times ranging from 15 min to 72 h. To investigate the adsorption mechanism, the temperature was kept constant at 22°C.

After the duration for adsorption was elapsed, the adsorbent was filtered under vacuum and the treated feed was collected in a vial for total sulfur and nitrogen analysis using an Antek analyzer. Following the N/S analysis, the adsorption efficiency was calculated using the formula shown below:

$$S \text{ removal efficiency (\%)} = \frac{S \text{ in the untreated feed (ppm)} - S \text{ in the treated feed}}{S \text{ in the untreated feed (ppm)}} \times 100 \quad (4.1)$$

The equilibrium capacity of the adsorbents was calculated using the following formula:

$$q_e = \frac{C_0 - C_e}{m} V \quad (4.2)$$

Where C_0 and C_e are the initial and equilibrium concentrations of sulfur (mg L^{-1}) respectively, V is the volume of the feed used (L), and m is the mass of the adsorbent (g).

4.3.1 Kinetic studies

To analyze the data from the adsorption experiments, two conventional kinetic models were used, pseudo-first and pseudo-second order models (Boahene et al., 2013; Malik, 2004). Figure 4.2 shows the adsorption kinetic curves for the pseudo-first-order model of adsorbents A, B and C for sulfur removal. The pseudo-first order model formula was rearranged for linearized data plotting and is shown below:

$$\ln(q_e - q_t) = \ln q_e - k_1 * t \quad (4.3)$$

Where q_e and q_t are amounts of sulfur compound adsorbed at equilibrium (q_e) and at various times (q_t) calculated in (mg g^{-1}) and k_1 is the rate constant of the pseudo-first-order model of adsorption (min^{-1}). The values of q_e and k_1 can be calculated using the intercept and slope of the linear plot of $\ln(q_e - q_t)$ versus t (see equation 4.3).

$$\frac{t}{q_t} = \frac{1}{k_2 q_e^2} + \frac{t}{q_e} \quad (4.4)$$

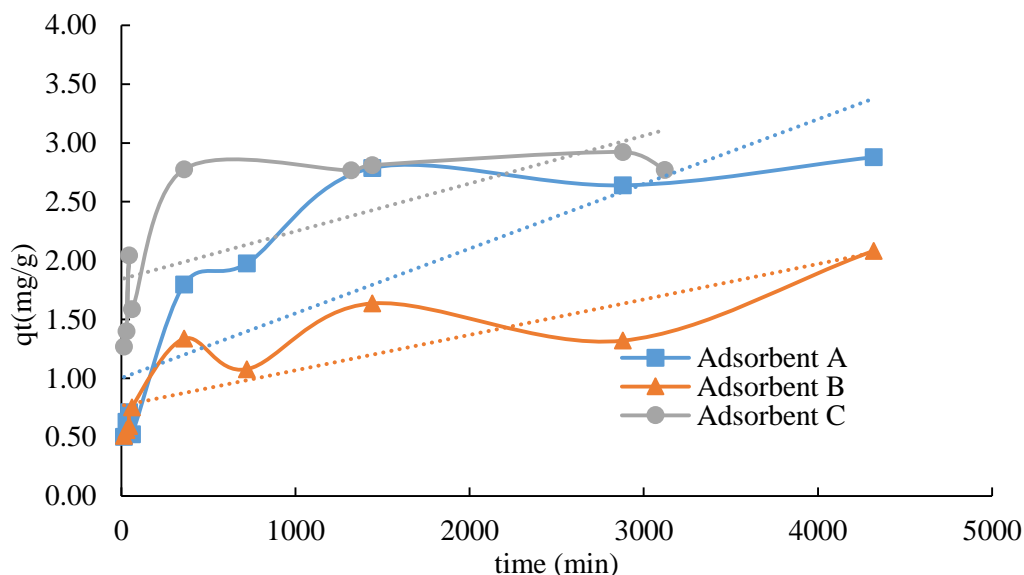


Figure 4.2 Pseudo first-order adsorption kinetics of adsorbents A, B and C. Temperature =22°C, feed to adsorbent ratio=5. The solid line is the results for the kinetic model; the dash line is pseudo first-order-model simulation

For the pseudo-first order model, values of q_e and k_1 were calculated, which are shown in Table 4.4, along with other kinetic parameters and correlation coefficients. The experimental data deviated considerably from the theoretical data. Also, the theoretical q_e values found from the first-order kinetic model did not give reasonable values. The kinetic parameters of the pseudo-second order model are also presented in Table 4.4. From this table, it can be seen that the pseudo-second order model (see equation 4.4) adequately fits the adsorption experimental data for all three adsorbents. This observation was corroborated by the correlation coefficient R^2 values obtained from this model. For adsorbents A and C the R^2 values were higher than for adsorbent B; however, the pseudo-first-order model did not show R^2 higher than 0.5. For the pseudo-second order model, both adsorbents A and C showed R^2 values greater than 0.99; suggesting a better correlation of the experimental data to the kinetic model. As it can be observed on Figure 4.3

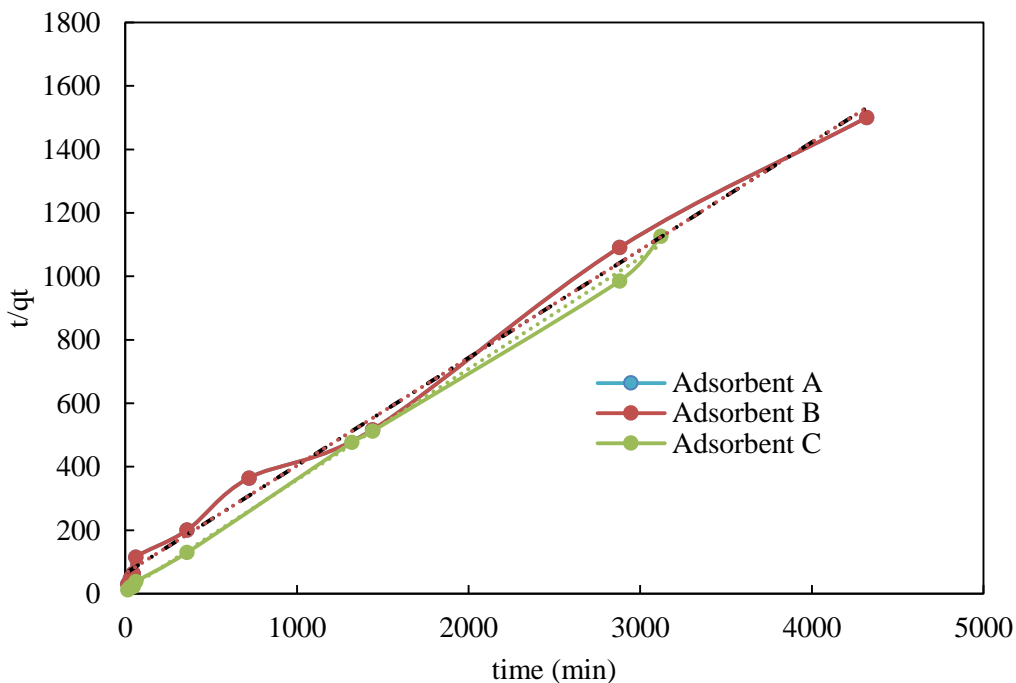


Figure 4.3. Pseudo first-order adsorption kinetics of adsorbents A, B and C. Temperature =22°C, feed to adsorbent ratio=5. The solid line is the results for the kinetic model; the dash line is pseudo first-order-model simulation.

Table 4.4 Kinetic parameters for pseudo-first and pseudo-second-order model

Adsorbent	Pseudo-first order model				Pseudo-second order model		
	q_e (exp) (mg·g ⁻¹)	q_e (cal) (mg·g ⁻¹)	K_1 (min ⁻¹)	R^2	q_e (cal) (mg·g ⁻¹)	K_2 (g·mg ⁻¹ ·min ⁻¹)	R^2
A	2.79	-0.00112	3.5E-04	0.39	1.01	1.59E-02	0.99
B	2.08	-0.00021	3.4E-05	0.18	1.20	1.22E-02	0.92
C	2.78	-0.00117	-9.0E-04	0.33	1.03	9.21E-03	0.99

Values for q_e (exp) and q_e (cal) highly differ for the pseudo-first and second order models, the negative k_1 values indicates that they are not significant for the model (Pan and Xing, 2010), as can be expected when looking at the R^2 values. Even though the q_e (exp) value for adsorbent B seems to be closer to the q_e (cal); this does not mean that it depends entirely on the adsorptive behavior. The R^2 for the pseudo-second order model for adsorbent B is the lowest with a value of ~ 0.92 when compared to those for adsorbents A and C; meaning that the pseudo-second order model fits better for adsorbents A and C adsorption data. The pseudo-second order model is also known as the double-exponential model or a two-step mechanism (Li et al., 1999). Michard et al. 1996, proposed a diffusion control mechanism consisted of two-steps. In the first one, a rapid uptake of adsorbate takes place; this involves internal and external diffusion. In the second step, the adsorption rate is controlled by the intraparticle diffusion before the adsorption reaches equilibrium. Therefore; the pseudo-second order model can be consider a diffusion model.

4.4 Adsorption thermodynamics

Using the reaction rate constant of the pseudo-second-order model, the activation energies of the three adsorbents were calculated following a method reported by Laidler, 1984. Using the Arrhenius equation, the activation energy, E_2 , was calculated as shown below:

$$\ln E_2 = -\frac{E_a}{RT} + \ln A \quad (4.5)$$

Moreover, using the data obtained from the adsorption experiments, the free activation energy (ΔG^0) was determined by assuming that the adsorption process happened spontaneously. The changes in enthalpy (ΔH_0) and entropy (ΔS_0) were also calculated using the equations shown below:

$$\Delta G^0 = -RT \ln K_D \quad (4.6)$$

$$K_D = \frac{q_e}{C_e} \quad (4.7)$$

$$\ln K_D = \frac{\Delta S^0}{R} - \frac{\Delta H^0}{RT} \quad (4.8)$$

Where ΔG^0 ($\text{kJ}\cdot\text{mol}^{-1}$) was calculated using the Van't Hoff equation, R is the universal gas constant, $8.314 \text{ J}\cdot\text{mol}^{-1}$, T is the absolute adsorption temperature in K, K_D is the adsorption equilibrium constant. Using the slope and intercept of the plot, $\ln K_D$ vs. $1/T$, ΔH^0 and ΔS^0 were calculated.

4.4.1. Adsorption thermodynamic studies

As part of this study, the activation energy (E_a) was calculated to provide an insight into the adsorption mechanisms. Using the Arrhenius equation, the activation energies were calculated for adsorbents A, B and C. Using temperature in the range of 295-314 K, the activation energy values of 8.27, -7.62 and 8.29 $\text{kJ}\cdot\text{mol}^{-1}$ were calculated for adsorbents A, B and C and are shown in Table 4.5. The values were obtained using the intercept and slope from the plot of $\ln k_2$ vs. $1/T$ for the three adsorbents (see Appendix A).

Table 4.5 Activation energy calculated values for adsorbents A, B and C.

Adsorbent	Activation energy (E_a) (kJ/mol)
A	8.27
B	-7.62
C	8.29

An activation energy E_a of 5~40 $\text{kJ}\cdot\text{mol}^{-1}$ corresponds to physical adsorption whereas 40~800 $\text{kJ}\cdot\text{mol}^{-1}$ corresponds to a chemical adsorption (Fei et al., 2017). The activation energy suggests that adsorbents A and C remove sulfur compounds through physical adsorption. This means that no chemical reactions take place during the adsorption, instead the sulfur molecules are attracted to the adsorbent by weak forces like Van der Waals or hydrogen bonding (Duan et al., 2014). On the other hand, adsorbent B has proven to have a poor adsorption activity. This can be attributed to its poor textural properties. Therefore, the activation energy values for adsorbent B can be neglected.

The free activation energy (ΔG^0), enthalpy (ΔH^0) and entropy (ΔS^0) are usually involved in an adsorption process. To evaluate if the adsorption of an adsorbate can happen spontaneously or not, the above parameters have to be determined. In this study, the free activation energy (ΔG^0) values

for a temperature of 295 K were found to be 9.6, 13.0 and 7.5 kJ·mol⁻¹, as shown in Table 4.6 for adsorbents A, B and C, respectively. For a temperature of 314 K, the values were 10.6, 11.8 and 8.4 kJ·mol⁻¹. The positive values of ΔG^0 mean that adsorption of sulfur compounds on adsorbents A,B and C is a slow process (Zhang et al., 2017). Using $\ln K_D$ vs. $1/T$ values (see figures shown in appendix B), enthalpy and entropy values were calculated for the three adsorbents using the intercept and slope.

Table 4.6 Free activation energy values for adsorbents A, B and C.

Temperature (K)	ΔG (kJ/mol)		
	<i>Adsorbent</i>		
	A	B	C
298	9.6	13.0	7.45
314	10.6	11.82	8.37

Enthalpy (ΔH^0) values for adsorbents A, B and C were calculated to be 15.5, -19.2 and 15.3 kJ·mol⁻¹, respectively as shown in Table 4.7. Positive values of ΔH^0 indicates that the adsorption process is endothermic (Foo and Hameed, 2010), meaning that the reaction consumes energy. The change of entropy (ΔS^0) values in the adsorption system were -85.2, 20.9 and -77.1 J·mol⁻¹ K⁻¹ for adsorbents A, B and C, respectively. Negative entropy values among adsorbents A and C indicate the absence of significant change in the internal structure of the adsorbent during the adsorption process. This is in accordance with the better textural properties of adsorbents A and C, compared to adsorbent B as reported previously (Botana de la Cruz et al., 2020).

Table 4.7 Enthalpy and entropy values for adsorbents A, B and C.

Adsorbent	ΔH (kJ/mol)	ΔS (J/mol K)
A	7.91	-59.65
B	-12.58	0.51
C	7.87	-52.19

4.5 Regeneration and reusability studies

Regeneration is a process in which the adsorbent is returned to its state prior to be used for adsorption. This has to be easily performed in order to reuse the adsorbents without affecting the viability of the process (Li et al., 2016). Thermal treatment, ultrasound and solvent extraction method have been used to regenerate the spent adsorbent. Solvent extraction has been reported to be the most efficient method to remove sulfur and nitrogen compounds (Han et al., 2014). Considering there are no SO_x and NO_x emissions, regeneration using solvent extraction might be consider an environmentally friendly process. Regeneration of the adsorbent is usually performed so the adsorbent can undergo further regeneration. Reusability studies provide the necessary information for industrial application as the adsorption process can be scale (Misra et al., 2018; Zolotareva et al., 2019).

The reusability of adsorbents was studied at the same process conditions (1:5 adsorbent to feed ratio, time=24 h, temperature= 22°C and 400 rpm) that were used for the screening of fresh adsorbents. After the 24 h adsorption reaction, the adsorbent was regenerated using 3 different solvents, chloroform, dichloromethane and carbon tetrachloride using a Soxhlet extraction set-up shown in Figure 4.4.

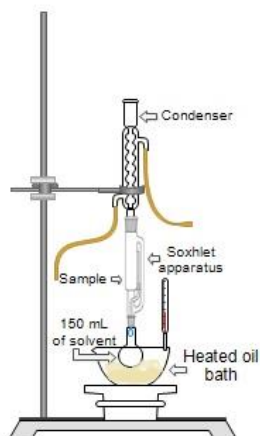


Figure 4.4 Schematic of Soxhlet extraction set-up used for regeneration.

The spent adsorbent was placed inside the soxhlet apparatus on a thimble and extracted with 150 mL of solvent. During the Soxhlet extraction, the solvent was placed in a 250 mL round-bottom flask connected to a reflux condenser in an immersed heated oil bath maintained at the boiling point of each solvent. The extraction was carried out for 8 h, and then adsorbent was dried and tested for reusability.

4.5.1 Regeneration and reusability studies

After the regeneration experiments, solvents were concentrated using a rotary evaporator and analyzed for their sulfur levels. The sulfur extraction efficiencies of chloroform, carbon tetrachloride and dichloromethane with adsorbent A (spent material) are shown in Figure 4.5.

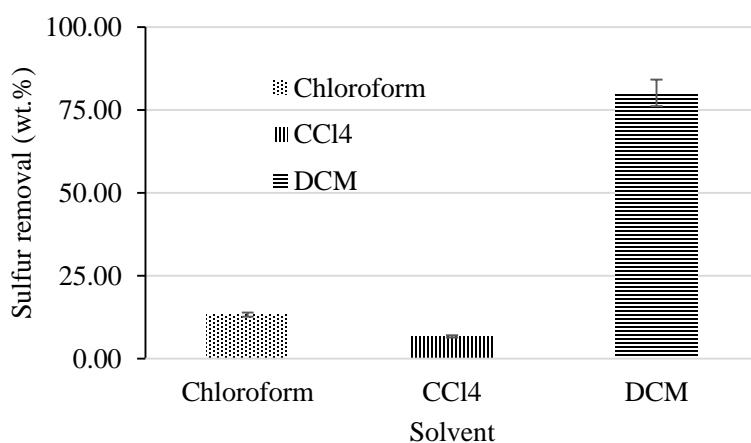


Figure 4.5 Sulfur removal from Adsorbent A after 8 h of regeneration with chloroform, carbon tetrachloride and dichloromethane

The highest sulfur removal was achieved using dichloromethane. It removed 80% of sulfur molecules that were adsorbed on adsorbent A. The reusability of adsorbent A was studied for three times by regenerating with DCM.

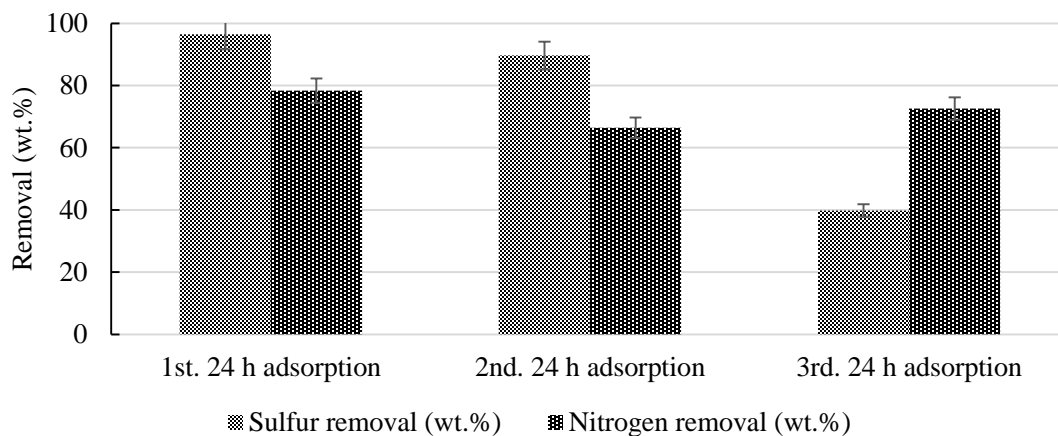


Figure 4.6 Reusability results for adsorbent A using dichloromethane as solvent

The fresh adsorbent showed 96.5% of sulfur removal. After the first regeneration, the sulfur removal efficiency dropped by only 7%. A significant drop was noted when adsorbent A was reused for the third time. The nitrogen analysis of the solvent extract was carried out to determine leaching of the immobilized EDA linker and π -acceptor during regeneration with DCM. The solvent extract of first and second regeneration contained 86.0 and 93.5 ppm of nitrogen respectively, due to leaching of EDA and DNF. The leaching of DNF from adsorbent A is expected to drop the number of available adsorption sites and thus its adsorption capacity after successive regenerations.

Chapter 5 : Conclusions and recommendations

5.1 Conclusions

The overall objective of this research work was to study the performance of π -acceptor immobilized alumina-based materials as adsorbent for the removal of sulfur and nitrogen impurities from liquid fuels. The goal was to improve the efficiency of hydrotreating in terms of less catalyst loading, lower reaction temperature, and low severity conditions by using an adsorption process as compared to typical hydrotreating process. The sub-objectives were (1) to investigate the effects of the proposed synthesis method and its impact on the adsorbent properties for sulfur and nitrogen compounds present in liquid fuels, and (2) to study process optimizations, kinetics and long-term stability of potential adsorbent identified in above sub-objective.

Three different charge-transfer complex (CTC) adsorbents for desulfurization of liquid fuels were prepared and characterized. The BET surface area measurement study evidenced the mesoporous nature of all three adsorbents based on their textural properties; surface area, pore size and pore volume. The FTIR, TGA and XRD studies confirmed the successful incorporation of the π -acceptor on the support. Furthermore, adsorption experiments were conducted with a model feed of 500 ppm sulfur. The CTC adsorbents prepared based on mesoporous alumina (Adsorbent A) and commercial γ -alumina (Adsorbent C) showed higher sulfur removal than the Ti incorporated material (Adsorbent B). The adsorbents successfully desulfurized the model feed used.

The poor performance of adsorbent B was due to leaching of the linker and π -acceptor in the adsorption medium (ULSD). This does not support the hypothesis that TiO_2 supported systems show high activity. No leaching of the linker and π -acceptor was observed with adsorbents A and C. The adsorption capacity profiles of adsorbents A and C are logarithmic with the monolayer and multilayer adsorptions. Between adsorbent A and C, it is concluded that adsorbent C is more suitable for sulfur removal due to the shorter equilibrium time of adsorption.

Furthermore, the optimization studies showed that the adsorption experiments should be conducted under ambient conditions ($\sim 22^\circ\text{C}$) as high sulfur removal was observed at this temperature. The pseudo-second-order model had the best fit with the kinetic data of all three adsorbents. **From the** kinetic studies, the activation energy (E_a) values were calculated, which indicated that the adsorption is physical in nature when adsorbents A and C are used for adsorption. The values of

free activation energy suggested that the adsorption of sulfur compounds was a slow process. Enthalpy values showed that adsorption on adsorbent A and C is endothermic. Entropy values indicated that adsorbent A and C experienced no significant change in their internal structure. The results of regeneration experiments showed that dichloromethane was relatively more effective as a solvent for regeneration, and the adsorbent A can be reused at least three times.

5.2 Recommendations

- Textural properties such as surface area, pore size and pore volume of the synthesized supports can be improved and enhance the adsorptive desulfurization and denitrogenation activity.
- An increase of the nitrogen concentration of the batch adsorption experiments might suggest leaching of the N-compounds (linker and π -acceptor) present in the adsorbent. The effect of the linker and π -acceptor loading onto the support can be tested to avoid leaching of these compounds onto the feed.
- For this study, pyridine and thiophene were used as nitrogen and sulfur compounds in the model feed. However, the presence of more nitrogen and sulfur compounds might show a different adsorptive efficiency among the adsorbents. Introducing more nitrogen and sulfur compounds on the feed can be explored and the affinity towards certain compounds can be analyzed.
- The used solvent should be separated from the pollutants and recycled. Also, the separated sulfur and nitrogen compounds should be reutilized for improving the economics of the entire process. Finally, techno-economic analysis of the entire process should be carried out for determining the viability of this technology.

References

- A.R Gonzalez-Elipse, G. Munuera, J. .. Espinos. 1989. "Compositional Changes Induced by 3.5 KeV Ar+ Ion Bombardment in Ni-Ti Oxide Systems." *Surface Science* 220:368–80.
- Abedi, Ali, Jackson Chitanda, Ajay K. Dalai, and John Adjaye. 2015. "Synthesis and Application of Functionalized Polymers for the Removal of Nitrogen and Sulfur Species from Gas Oil." *Fuel Processing Technology* 131:473–82.
- Abedi, Ali, Jackson M. Chitanda, Ajay K. Dalai, and John Adjaye. 2016. "Graft Copolymerization of Glycidyl Methacrylate and Ethylene Glycol Dimethacrylate on Alumina for the Removal of Nitrogen and Sulfur Compounds from Gas Oil." *Industrial and Engineering Chemistry Research* 55(35):9408–15.
- Ahmed, M. A. 2011. "Structural and Nano-Composite Features of TiO₂ – Al₂O₃ Powders Prepared by Sol – Gel Method." 509:2154–59.
- Akelah, Ahmed and David C. Sherrington. 1981. "Application of Functionalized Polymers in Organic Synthesis." *Chemical Reviews* 81(6):557–87.
- Almarri, Masoud, Xiaoliang Ma, and Chunshan Song. 2009. "Selective Adsorption for Removal of Nitrogen Compounds from Liquid Hydrocarbon Streams over Carbon- and Alumina-Based Adsorbents." *Industrial and Engineering Chemistry Research* 48(2):951–60.
- Alphonse, Pierre and Benjamin Faure. 2013a. "Microporous and Mesoporous Materials Synthesis of Highly Porous Alumina-Based Materials." *Microporous and Mesoporous Materials* 181:23–28.
- Alphonse, Pierre and Benjamin Faure. 2013b. "Synthesis of Highly Porous Alumina-Based Materials." *Microporous and Mesoporous Materials* 181:23–28.
- Auerbach, Scott, Kathleen Carrado, Prabir Dutta, Shivaji Sircar, and Alan Myers. 2003. "Gas Separation by Zeolites." *Handbook of Zeolite Science and Technology*.
- Badoga, Sandeep, Rajesh V. Sharma, Ajay K. Dalai, and John Adjaye. 2014. "Hydrotreating of Heavy Gas Oil on Mesoporous Mixed Metal Oxides (M-Al₂O₃, M = TiO₂, ZrO₂, SnO₂) Supported NiMo Catalysts: Influence of Surface Acidity." *Industrial and Engineering Chemistry Research* 53(49):18729–39.
- Badoga, Sandeep, Rajesh V. Sharma, Ajay K. Dalai, and John Adjaye. 2015. "Synthesis and Characterization of Mesoporous Aluminas with Different Pore Sizes: Application in NiMo Supported Catalyst for Hydrotreating of Heavy Gas Oil." *Applied Catalysis A: General* 489:86–97.
- Badoga, Sandeep, Ketaki Sohani, Ying Zheng, and Ajay K. Dalai. 2017. "Mesoporous Alumina and Alumina-Titania Supported KCuFe Catalyst for Fischer-Tropsch Synthesis: Effects of CO₂ and CH₄ Present in Syngas." *Fuel Processing Technology* 168(August):140–51.
- Baia, Luana V., Wallace C. Souza, Ricardo J. F. De Souza, Cláudia O. Veloso, Sandra S. X. Chiaro, and Marco Antonio G. Figueiredo. 2017. "Removal of Sulfur and Nitrogen Compounds from Diesel Oil by Adsorption Using Clays as Adsorbents." *Energy and Fuels* 31(11):11731–42.
- Bedda, K., Hamada, B., Semikin, K.V., Kuzichkin, N. V. 2019. "Petroleum and Coal

- Desulfurization of Light Cycle Oil by Extraction with Polar Organic Solvents.” 61:1352–60.
- Biesinger, Mark C., Leo W. M. Lau, Andrea R. Gerson, and Roger St C. Smart. 2010. “Resolving Surface Chemical States in XPS Analysis of First Row Transition Metals, Oxides and Hydroxides: Sc, Ti, V, Cu and Zn.” *Applied Surface Science* 257(3):887–98.
- Biswas, Piyali, Prabhu Narayanasarma, Chandra Mouli Kotikalapudi, Ajay K. Dalai, and John Adjaye. 2011. “Characterization and Activity of ZrO₂ Doped SBA-15 Supported NiMo Catalysts for HDS and HDN of Bitumen Derived Heavy Gas Oil.” *Industrial and Engineering Chemistry Research* 50(13):7882–95.
- Boahene, Philip E., Kapil K. Soni, Ajay K. Dalai, and John Adjaye. 2013. “Hydroprocessing of Heavy Gas Oils Using FeW/SBA-15 Catalysts: Experimentals, Optimization of Metals Loading, and Kinetics Study.” *Catalysis Today* 207:101–11.
- Bokade, Vijay V. and Ganapati D. Yadav. 2009. “Transesterification of Edible and Nonedible Vegetable Oils with Alcohols over Heteropolyacids Supported on Acid-Treated Clay.” *Industrial and Engineering Chemistry Research* 48(21):9408–15.
- Botana de la Cruz, Anakaren, Philip Boahene, Sundaramurthy Vedachalam, Ajay K. Dalai, and John Adjaye. 2020. “Adsorptive Desulfurization through Charge-Transfer Complex Using Mesoporous Adsorbents.” *Fuel* 269(February):117379.
- Bu, Jie, Gabriel Loh, Chuandayani Gunawan Gwie, Silvia Dewiyanti, Michael Tasrif, and Armando Borgna. 2011. “Desulfurization of Diesel Fuels by Selective Adsorption on Activated Carbons: Competitive Adsorption of Polycyclic Aromatic Sulfur Heterocycles and Polycyclic Aromatic Hydrocarbons.” *Chemical Engineering Journal* 166(1):207–17.
- Canada, Government of. n.d. “Sulphur-Gasoline @ Www.Canada.Ca.”
- Chang, Hua and Zong Xin Wu. 2009. “Experimental Study on Adsorption of Carbon Dioxide By 5A Molecular Sieve for Helium Purification of High-Temperature Gas-Cooled Reactor.” *Industrial and Engineering Chemistry Research* 48(9):4466–73.
- Chiou, Ming Shen and Hsing Ya Li. 2002. “Equilibrium and Kinetic Modeling of Adsorption of Reactive Dye on Cross-Linked Chitosan Beads.” *Journal of Hazardous Materials* 93(2):233–48.
- Chitanda, Jackson M., Prachee Misra, Ali Abedi, Ajay K. Dalai, and John D. Adjaye. 2015. “Synthesis and Characterization of Functionalized Poly(Glycidyl Methacrylate)-Based Particles for the Selective Removal of Nitrogen Compounds from Light Gas Oil: Effect of Linker Length.” *Energy and Fuels* 29(3):1881–91.
- Duan, Feifei, Chaoqiu Chen, Guizhen Wang, Yongzhen Yang, Xuguang Liu, and Yong Qin. 2014. “Efficient Adsorptive Removal of Dibenzothiophene by Graphene Oxide-Based Surface Molecularly Imprinted Polymer.” *RSC Advances* 4(3):1469–75.
- Duprez, Daniel, Adam F. Lee, Karen Wilson, Sandeep Badoga, Rajesh V. Sharma, Ajay K. Dalai, John Adjaye, S. K. Maity, J. Ancheyta, L. Soberanis, F. Alonso, M. E. Llanos, Sandeep Badoga, Rajesh V. Sharma, Ajay K. Dalai, John Adjaye, Vahid Vosoughi, Sandeep Badoga, Ajay K. Dalai, Nicolas Abatzoglou, John Adjaye, Yongfeng Hu, Jie Bu, Gabriel Loh, Chuandayani Gunawan Gwie, Silvia Dewiyanti, Michael Tasrif, Armando Borgna, Hong Yang, Jinwen Chen, Craig Fairbridge, Yevgenia Briker, Yu Jie Zhu, and

- Zbigniew Ring. 2011. "Inhibition of Nitrogen Compounds on the Hydrodesulfurization of Substituted Dibenzothiophenes in Light Cycle Oil." *Fuel Processing Technology* 489(1):86–97.
- Duprez, Daniel and Karen Wilson. 2009. "An Efficient Route to Highly Organized , Tunable Macroporous - Mesoporous." 12896–97.
- Espantaleón, A. G., J. A. Nieto, M. Fernández, and A. Marsal. 2003. "Use of Activated Clays in the Removal of Dyes and Surfactants from Tannery Waste Waters." *Applied Clay Science* 24(1–2):105–10.
- Favvas, Evangelos P., Nikolaos S. Heliopoulos, Sergios K. Papageorgiou, Athanasios Ch Mitropoulos, George C. Kapantaidakis, and Nick K. Kanellopoulos. 2015. "Helium and Hydrogen Selective Carbon Hollow Fiber Membranes: The Effect of Pyrolysis Isothermal Time." *Separation and Purification Technology* 142:176–81.
- Fei, Liu, Jingwei Rui, Rijing Wang, Yanfei Lu, and Xiaoxia Yang. 2017. "Equilibrium and Kinetic Studies on the Adsorption of Thiophene and Benzothiophene onto NiCeY Zeolites." *RSC Advances* 7(37):23011–20.
- Fleming, Hubert L., P. Kenneth, and K. Emmanuel. 1988. "United States Patent (19) Patent Number : 4762537." (19).
- Foo, K. Y. and B. H. Hameed. 2010. "Insights into the Modeling of Adsorption Isotherm Systems." *Chemical Engineering Journal* 156(1):2–10.
- Fu, Jinmei, Geoffrey C. Klein, Donald F. Smith, Sunghwan Kim, Ryan P. Rodgers, Christopher L. Hendrickson, and Alan G. Marshall. 2006. "Comprehensive Compositional Analysis of Hydrotreated and Untreated Nitrogen-Concentrated Fractions Syncrude Oil by Electron Ionization, Field Desorption Ionization, and Electrospray Ionization Ultrahigh-Resolution FT-ICR Mass Spectrometry." *Energy and Fuels* 20(3):1235–41.
- Gonz, V. and E. Sastre. 2001. "Thermally Stable Mesoporous Alumina Synthesized with Non-Ionic Surfactants in the Presence of Amines." 45:203–10.
- Guevara, A., A. Alvarez, and M. Vrinat. 2008. "Effect of TiO₂-Al₂O₃sol-Gel Supports on the Superficial Ni and Mo Species in Oxidized and Sulfided NiMo/TiO₂-Al₂O₃catalysts: Influence on Dibenzothiophene Hydrodesulfurization." *Catalysis Letters* 126(3–4):268–74.
- Ha, Jeong W., Tenzing Japhe, Tesfamichael Demeke, Bertin Moreno, and Abel E. Navarro. 2018. "Clean Technologies on the Removal and Desorption of Sulfur Compounds from Model Fuels with Modified Clays." 58–69.
- Han, Xue, Hongfei Lin, and Ying Zheng. 2014. "Regeneration Methods to Restore Carbon Adsorptive Capacity of Dibenzothiophene and Neutral Nitrogen Heteroaromatic Compounds." *Chemical Engineering Journal* 243:315–25.
- Heilig, Morton L. 1994. "United States Patent Office." *Computer Graphics* 28(2):131–34.
- Hendricks, David. 2011. *Water Treatment Unit Processes*. Boca Raton: Taylor and Francis Group, LLC.
- Hentze, H. P. and M. Antonietti. 2002. "Porous Polymers and Resins for Biotechnological and Biomedical Applications." *Reviews in Molecular Biotechnology* 90(1):27–53.
- Herbert, Javier, Víctor Santes, Maria Teresa Cortez, René Zárate, Leonardo Díaz, Ali Abedi,

- Jackson M. Chitanda, Ajay K. Dalai, John Adjaye, M. A. Ahmed, Silvester Tursiloadi, Hiroaki Imai, Hiroshi Hirashima, Jae Hyung Kim, Xiaoliang Ma, Anning Zhou, and Chunshan Song. 2005. "Catalytic Hydrotreating of Heavy Gasoil FCC Feed over a NiMo/ γ -Al₂O₃-TiO₂ Catalyst: Effect of Hydrogen Sulfide on the Activity." *Catalysis Today* 111(1–2):74–83.
- Hernández-Maldonado, Arturo J. and Ralph T. Yang. 2003. "Desulfurization of Commercial Liquid Fuels by Selective Adsorption via π -Complexation with Cu(I)-Y Zeolite." *Industrial and Engineering Chemistry Research* 42(13):3103–10.
- Jayaraman, Ambalavanan, Frances H. Yang, and Ralph T. Yang. 2006. "Effects of Nitrogen Compounds and Polyaromatic Hydrocarbons on Desulfurization of Liquid Fuels by Adsorption via π -Complexation with Cu(I)Y Zeolite." *Energy and Fuels* 20(3):909–14.
- Kale, S., S. B. Umbarkar, M. K. Dongare, R. Eckelt, U. Armbruster, and A. Martin. 2015. "Selective Formation of Triacetin by Glycerol Acetylation Using Acidic Ion-Exchange Resins as Catalyst and Toluene as an Entrainer." *Applied Catalysis A: General* 490:10–16.
- Khodabandeh, Shervin and Mark E. Davis. 2014. "Synthesis of Pure Alumina Mesoporous Materials." *Chemistry of Materials* 4756(5):1451–64.
- Kim, Jae Hyung, Xiaoliang Ma, Anning Zhou, and Chunshan Song. 2006. "Ultra-Deep Desulfurization and Denitrogenation of Diesel Fuel by Selective Adsorption over Three Different Adsorbents: A Study on Adsorptive Selectivity and Mechanism." *Catalysis Today* 111(1–2):74–83.
- Laidler, Keith J. 1984. "The Development of the Arrhenius Equation." *Journal of Chemical Education* 61(6):494–98.
- Lazzaroni, R. and M. Hecq. 2003. "Growth of Ultrathin Ti Films Deposited on SnO₂ by Magnetron Sputtering." *Thin Solid Films* 437(03):57–62.
- Lemaire, Marc, Michéle Monnet, Michel Vrinat, Valérie Lamure, Emmanuelle Sanson, and Alexandra Milenkovic. 2002. "Method for Separating Benzothiophene Compounds from Hydrocarbon Mixture Containing Them, and Hydrocarbon Mixture Obtained by Said Method." *US. PATENT DOCUMENTS* 1(12):1–5.
- Li, Chong Jiu, Ran Zhao, Meng Qi Peng, Hao Liu, Gang Yu, and Dong Sheng Xia. 2015. "Study on Desulfurization and Denitrification by Modified Activated Carbon Fibers with Visible-Light Photocatalysis." *Ranliao Huaxue Xuebao/Journal of Fuel Chemistry and Technology* 43(12):1516–22.
- Li, Gang, Penny Xiao, Paul Webley, Jun Zhang, Ranjeet Singh, and Marc Marshall. 2008. "Capture of CO₂ from High Humidity Flue Gas by Vacuum Swing Adsorption with Zeolite 13X." *Adsorption* 14(2–3):415–22.
- Li, Pam H. Y., Roderick L. Bruce, and Malcolm D. Hobday. 1999. "A Pseudo First Order Rate Model for the Adsorption of an Organic Adsorbate in Aqueous Solution." *Journal of Chemical Technology and Biotechnology* 74(1):55–59.
- Li, Weiwei, Jingwen Chen, Guojing Cong, Lei Tang, Qun Cui, and Haiyan Wang. 2016. "Solvent Desulfurization Regeneration Process and Analysis of Activated Carbon for Low-Sulfur Real Diesel." *RSC Advances* 6(24):20258–68.
- Li, Xiaojuan, Xingwang Zhang, and Lecheng Lei. 2009. "Preparation of CuNaY Zeolites with

- Microwave Irradiation and Their Application for Removing Thiophene from Model Fuel.” *Separation and Purification Technology* 64(3):326–31.
- Li, Y. Y., S. P. Perera, and B. D. Crittenden. 1998. “Zeolite Monoliths for Air Separation Part 2: Oxygen Enrichment, Pressure Drop and Pressurization.” *Chemical Engineering Research and Design* 76(8 A8):931–41.
- Lin, J. X., S. L. Zhan, M. H. Fang, and X. Q. Qian. 2007. “The Adsorption of Dyes from Aqueous Solution Using Diatomite.” *Journal of Porous Materials* 14(4):449–55.
- Lin, Junxiong and Lan Wang. 2009. “Comparison between Linear and Non-Linear Forms of Pseudo-First-Order and Pseudo-Second-Order Adsorption Kinetic Models for the Removal of Methylene Blue by Activated Carbon.” *Frontiers of Environmental Science and Engineering in China* 3(3):320–24.
- Liu, Bing, Xiaochen Xu, Yuan Xue, Lifen Liu, and Fenglin Yang. 2020. “Simultaneous Desulfurization and Denitrification from Flue Gas by Catalytic Ozonation Combined with NH₃/(NH₄)₂S₂O₈ Absorption: Mechanisms and Recovery of Compound Fertilizer.” *Science of the Total Environment* 706:136027.
- Macaud, Mathieu, Marc Sévignon, Alain Favre-Réguillon, Marc Lemaire, Emmanuelle Schulz, and Michel Vrinat. 2004. “Novel Methodology toward Deep Desulfurization of Diesel Feed Based on the Selective Elimination of Nitrogen Compounds.” *Industrial & Engineering Chemistry Research* 43(24):7843–49.
- Maity, S. K., J. Ancheyta, Mohan S. Rana, and P. Rayo. 2006. “Alumina - Titania Mixed Oxide Used as Support for Hydrotreating Catalysts of Maya Heavy Crude - Effect of Support Preparation Methods.” *Energy and Fuels* 20(2):427–31.
- Maity, S. K., J. Ancheyta, L. Soberanis, F. Alonso, and M. E. Llanos. 2003. “Alumina-Titania Binary Mixed Oxide Used as Support of Catalysts for Hydrotreating of Maya Heavy Crude.” *Applied Catalysis A: General* 244(1):141–53.
- Malik, P. K. 2004. “Dye Removal from Wastewater Using Activated Carbon Developed from Sawdust: Adsorption Equilibrium and Kinetics.” *Journal of Hazardous Materials* 113(1–3):81–88.
- Mccabe, Peter J. 2020. “Fossil Energy.” *Fossil Energy*.
- Mckay, G. and Northern Ireland. 1985. “The Adsorption of Various Pollutants from Aqueous Solutions onto Activated Carbon.” *Water Research* 19(4):491–95.
- McKay, G., M. J. Bino, and A. R. Altamemi. 1985. “The Adsorption of Various Pollutants from Aqueous Solutions on to Activated Carbon.” *Water Research* 19(4):491–95.
- Meille, Valérie, Emmanuelle Schulz, Michel Vrinat, and Marc Lemaire. 1998. “A New Route towards Deep Desulfurization: Selective Charge Transfer Complex Formation.” *Chemical Communications* (3):305–6.
- Michard, P., E. Guibal, T. Vincent, and P. Le Cloirec. 1996. “Sorption and Desorption of Uranyl Ions by Silica Gel: PH, Particle Size and Porosity Effects.” *Microporous Materials* 5(5):309–24.
- Milenkovic, Alexandra, David Loffreda, Emmanuelle Schulz, Henry Chermette, De Lyon, Paris Sud, Paris Xi, and Orsay Cedex. 2004. “And Experimental Study.” 1169–80.

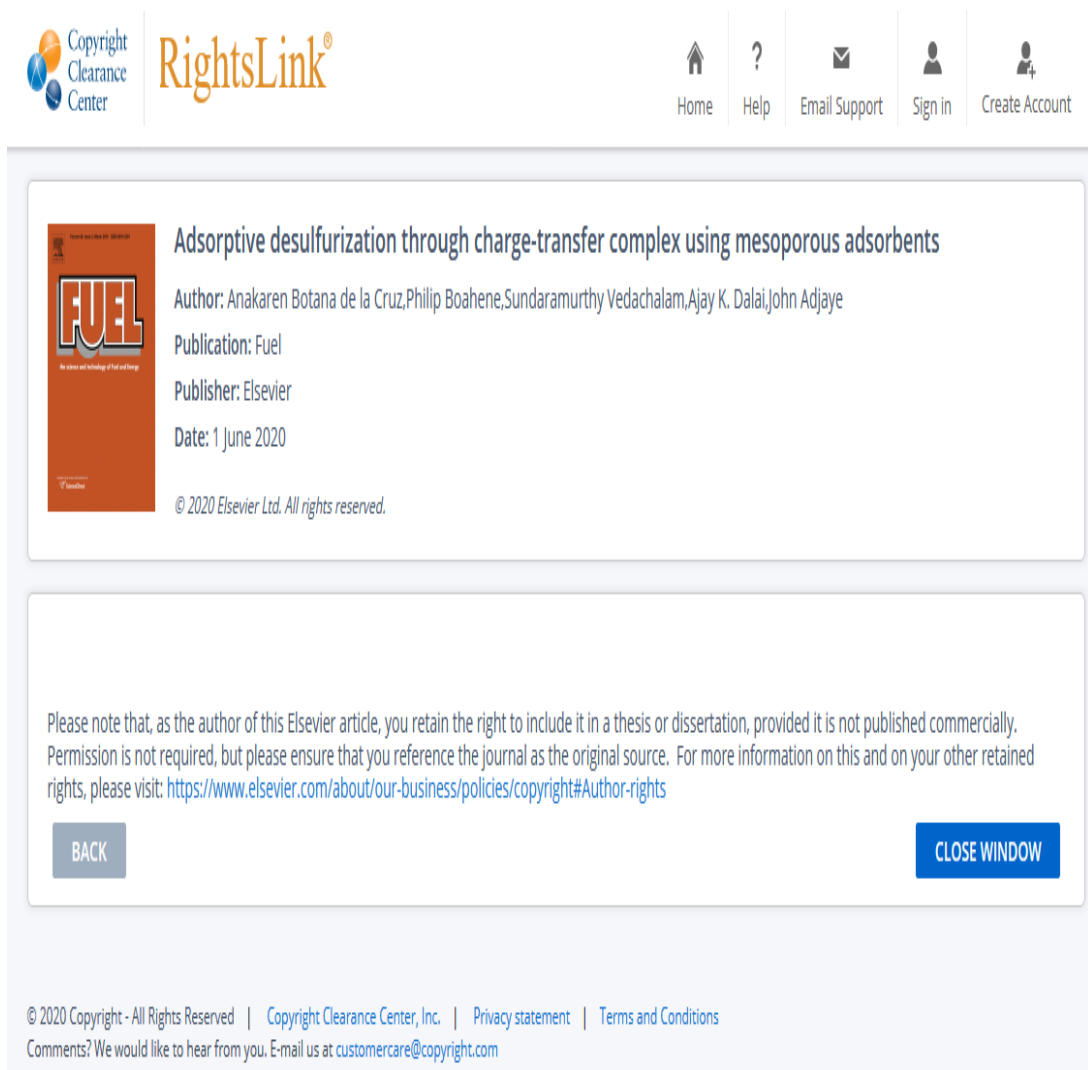
- Milenkovic, Alexandra, Emmanuelle Schulz, Valérie Meille, David Loffreda, Michel Forissier, Michel Vrinat, Philippe Sautet, and Marc Lemaire. 1999. "Selective Elimination of Alkyldibenzothiophenes from Gas Oil by Formation of Insoluble Charge-Transfer Complexes." *Energy and Fuels* 13(4):881–87.
- Misra, Prachee. 2017. "Desulfurization and Denitrogenation of Bitumen-Derived Gas Oils Using Functionalized Polymers." (May):1–164.
- Misra, Prachee, Sandeep Badoga, Ajay K. Dalai, and John Adjaye. 2018. "Enhancement of Sulfur and Nitrogen Removal from Heavy Gas Oil by Using Polymeric Adsorbent Followed by Hydrotreatment." *Fuel* 226(April):127–36.
- Misra, Prachee, Jackson M. Chitanda, Ajay K. Dalai, and John Adjaye. 2015a. "Immobilization of Fluorenone Derived π -Acceptors on Poly (GMA-Co-EGDMA) for the Removal of Refractory Nitrogen Species from Bitumen Derived Gas Oil." *Fuel* 145:100–108.
- Misra, Prachee, Jackson M. Chitanda, Ajay K. Dalai, and John Adjaye. 2015b. "Immobilization of Fluorenone Derived π -Acceptors on Poly (GMA-Co-EGDMA) for the Removal of Refractory Nitrogen Species from Bitumen Derived Gas Oil." *Fuel* 145:100–108.
- Misra, Prachee, Jackson M. Chitanda, Ajay K. Dalai, and John Adjaye. 2016. "Selective Removal of Nitrogen Compounds from Gas Oil Using Functionalized Polymeric Adsorbents: Efficient Approach towards Improving Denitrogenation of Petroleum Feedstock." *Chemical Engineering Journal* 295:109–18.
- Mochida, Isao, Yozo Korai, Masuaki Shirahama, Shizuo Kawano, Tomohiro Hada, Yorimasa Seo, Masaaki Yoshikawa, and Akinori Yasutake. 2000. "Removal of SO_x and NO_x over Activated Carbon Fibers." *Carbon* 38(2):227–39.
- Munakata, Kenzo, Teruki Fukumatsu, Satoshi Yamatsuki, and Kenji Tanaka. 1999. "Adsorption Equilibria of Krypton, Xenon, Nitrogen and Their Mixtures on Molecular Sieve 5A and Activated Charcoal." *Journal of Nuclear Science and Technology* 36(9):818–29.
- Nathan, Andrew J. and Andrew Scobell. 2012. "How China Sees America." *Foreign Affairs* 91(5):2.1-2.54.
- Niesz, Krisztian, Peidong Yang, and Gabor A Somorjai. 2005. "Sol-Gel Synthesis of Ordered Mesoporous Alumina." *RSC Advances* 1986–87.
- Niesz, Krisztian, Peidong Yang, and Gabor A. Somorjai. 2005. "Sol-Gel Synthesis of Ordered Mesoporous Alumina." *Chemical Communications* (15):1986–87.
- Pan, Bo and Baoshan Xing. 2010. "Adsorption Kinetics of 17 α -Ethinyl Estradiol and Bisphenol A on Carbon Nanomaterials. I. Several Concerns Regarding Pseudo-First Order and Pseudo-Second Order Models." *Journal of Soils and Sediments* 10(5):838–44.
- Pouilleau, J., D. Devilliers, F. Garrido, S. Durand-vidal, and E. Mah. 1997. "Structure and Composition of Passive Titanium Oxide Films." *Materials Science and Engineering* B47:235–43.
- Puoci, Francesco Iemma, Francesca Gianfranco, Unile Cirillo, Giuseppe. 2008. "Polymer in Agriculture: A Review." *American Journal of Agricultural and Biological Sciences* 299(314).
- El Qada, Emad N., Stephen J. Allen, and Gavin M. Walker. 2006. "Adsorption of Methylene

- Blue onto Activated Carbon Produced from Steam Activated Bituminous Coal: A Study of Equilibrium Adsorption Isotherm.” *Chemical Engineering Journal* 124(1–3):103–10.
- Qi, Liqiang, Zhikai Zhao, Ruitao Wang, Weiheng Gao, Jingxin Li, and Yajuan Zhang. 2020. “Simultaneous Desulfurization and Denitri Fi Cation Using La – Ce – V – Cu – ZSM - 5 Catalysts in an Electrostatic Precipitator.”
- Rendon-Rivera, A., M. A. Cortes-Jacome, E. Lopez-Salinas, M. L. Mosqueira, and J. A. Toledo-Antonio. 2016. “Adsorption of Nitrogen and Sulphur Organic-Compounds on Titania Nanotubes.” *International Journal of Engineering Research & Science* 2(8):156–66.
- Richardson, Louis L. 1978. “Use of Bleaching, Clays, in Processing Edible Oils.” *Journal of the American Oil Chemists’ Society* 55(11):777–80.
- Rizwan, Danish, Ajay K. Dalai, and John Adjaye. 2013. “Synthesis of Novel Polymer Poly(Glycidyl Methacrylate) Incorporated with Tetranitrofluorenone for Selective Removal of Neutral Nitrogen Species from Bitumen-Derived Heavy Gas Oil.” *Fuel Processing Technology* 106:483–89.
- Ronald F. Ziolo, Webster, N. Y. ..., Canada; Elizabeth C. Kroll, Hamilton, Javier Tejada Palacios; Xixiang, and Spain Zhang, both of Barcelona. 1995. “Magnetc Refrgerant Compostions and Processes for Makng and Usng.” 11.
- Sampanthar, Jeyagowry T., Huang Xiao, Jian Dou, Teo Yin Nah, Xu Rong, and Wong Pui Kwan. 2006. “A Novel Oxidative Desulfurization Process to Remove Refractory Sulfur Compounds from Diesel Fuel.” *Applied Catalysis B: Environmental* 63(1–2):85–93.
- Sano, Yosuke, Ki Hyouk Choi, Yozo Korai, and Isao Mochida. 2004. “Selection and Further Activation of Activated Carbons for Removal of Nitrogen Species in Gas Oil as a Pretreatment for Its Deep Hydrodesulfurization.” *Energy and Fuels* 18(3):644–51.
- Santos, Aaron L., Rodrigo A. Reis, Vinicius Rossa, Marcelo M. Reis, André L. H. Costa, Cláudia O. Veloso, Cristiane A. Henriques, Fátima M. Z. Zotin, Márcio L. L. Paredes, Erika B. Silveira, and Sandra S. X. Chiaro. 2012. “Silica-Alumina Impregnated with Cerium, Nickel, and Molybdenum Oxides for Adsorption of Sulfur and Nitrogen Compounds from Diesel.” *Materials Letters* 83:158–60.
- Sarda, K. K., A. Bhandari, K. K. Pant, and Sapna Jain. 2012. “Deep Desulfurization of Diesel Fuel by Selective Adsorption over Ni/Al 2O 3 and Ni/ZSM-5 Extrudates.” *Fuel* 93:86–91.
- Satterfield, Charles N. 1996. *Heterogeneous Catalysis in Industrial Practice 2nd E.* 2nd Editio. Krieger Publishing Company.
- Schirmer, W. 1999. “Physical Chemistry of Surfaces.” *Zeitschrift Für Physikalische Chemie* 210(Part_1):134–35.
- Sévignon, Marc, Mathieu Macaud, Alain Favre-Réguillon, Jürgen Schulz, Muriel Rocault, René Faure, Michel Vrinat, and Marc Lemaire. 2005. “Ultra-Deep Desulfurization of Transportation Fuels via Charge-Transfer Complexes under Ambient Conditions.” *Green Chemistry* 7(6):413–20.
- Shan, Jia Hui, Xiao Qin Liu, Lin Bing Sun, and Rong Cui. 2008. “Cu-Ce Bimetal Ion-Exchanged Y Zeolites for Selective Adsorption of Thiophenic Sulfur.” *Energy and Fuels* 22(6):3955–59.

- Silva, Alysson M. A., Eduardo H. M. Nunes, Douglas F. Souza, Dana L. Martens, João C. Diniz da Costa, Manuel Houmard, and Wander L. Vasconcelos. 2015. "Effect of Titania Addition on the Properties of Freeze-Cast Alumina Samples." *Ceramics International* 41:10467–75.
- Silveira, E., C. Veloso, A. Costa, C. Henriques, F. Zotin, M. Paredes, R. Reis, and S. Chiaro. 2015. "Influence of Metal Oxides Impregnated on Silica-Alumina in the Removal of Sulphur and Nitrogen Compounds from a Hydrotreated Diesel Fuel Stream." *Adsorption Science and Technology* 33(2):105–16.
- Sismanoglu, T. and S. Pura. 2001. "Adsorption of Aqueous Nitrophenols on Clinoptilolite." *Colloids and Surfaces A: Physicochemical and Engineering Aspects* 180(1–2):1–6.
- Song, Chunshan. 2003. "An Overview of New Approaches to Deep Desulfurization for Ultra-Clean Gasoline, Diesel Fuel and Jet Fuel." *Catalysis Today* 86(1–4):211–63.
- Speight, James G. 2020. "Fossil Energy." *Fossil Energy* 17–45.
- Sumathi, S., S. Bhatia, K. T. Lee, and A. R. Mohamed. 2009. "Performance of an Activated Carbon Made from Waste Palm Shell in Simultaneous Adsorption of SO_x and NO_x of Flue Gas at Low Temperature." *Science in China, Series E: Technological Sciences* 52(1):198–203.
- Sumathi, S., S. Bhatia, K. T. Lee, and A. R. Mohamed. 2010. "Selection of Best Impregnated Palm Shell Activated Carbon (PSAC) for Simultaneous Removal of SO₂ and NO_x." *Journal of Hazardous Materials* 176(1–3):1093–96.
- Takahashi, Akira, Frances H. Yang, and Ralph T. Yang. 2002. "New Sorbents for Desulfurization by π -Complexation: Thiophene / Benzene Adsorption." 2487–96.
- Tang, Hu, Weijie Zhou, and Lina Zhang. 2012. "Adsorption Isotherms and Kinetics Studies of Malachite Green on Chitin Hydrogels." *Journal of Hazardous Materials* 209–210:218–25.
- Toor, Saqib S., Harvind Reddy, Shuguang Deng, Jessica Hoffmann, Dorte Spangsmark, Linda B. Madsen, Jens Bo Holm-Nielsen, and Lasse A. Rosendahl. 2013. "Hydrothermal Liquefaction of Spirulina and Nannochloropsis Salina under Subcritical and Supercritical Water Conditions." *Bioresource Technology* 131:413–19.
- Tursiloadi, Silvester, Hiroaki Imai, and Hiroshi Hirashima. 2004. "Preparation and Characterization of Mesoporous Titania-Alumina Ceramic by Modified Sol-Gel Method." *Journal of Non-Crystalline Solids* 350:271–76.
- Ullah, K. R., R. Saidur, H. W. Ping, R. K. Akikur, and N. H. Shuvo. 2013. "A Review of Solar Thermal Refrigeration and Cooling Methods." *Renewable and Sustainable Energy Reviews* 24:499–513.
- Vaez, Mohammad, Abdolsamad Zarringhalam Moghaddam, and Somayeh Alijani. 2012. "Optimization and Modeling of Photocatalytic Degradation of Azo Dye Using a Response Surface Methodology (RSM) Based on the Central Composite Design with Immobilized Titania Nanoparticles." *Industrial and Engineering Chemistry Research* 51(11):4199–4207.
- Velu, S., Chunshan Song, Clean Fuels, Catalysis Program, and Geo-environmental Engineering. 2002. "Zeolite-Based Adsorbents for Desulfurization of Jet Fuel by Selective Adsorption." *Fuel Chemistry* 47(2):447–48.
- Vosoughi, Vahid, Sandeep Badoga, Ajay K. Dalai, and Nicolas Abatzoglou. 2017. "Modification

- of Mesoporous Alumina as a Support for Cobalt-Based Catalyst in Fischer-Tropsch Synthesis.” *Fuel Processing Technology* 162:55–65.
- Vural, Ufuk. 2020. “Waste Mineral Oils Re-Refining With Physicochemical Methods.” *Turkish Journal of Engineering* 4(2):62–69.
- Wachs, Israel E. 2005. “Recent Conceptual Advances in the Catalysis Science of Mixed Metal Oxide Catalytic Materials.” *Catalysis Today* 100(1–2):79–94.
- Weber, Rainer, Hans-dieter Block, and Norbert Lonhoff. 1991. “United States Patent [151 Date of Patent :” (19):3–5.
- Wu, Xiaohui, Bo Yue, Yi Su, Qi Wang, Qifei Huang, Qunhui Wang, and Hongying Cai. 2017. “Pollution Characteristics of Polycyclic Aromatic Hydrocarbons in Common Used Mineral Oils and Their Transformation during Oil Regeneration.” *Journal of Environmental Sciences (China)* 56(200 L):247–53.
- Yang, Hong, Jinwen Chen, Craig Fairbridge, Yevgenia Briker, Yu Jie Zhu, and Zbigniew Ring. 2004. “Inhibition of Nitrogen Compounds on the Hydrodesulfurization of Substituted Dibenzothiophenes in Light Cycle Oil.” *Fuel Processing Technology* 85(12):1415–29.
- Yang, Ralph T., Akira Takahashi, and Frances H. Yang. 2001. “New Sorbents for Desulfurization of Liquid Fuels by π -Complexation.” 6236–39.
- Yang, Yuqing, Shongming Huang, Robert Vassov, Brad Pinno, and Sophan Chhin. 2020. “Climate-Sensitive Height – Age Models for Top Height Trees in Natural and Reclaimed Oil Sands Stands in Alberta , Canada.” 307(November 2019):297–307.
- Yitzhaki, D. 1995. “Deep Desulfurization of Heavy Atmospheric Gas Oil With Co-Mo-Al Catalysts - Effect of Sulfur Adsorption.” *Applied Catalysis A-General* 122(2):99–110.
- Yoosuk, Boonyawan, Arnan Silajan, and Pattarapan Prasassarakich. 2020. “Deep Adsorptive Desulfurization over Ion-Exchanged Zeolites: Individual and Simultaneous Effect of Aromatic and Nitrogen Compounds.” *Journal of Cleaner Production* 248:119291.
- Yuan, Quan, An-Xiang Yin, Chen Luo, Ling-Dong Sun, Ya-Wen Zhang, Wen-Tao Duan, Hai-Chao Liu, and Chun-Hua Yan. 2008. “Facile Synthesis for Ordered Mesoporous γ -Aluminas with High Thermal Stability.” *Journal of the American Chemical Society* 130(11):3465–72.
- Zhang, Yong, Feng Yu, Wenping Cheng, Jiancheng Wang, and Juanjuan Ma. 2017. “Adsorption Equilibrium and Kinetics of the Removal of Ammoniacal Nitrogen by Zeolite X/Activated Carbon Composite Synthesized from Elutrilithe.” *Journal of Chemistry* 2017.
- Zhou, Keqing, Qiangjun Zhang, Biao Wang, Jiajia Liu, Panyue Wen, Zhou Gui, and Yuan Hu. 2014. “The Integrated Utilization of Typical Clays in Removal of Organic Dyes and Polymer Nanocomposites.” *Journal of Cleaner Production* 81:281–89.
- Zolotareva, Darya, Alexey Zazybin, Khadichakhan Rafikova, Valery M. Dembitsky, Anuar Dauletbakov, and Valentina Yu. 2019. “Ionic Liquids Assisted Desulfurization and Denitrogenation of Fuels.” *Vietnam Journal of Chemistry* 57(2):133–63.

Appendix A: Permission to reuse submitted paper Tables and Figures



The screenshot displays the Copyright Clearance Center RightsLink interface. At the top left, the Copyright Clearance Center logo and the RightsLink logo are visible. On the top right, there are navigation links: Home, Help, Email Support, Sign in, and Create Account. The main content area shows a card for an article titled "Adsorptive desulfurization through charge-transfer complex using mesoporous adsorbents". The card includes a thumbnail of the journal cover for "FUEL", the author list "Anakaren Botana de la Cruz, Philip Boahene, Sundaramurthy Vedachalam, Ajay K. Dalai, John Adjaye", the publication "Fuel", the publisher "Elsevier", and the date "1 June 2020". Below the article details, there is a copyright notice: "© 2020 Elsevier Ltd. All rights reserved." Below the article card, a text box contains a permission notice: "Please note that, as the author of this Elsevier article, you retain the right to include it in a thesis or dissertation, provided it is not published commercially. Permission is not required, but please ensure that you reference the journal as the original source. For more information on this and on your other retained rights, please visit: <https://www.elsevier.com/about/our-business/policies/copyright#Author-rights>". At the bottom of this text box are two buttons: "BACK" and "CLOSE WINDOW". At the very bottom of the interface, there is a footer with copyright information: "© 2020 Copyright - All Rights Reserved | Copyright Clearance Center, Inc. | Privacy statement | Terms and Conditions" and a contact note: "Comments? We would like to hear from you. E-mail us at customer-care@copyright.com".

Figure A.1. Permission to use published article, tables and Figures for Chapter 3

Appendix B: Additional table of results from process parameter optimization studies and activation energy (E_a) plots for adsorbents A, B and C

Adsorbent A					
Sample name	Adsorbent loading (g)	Temperature	Time (min)	Sulfur concentration (ppm)	Sulfur removal (%)
A22	0.75	22°C	60	166.7	69.2
B22	0.75		27	140.8	74.0
C22	0.25		60	236	56.4
D22	0.25		27	428.5	20.8
A60	0.75	60°C	60	177.7	67.2
B60	0.75		27	206.4	61.8
C60	0.25		60	290.4	46.3
D60	0.25		27	327.1	39.5
A41	0.5	41°C	43	222.6	58.9
B41	0.5		43	128.1	76.3
C41	0.5		71	215.1	60.2
D41	0.5		43	222.5	58.9
E41	0.5		43	143.8	73.4
F41	0.5		43	204.4	62.2
G41	0.5		15	238.6	55.9
H41	0.5		43	221.5	59.1
I41	0.92		43	327.7	39.4
J41	0.08		43	328.6	39.3
A73	0.5		73°C	43	522.5

Figure B.1. Optimization result table for adsorbent A

Adsorbent B					
Sample name	Adsorbent loading (g)	Temperature	Time (min)	Sulfur concentration (ppm)	Sulfur removal (%)
TA22	0.75	22°C	60	379.5	29.9
TB22	0.75		27	414	23.5
TC22	0.25		60	394.5	27.1
TD22	0.25		27	340.2	37.1
TA60	0.75	60°C	60	259.9	52.0
TB60	0.75		27	258	52.3
TC60	0.25		60	289.9	46.4
TD60	0.25		27	231.5	57.2
TA41	0.5	41°C	43	282.3	47.8
TB41	0.5		43	292	46.0
TC41	0.5		71	313.7	42.0
TD41	0.5		43	297.3	45.0
TE41	0.5		43	271.1	49.9
TF41	0.5		43	324	40.1
TG41	0.5		15	334.4	38.2
TH41	0.5		43	320.9	40.7
TI41	0.92		43	300	44.5
TJ41	0.08		43	246.1	54.5
TA73	0.5		73°C	43	360.9

Figure B.2. Optimization result table for adsorbent B

Sample name	Adsorbent C				
	Adsorbent loading (g)	Temperature	Time (min)	Sulfur concentration (ppm)	Sulfur removal (wt.%)
CA22	0.75	22°C	60	83.30	80.94
CB22	0.75		27	60.80	86.09
CC22	0.25		60	323.70	25.93
CD22	0.25		27	108.80	75.10
CA60	0.75	60°C	60	96.45	77.93
CB60	0.75		27	88.68	79.71
CC60	0.25		60	263.36	39.73
CD60	0.25		27	97.33	77.73
CA41	0.50	41°C	43	221.30	49.36
CB41	0.50		43	95.03	62.43
CC41	0.50		71	275.50	36.96
CD41	0.50		43	61.20	58.69
CE41	0.50		43	93.20	62.77
CF41	0.50		43	126.70	59.58
CG41	0.50		15	92.20	78.90
CH41	0.50		43	224.20	48.70
CI41	0.92		43	60.90	86.06
CJ41	0.08		43	416.70	4.65
CA73	0.50	73°C	43	259.79	40.55

Figure B.3. Optimization result table for adsorbent C

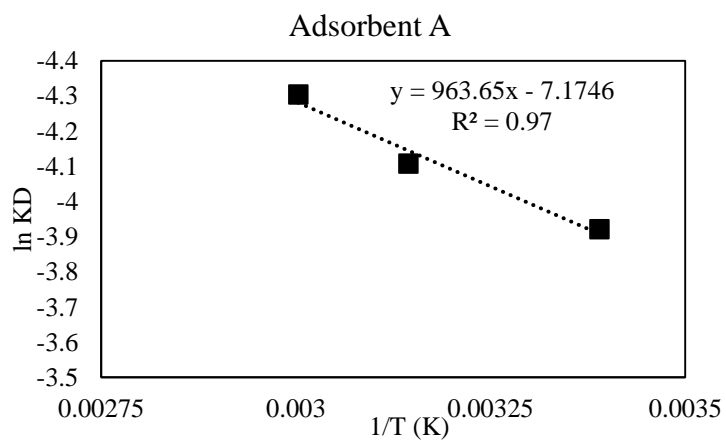


Figure B.4. Activation energy (E_a) plot $\ln K_D$ vs. $1/T$ (K^{-1}) for adsorbent A

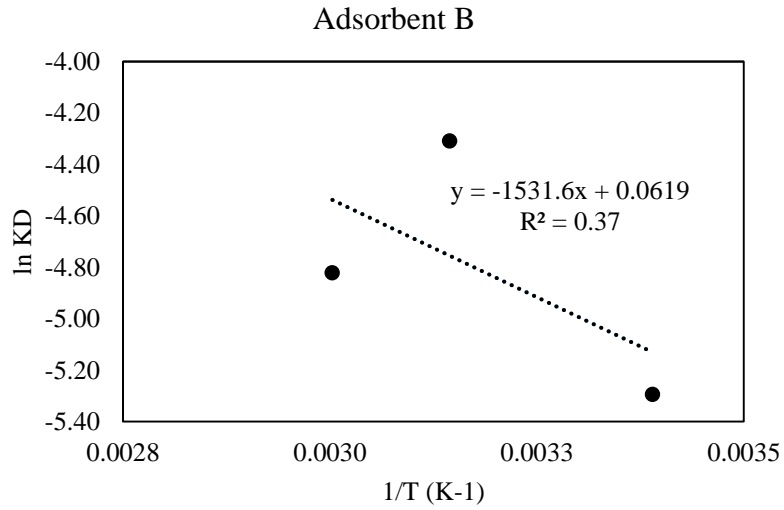


Figure B.5. Activation energy (E_a) plot $\ln K_D$ vs. $1/T$ (K⁻¹) for adsorbent B

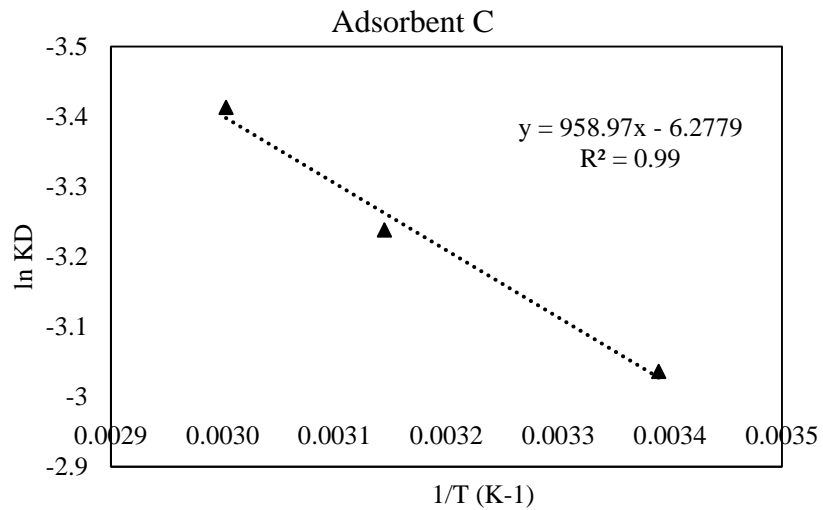


Figure B.6. Activation energy (E_a) plot $\ln K_D$ vs. $1/T$ (K⁻¹) for adsorbent C

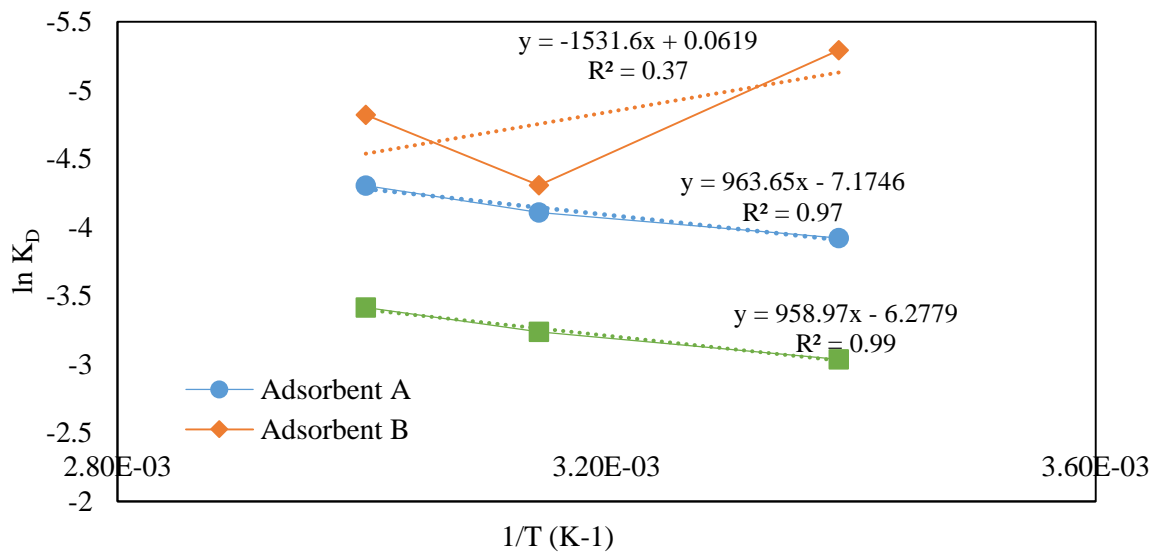


Figure B.7. Free activation energy, enthalpy and entropy plots for adsorbents A, B and C